CENTER FOR INFRASTRUCTURE ENGINEERING STUDIES

Optimization of HPC for Missouri Bridge Structures

By

Dr. John J. Myers

Mahmut Ekenel

And

Brian Sides

University Transportation Center Program at

The University of Missouri-Rolla

UTC
R79

Disclaimer

Technical Report Documentation Page

1. Report No.

UTC R79

2. Government Accession No.

3. Recipient's Catalog No.

4. Title and Subtitle

Optimization of HPC for Missouri Bridge Structures

5. Report Date

June 2003

6. Performing Organization Code

7. Author/s

Dr. John J. Myers, Mahmut Ekenel, and Brian Sides

8. Performing Organization Report No.

RG001232 OT079

9. Performing Organization Name and Address

Center for Infrastructure Engineering Studies/UTC program
University of Missouri - Rolla
223 Engineering Research Lab
Rolla, MO 65409

10. Work Unit No. (TRAIS)

11. Contract or Grant No.

DTRS98-G-0021

12. Sponsoring Organization Name and Address

U.S. Department of Transportation
Research and Special Programs Administration
400 7th Street, SW
Washington, DC 20590-0001

13. Type of Report and Period Covered

Final

14. Sponsoring Agency Code

15. Supplementary Notes

16. Abstract

Commercially available materials will be used throughout this investigation for laboratory produced concrete. Optimization of mix proportions will be accomplished through a trial batching series investigating the interaction of various materials in the production of HPC. The trial series will involve mix designs with the following upper and lower bound limits: w/cm ratio of 0.2 to 0.45 by wt., coarse aggregate content 36 to 44 % by wt., and fine aggregate content 25 to 40 % by wt. Performance will focus on durability enhancement and mechanical property performance such as strength-gain and elastic modulus.

17. Key Words

High performance concrete, high-strength concrete, quality assurances, quality control, mix proportioning.

18. Distribution Statement

No restrictions. This document is available to the public through the National Technical Information Service, Springfield, Virginia 22161.

19. Security Classification (of this report)

unclassified

20. Security Classification (of this page)

unclassified

21. No. Of Pages

22. Price

Form DOT F 1700.7 (8-72)

OPTIMIZATION & DURABILITY OF HIGH STRENGTH / HIGH PERFORMANCE CONCRETE PRODUCED USING LOCALLY AVAILABLE MATERIALS IN THE STATE OF MISSOURI

A study was undertaken on the optimization of high strength (HSC) and high performance concrete (HPC) mixtures using locally available materials obtained in the State of Missouri. Thirty-six (36) different mixtures were produced that were categorized as HSC; eighteen (18) mixtures were categorized as HPC. 30% fly ash replacement by cement weight was utilized in both the HSC and HPC mixtures, and Grade 100 ground granulated blast-furnace slag (GGBFS) was also substituted by 5% of the cement in some of the mixtures. Mineral admixtures were expected to reduce the concrete material costs, enhance durability, increase recycling of these materials and reduce CO_2 production. The HSC mixtures included locally available Limestone coarse aggregate. Three different coarse aggregate sources in Missouri were used in the HPC mixtures including a Limestone, Trap Rock, and River Gravel. Laboratory test results concluded that mixtures of HSC and HPC without cement replacement displayed higher strength development at the end of 56-day compared to the mixtures in which Class F fly ash and Class F fly ash-GGBFS blend were utilized as a cementitious replacement material. The HPC mixtures batched with limestone showed higher compressive strength relative to the mixtures prepared with other coarse aggregate types mentioned above. All the air-entrained mixtures performed well under 300 freezing & thawing cycles, however, the samples in which GGBFS was utilized performed poorly relative to the other samples. Similar lower performance was obtained from the same samples in chloride permeability tests, in which fly ash substituted samples performed outstanding in both the HSC and HPC series.

Acknowledgments

The present research was funded by University of Missouri Research Board and the University Transportation Center (UTC) at the University of Missouri-Rolla (UMR). The authors are thankful to several manufacturers in the State of Missouri, USA, who donated materials used in this research study. Their names are not mentioned herein to prevent any concern of commercialism. The authors would also like to acknowledge Mr. Brian Sims for his effort on this project as undergraduate research assistants.

Table of Contents

List of Figures

List of Appendices Figures

List of Tables

List of Appendices Tables

Notations &Abbreviations:

AEA	Air Entrainment Agent
ASTM	American Society for Testing & Materials
C.Ag.	Coarse aggregate
F. Ag.	Fine aggregate
FA	Fly ash
f’c	Compressive strength
GGBS	Ground granulated blast-furnace slag
HPC	High performance concrete
HSC	High strength concrete
MOE	Modulus of Elasticity
HRWR	High range water reducer
P.Cem.	Portland cement
LS	Limestone
RG	River Gravel
TR	Trap Rock
w/c	Water per cementitious ratio

CHAPTER 1: INTRODUCTION

1.1 Introduction and Problem Statement

Increasing public and commercial use of existing bridges, highways, and local streets has generated major problems for city, state, and federal governments, especially when traffic loads exceed the level for which a structure is design. When these members were built years ago, engineers often underestimated the required conditions, not anticipating the high levels of heavy truck traffic these members now must carry. Durability of these structures, or by another saying, the long-term deterioration of these structures caused by environmental conditions, which is also accelerated by either application of an inappropriate specification or the use of improper materials and construction practice, was another issue that attracted attention, especially after 1970's. These issues became clearer after a report is published by National Materials Advisory in 1987 [Mehta, 1997]. According to this report, approximately 253,000 concrete bridge decks, some of them less than 20 years old, were in varying states of deterioration and structurally or functionally deficient.

Figure 1.1 A deteriorated bridge pier & deck on Highway 44

A recent report released for congress by FHWA in 1997 on the status of the Nations highway bridges. According to this report, 31% of the 581,862 bridges are substandard, 17% are classified as "structurally insufficient", meaning they are either closed or require immediate rehabilitation to remain open, 14% are "functionally obsolete", meaning that they do not meet current standards. These bridges, as well as the connected highways will soon require extensive repair or replacement. Consequently, the durability of concrete is being taken much more seriously now then before. Figure 1.1 shows a deteriorated bridge because of heavy traffic loads and chemical attack on Highway 44.

When deterioration of concrete structures because of durability issues became more viable after 1970's, the construction companies in United States gradually moved toward the use of higher strength concrete mixtures. However, a report published by National Cooperative Highway Research Program (NCHRP) in 1995 by Rogella et al changed this concept. It was mentioned in this report that more than 100,000 high strength concrete bridge decks developed full depth transverse cracks spaced 3 to 10 ft (1 to 3 m) before the concrete was one month old [Mehta, 1997]. Hence, since the cost of replacing these structures are more costly than repair and rehabilitation of only minor maintenance expense, alternative methods are being sought.

One viable alternative to repair or replacement of the existing deteriorated concrete bridge members is the use of high strength concrete (HSC) in girder applications where strength and durability issues are main concerns, and high performance concrete (HPC) in deck applications where durability performance is primary characteristic of interest [ACI 363R; Alampalli, 2000]. High performance concrete (HPC) has been used more widely in recent years. Some examples for the primary applications of HPC in United States have been in the high buildings; as well as bridges and highways, and aircraft aprons, where the structural members are subject to high traffic loads and severe environmental conditions. The Federal Highway Administration (FHWA) has investigated a significant amount of research dollars into the use and application of high performance concrete relative to highway applications. HPC is not a revolutionary concrete; it is a development of the conventional concrete used in the past. The difference is, HPC meets special performance and uniformity requirements that cannot always be obtained by using conventional ingredients and methods, such as enhancement of placement and compaction without segregation, early-age strength, curing, toughness, volume stability, or service life in a severe environment [Zia, 1993].

The HPC used to be also named as high strength concrete (HSC), however, the current name took place when the researchers realized that the durability should be a required specification as well as high strength in many cases. High strength does not necessarily mean a low permeability and high durability in service. Consequently, HPC has been designed to be more durable, and if necessary, stronger than conventional concrete. One another reason that HPC is preferred against to HSC is the concrete crack resistance. HSC are prone to cracking more than any other concrete because of the increase in strength would yield to increase in elastic modulus and reduce the creep coefficient, which would also have an adverse effect on concrete crack resistance (extensibility)[Mehta, 1997].

The increased durability of HPC is based on the moderately high strength and low permeability. The basic concept of providing these two major properties is using low w/c ratio with high cement content, and in many cases more than one supplementary cementitious material, such as fly ash, silica fume, and ground granulated blast-furnace slag, to name a few. When these properties come together, it provides a discontinuous capillary pore system, which is essential for high durability and longer life in severe environments. The main advantages of being high durable concrete are increased service life and reduced maintenance costs of the concrete structures. Because of these reasons, an increasing demand for HPC can be seen in recent years.

In production of HPC, it is necessary to get the maximum performance from all of the materials. The materials should be well identified, and their behavior when combined in a concrete mixture should be examined. Any material that presents incompatibilities will yield to detrimental effects to fresh properties, as well as hardened properties of concrete [Shah, 1994]. HPC normally contains Portland cement, aggregate and water, as well as chemical or mineral admixtures (in many cases both), and more than one supplementary mineral admixture. Mineral admixtures were expected to reduce the concrete material costs, enhance durability, increase recycling of these materials and reduce CO_2 production [Mehta, 1986; Malhotra, 1996]. A well-graded aggregate is also required for providing low volumes of pores. Moreover, the strength of aggregate is important when a long-term strength and durability of concrete is required. Hence good quality of aggregate is necessary to ensure good bond between the coarse aggregate participles and the matrix [Neville, 1996]. The quality of aggregate also plays an important role in the applications where high modulus of elasticity (MOE) is properly sought [Neville, 1996].

In the mechanical point of view, HPC provides significantly more structural improvement. An example of this case is the bridge design, in which substantial benefits can be obtained by utilizing the HPC. Since it has also been designed with high strength properties, the number of beams per bent line can be significantly reduced in a bridge, and the span lengths between bridge piers can be longer than conventional ones. Longer member spans allow for the reduction of substructure elements, of which are approximately 50% overall construction costs associated with a bridge (based on a national average). As a result of using fewer or longer spanning members, HPC can result in reduced construction costs. The utilization of HPC for prestressed concrete bridge girders also results in design flexibility for the bridge designer. In addition to these, HPC results in reduced maintenance costs, and an extended service life from 40 to 75 years for the structure, fewer work zone related user delays, less potential for work-zone related accidents, and less disruption to the community.

1.2 Research Objectives

The main objective of this research is to optimize the use of HPC by using the materials that are locally available in the state of Missouri. Optimization is focused on the examination of the short and long-term durability of high performance concrete, as well as its mechanical properties, such as compressive strength and modulus of elasticity (MOE). Aggregates have been investigated to identify aggregate sources that are most appropriate for enhanced durability performance and for the production of HPC in Missouri.

One another goal of this investigation is to investigate quality control or specification issues and provide recommendations for HPC, related to the use and placement of HPC concrete in bridge structures based on the optimized mix designs, and local materials investigated. Since HPC concretes are known as cohesive, the findings of this research will provide guidelines for the placement and transportation of HPC, and control of the fresh characteristics such as premature loss of workability and segregation.

In addition of the above-mentioned objectives, the aim of the research also intents to advance the science of HPC, and the current state-of-the-art. For this purpose, an investigation has been conducted on the impact of air entrainment on the durability performance of HPC; and the current assumptions such as, the air entrainment may not be warranted for freezing & thawing resistance of high strength concrete with low w/c ratio due to a discontinuous capillary network and lack of freezable water have been asserted. Moreover, the role of aggregate on failure mechanism has been studied. The aggregate-paste bond, and the paste matrix to distinguish if a weak link failure mechanism can be predicted at a given material content level have also been examined.

1.3 Scope of Research Program

The scope of this investigation is to determine the behavior of high strength/high performance concrete, produced by using the locally available materials of Missouri State, under mechanical and durability tests. Some fresh property tests have also been performed on the concrete batches under investigation. A large number of specimens were cast, moist cured, and tested to generate and analyze specific data on the fresh, mechanical and durability properties of HSC/HPC. The influence of matrix constituents and proportions on these properties is also examined. The mechanical properties of interest included compressive strength, and modulus of elasticity; fresh properties consist the tests of air content and slump; finally, durability tests covered a big range from permeability, abrasion resistance, to freeze-thaw resistance.

CHAPTER 2: LITERATURE REVIEW

The following discussion presented in Chapter 2 is a literature review on high strength and high performance concrete conducted and summarized by Myers (1998).

2.1 Fundamental Mechanisms of High Strength / High Performance Concrete

In the development of mix proportions for high strength/high performance concrete (HS/HPC), the content of three components must be optimized to produce a mix design satisfying hardened or fresh concrete property requirements. These include the strength of the coarse aggregate, the strength of the paste, and the strength of the paste-to-aggregate bond [Mindness, 1985]. The load-bearing capacity of HS/HPC is determined by the weakest of these three components. This concept of the weakest component controlling the strength of the concrete is refereed to as the “Three Link Chain” concrete theory and is schematically presented in Figure 2.1. In producing the most efficient mix design utilizing readily available materials, it is important to optimize each component to maximize the strength potential. Furthermore, the compatibility among the constituents plays a very important role in the development of high strength mixes as discussed herein.

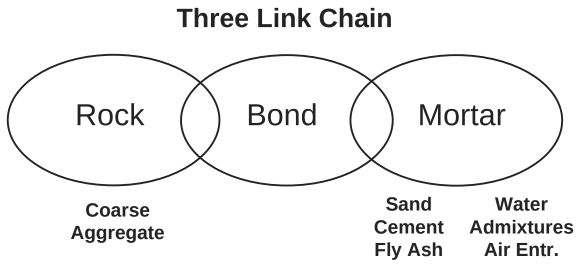

Figure 2.1: “Three Link Chain” concrete theory [Myers (1998)]

2.1.1 Aspects of Cement Hydration

Before discussing the individual constituents and the manner in which they affect the strength of the concrete, it is important to understand the chemical and physical aspects of cement hydration. Portland cement is composed of five major crystalline compounds. These components are tricalcium silicate (C_3S), dicalcium silicate (C_2S), tricalcium aluminate (C_3A), tetracalcium aluminoferrite (C_4AF), and gypsum (CSH_2). C_3S and C_2S are the most important ingredients that affect the strength development while the C_3A, C_4AF, CSH_2, and alkaline compounds are important during the clinker production and regulation of setting and other rheological properties of fresh concrete. In the presence of water, the silicates and aluminates hydrate and precipitate calcium silicate hydrate (C-S-H), calcium hydroxide ($Ca[OH]_2$), and calcium sulfoaluminate ($C_6AS_3H_{32}$). Mindness and Young [2] assert that cement hydration is an exothermic reaction where the reaction kinetics may be followed by isothermal calorimetry. An isothermic curve for an ordinary portland cement is illustrated in Figure 2.2. The rate of strength gain of the cement is approximately proportional to the area under the rate of heat evolution curve.

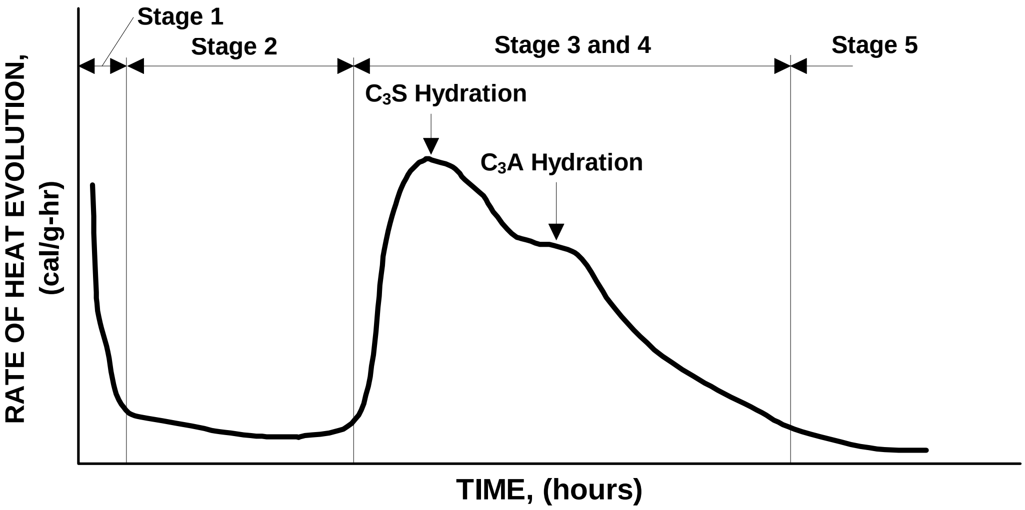

Figure 2.2: Rate of heat evolution during hydration of Portland cement [Myers, 1998]

Stage 1 is a period of rapid evolution of heat and marks the rapid dissolution of C_3A, C_3S, and gypsum is water. A very alkaline solution results with a pH of over 12. Exothermic hydrolysis of ions slows down within approximately ten minutes due to the formation of ettringite which resembles stubby rods on the outer surface of the gel layer surrounding the cement grains. Gypsum is added to form ettringite during the plastic state to curb the vigorous initial reaction of C_3A with water. The formation of ettringite is given by the following:

$$\underset{\text{tricalcium aluminate}}{C_3A} + \underset{\text{gypsum}}{3CSH_2} + \underset{\text{water}}{26H} \Rightarrow \underset{\text{ettringite}}{C_6AS_3H_{32}} \quad \textbf{(2.1)}$$

Stage 2 is a dormant period where the hydrolysis of ions continues but significant hydration does not occur for a period of two to four hours. This is caused by a requirement to achieve a certain ion concentration in the solution before crystal nuclei can form. When calcium and hydroxide ions reach a certain concentration in the solution, hydration of C_3S proceeds rapidly and the initiation of the acceleration period (Stage 3) begins. This is characterized by a strong heat evolution and the following reaction:

$$\underset{\text{tricalcium silicate}}{2C_3S} + \underset{\text{water}}{6H} \Rightarrow \underset{\text{C-S-H}}{C_3S_2H_3} + \underset{\text{calcium hydroxide}}{3CH} \quad \textbf{(2.2)}$$

Calcium hydroxide (CH) crystallizes from solution while the calcium silicate hydrate (C-S-H) develops around the cement grains forming a relatively porous shell initially. As hydration continues, the shell increases and forms a barrier through which water must flow to reach the cement particles and ions must diffuse to reach the growing crystals that nucleate on the ettringite rods. Hydration becomes diffusion controlled at this juncture resulting in a deceleration of hydration of C_3S (Stage 4). Reactions which are diffusion-controlled are quite slow and become slower as the thickness of the diffusion barrier increases. When sulfate concentration is depleted by the formation of ettringite, ettringite further reacts with C_3A and water to form monosulfoaluminate (AFm). The formation of AFm is expressed by the following reaction:

$$\underset{\text{tricalcium aluminate}}{2C_3A} + \underset{\text{ettringite}}{C_6AS_3H_{32}} + \underset{\text{water}}{4H} \Rightarrow \underset{\text{AFm}}{3C_4ASH_{12}} \quad \textbf{(2.3)}$$

The renewed growth of ettringite crystals are more acicular and their formation with C3A is associated with this secondary peak. Once hydration is completely diffusion-controlled a steady state period has been reached (Stage 5). This steady state reaction stage is primary relevant to the later age strength gain of the concrete mix design.

2.1.2 Portland Cement Paste

The total porosity, pore size distribution, and the presence of flaws within its structure are properties of the paste which have been found to have a significant effect on strength [Mindness (1985)]. As the total porosity of the paste increases, the strength decreases. The pore size also effects the strength of the paste. Large pores are considered to be more detrimental to the strength of the paste than the small pores. In some cases [Hester, 1985] lowering the water-to- cementitious (w/cm) ratio may reduce the strength of the concrete if the cement grains are not dispersed properly. This may be caused by low slump of the concrete or poor compaction of the mix associated with the low slump of a concrete. However, this is generally not a concern when a mid or high range water reducer is used in conjunction with a low water-to-cementitious material ratio. Figure 2.3 presents the volume relationships among the constituents schematically.

Capillary and gel pores are two types of pores in cement paste. Capillary pores represent the voids in the paste that have not yet been filled with hydration products while the gel pores are the infinitesimal interconnected space that exist between the gel particles. The pore system plays a major role in determining the permeability of the concrete.

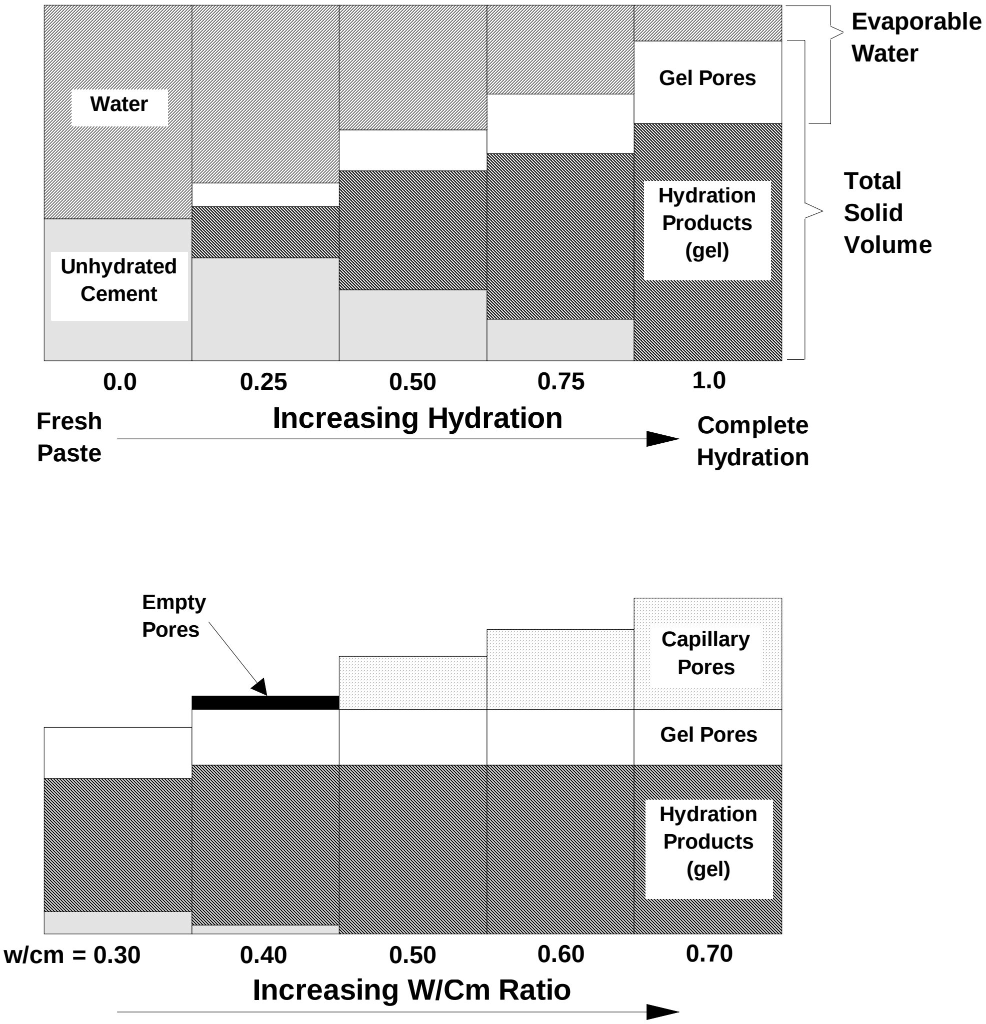

Figure 2.3: Volume relationships among constituents of hydrated pastes [Mindness, 1981]

Immediately surrounding the aggregates is a layer of paste known as the transition zone. The transition zone may be 10 to 50 μm thick in conventional concretes. The thickness is dependent upon a number of variables including the w/cm ratio and the aggregate size. In freshly placed conventional concrete, the bleed water deposits around the coarse aggregate particles forming a water film. The water film is thicker with larger aggregate sizes under identical conditions. This higher w/cm ratio at the transition zone causes the formation of larger crystals of ettringite and calcium hydroxide (CH) resulting in a more porous microstructure than in the bulk hydrated cement paste. Calcium hydroxide crystals grow with their c-axis perpendicular to the surface of the coarse aggregate which affects the paste-to-aggregate bond in a detrimental manner. The higher the w/cm ratio at the transition zone, the thicker the transition zone and the greater number of CH crystals which are oriented perpendicular to the aggregate resulting in weaker bond characteristics. Most experts [Mindness, 1981, Mehta, Skalny, Swamy, Unpublished] agree that the transition zone is the weak link for conventional concretes. For the purposes of this presentation, conventional concretes are concretes without chemical or mineral admixtures generally less than 41.4 MPa (6,000 psi) in strength. The aggregate particles and paste components for conventional concretes are generally not the weak link since microcracking in the transition zones are already present due to drying and cooling even before the concrete is subjected to loading. The weak nature of the transition zone and this presence of microcracking are mainly responsible for the inelastic behavior of concrete and its associated loss of stiffness relative to these two components. For the case of HS/HPC’s, the cement paste is denser when compared to conventional concretes [Sarkar, 1987]. Both conventional concretes and HS/HPC are composed of calcium silicate hydrate (C-S-H) and CH, but their proportions and morphologies are different. In HS/HPC, the CH content is significantly lower and less crystallized which is attributed to a low w/cm ratio. The lack of water in HS/HPC’s inhibits the formation of CH crystals since the solution is required to be supersaturated before CH crystals can form. Since the presence of CH in the transition zone is inhibited, C-S-H is in direct contact with the coarse aggregate particle resulting in an improved bonding between the aggregate particle and mortar. Therefore, in HS/HPC’s, the transition zone may or may not be the “weak link” dependent upon the composition and characteristics of the aggregate and mortar. Additionally, both the total porosity and the average pore size are reduced in HS/HPC’s resulting in low permeability as discussed in Section 2.3.2. The generally low w/cm ratio of HS/HPC results in the improved durability performance as discussed in subsequent sections.

2.1.3 Effect of Chemical Admixtures

The use of chemical admixtures in the production of HS/HPC’s can significantly improve the quality of the concrete. In order to select the best type and dosage rate of a chemical admixture for a HS/HPC, the admixture should be optimized and tested under the expected field conditions. Chemical admixtures may be separated into several general groups including water reducers and retarders, high range water reducers, air entraining admixtures, and accelerating admixtures.

2.1.3.1 Water Reducers and Retarders. The high cementitious material content and generally low w/cm ratio, have made the use of water reducers and retarders a necessity for the production of high strength concrete. Water reducers are an effective means of decreasing a high mixing water demand for proper workability. Water reducers lower a given w/cm ratio while maintaining a given slump resulting in improved concrete strength, impermeability, and durability. The use of retarding admixtures also reduces the mixing water requirement, but more importantly prolongs the plastic state of the concrete mix and aids in reducing the temperature rise of the fresh concrete due to the heat of hydration. Most HS/HPC's incorporate very high contents of cement where high heat of hydration temperatures is encountered. These high temperatures can impact mechanical and material property development. By reducing the temperature rise during initial hydration, the later-age properties of the concrete including strength and elastic modulus can be improved. Longer set times, particularly during hot-weather concreting, can benefit the overall quality of the concrete. This aspect of controlling the peak heat of hydration is discussed in greater detail in Chapter Eight

2.1.3.2 High Range Water Reducers. The use of high range water reducers (HRWR), often referred to as a superplasticizer, is considered to be very important in the production of very high strength concretes with compression strengths in excess of 68.9 MPa (10,000 psi). The use of a HRWR in a HS/HPC mix allows for a significant reduction in the w/cm ratio below a value of 0.40. HRWR's are high molecular weight anionic surfactants derived from sulfonated formaldehyde of naphthalene or melamine. HRWR's deflocculate the clumps of cement grains and fluidize the mixture. The higher dosage rates of HRWR over mid-range or conventional water reducers allows for an increased and more uniform dispersion of hydration products and thereby a more effective use or optimization of the cementitious material. In effect, Philleo [1986] explained that the water is used more efficiently since the cement particles are more evenly distributed, and their surface is more accessible to water for hydration to occur more expeditiously. The use of a HRWR lessens the sensitivity of the concrete strength to low w/cm ratios [Hester, 1985]. This may be attributed to the more efficient use of the materials.

2.1.3.3 Accelerating Admixtures. Set-accelerating admixtures are used to increase the rate of hydration of C_3S thereby reducing the length of the dormant period (Stage 2). Applications may include emergency concrete repair where very rapid development of rigidity is required or for cold weather concreting where they can offset delay caused by cold temperatures. The use of set-accelerating admixtures with HS/HPC is generally not recommended since it increases the heat of hydration and detrimentally affects the long-term properties of the concrete. Furthermore, in many cold weather concreting applications, temperature related placement concerns are reduced due to the high cement content of most HS/HPC mix designs. The high performance concrete beams and decks associated with this study are a prime example.

2.1.4 Effect of Mineral Admixtures

The use of mineral admixtures mainly consist of fly ash, slags, and silica fume. All of these materials are able to react with calcium hydroxide and said to have pozzolanic activity and are thereby referred to as pozzolans. A pozzolan contains amorphous silica which is sufficiently reactive to combine with calcium hydroxide to form C-S-H in the presence of water. The pozzolanic reaction is given by:

$$\text{CH} + \text{S} + \text{H} \Rightarrow \text{C-S-H} \quad \textbf{(2.4)}$$

When a pozzolan is combined with cement, it will react with the calcium hydroxide formed during hydration. The pozzolanic reaction does not begin until CH is produced by the cementitious reaction. The reaction with the pozzolan converts the CH crystals to the highly cementitious C-S-H. The strength of the paste is thereby increased while the permeability is decreased. However, since the pozzonlanic reaction does not occur until CH becomes available for reaction, it does not contribute to the concrete strength until later ages. Since the cementitious and pozzolanic reactions occur at different times, the hydration temperature at any given time is generally lower than that of a concrete containing the same volume of portland cement. The control of temperature can be beneficial in most situations as previously discussed. The effect on the properties of fresh and hardened concrete of each of these mineral admixtures depends on the chemical and physical properties of each. While each mineral admixture will vary depending on its source, there are characteristics which generally apply to each type.

In terms of usage on a national basis, the material which is locally available is generally the mineral admixture of choice by concrete producers. When used as a replacement material by producers, the mineral admixture generally reduces the cost of the cementitious material. Along the northern rust belt, slags, fly ash, and silica fume are more typically used while fly ashes are used in the south and southwest. Therefore, it is mainly an economic criteria which drives the usage of a particular mineral admixture in a region.

2.1.4.1 Fly Ash. Fly ash is a by-product produced in the coal burning process. When the coal is burned, the impurities in the coal which do not burn are suspended in the flue gases. These particles are called fly ash. Because of environmental concerns, the fly ash is removed from the flue gases by mechanical collectors and electrostatic precipitators before they are discharged into the atmosphere. Fly ash particles are typically smooth and spherical in shape and range in diameter from 1 to 150 μm depending on the type of collection system.

Based on its composition, fly ash is classified into two groups: ASTM Class C or high calcium fly ash, and ASTM Class F or low calcium fly ash. Class F fly ash is generally produced from the combustion of anthracite or bituminous coals. Due to their low calcium oxide content, these fly ashes require an external source of calcium for their reaction. Diamond and Lopez-Flores found [9] that mortars with a 30 percent Class F fly ash replacement achieved equal strength with reference mortars at ninety days. The pozzolanic reaction for Class F fly ash begins after approximately two weeks [Mehta, 1983]. In some cases, Class F fly ash may contain approximately five percent by weight cenospheres or plerospheres [Fisher, 1978; Lauf, 1982]. Cenospheres are hollow and empty, whereas plerospheres are hollow but contain smaller spheres inside. Class F fly ash also typically has a carbon content of two to ten percent due to incomplete combustion of the coal. A measure of its carbon content is indicated by the loss of ignition (LOI) of a fly ash. Generally concretes having a high LOI level require a higher dosage of air entraining admixtures for a given air content since the carbon particles absorb some of the air-entraining admixture.

Class C fly ash is produced primarily from the combustion of lignite or subbituminous coals. Class C fly ash has a relatively high calcium oxide content, between 15 and 30 percent. Class C fly ash exhibits both cementitious and pozzolanic behavior. It has been reported [Diamond, 1981] that mortars with a 30 percent Class C fly ash replacement achieved equal strength with reference mortars at seven days. Class C fly ashes contain less than one percent carbon. Thus the impact of a Class C fly ash on air entraining dosage is minimal.

The rheological behavior of concrete is affected to a great extent by the addition of fly ash. When added as a replacement of cement, fly ash results in a more workable mix due to its spherical shape and enables the producer to reduce the w/cm ratio for a given slump thereby resulting in an increase in strength and other mechanical properties. This characteristic coupled with the reduction in hydration temperatures makes fly ash a very desirable component in producing HS/HPC.

2.1.4.2 Slag. There are three main types of slag which include two blast furnace slags (granulated and pelletized) and one steel slag. Non-ferrous slag is not being used as an admixture in concrete [Mehta, 1983].

Blast furnace slag is a by-product in the production of pig iron. The type of blast slag is determined by the method used for cooling the molten slag. If the liquid slag is quenched using water, granulated slag results. If the liquid slag is quenched with air and water, pelletized slag results. Both materials must be ground to a fineness of 400 to 600 m^2/kg to exhibit satisfactory cementitious and pozzolanic characteristics [Mehta, 1983]. Water demand for slags is generally higher than for an equal volume of cement due to its coarse texture and higher fineness. However, these slags can exhibit similar strengths equal to reference concrete at seven days [Hogan, 1981].

Steel slag is produced in the conversion of pig iron to steel. The liquid slag is quenched with water and ground fine. It exhibits both cementitious or pozzolanic characteristics similar to the granulated and pelletized slags.

Other slag materials such as non-ferrous slags produced from metallic copper, nickel, and lead do exhibit pozzolanic characteristics, but are currently not being used as a mineral admixture.

2.1.4.3 Silica Fume. Silica fume is produced in electric arc furnaces during the production of metallic silicon and ferrosilicon alloys. These are smooth and spherical particles which are nearly pure silicon dioxide and one hundred times finer than cement and fly ash particles. Silica fume is highly pozzolanic in nature and can achieve equal strengths with reference concrete at fourteen days. Due to the fineness of the particles, silica fume has an extremely high water demand and requires the use of a water reducer. To achieve adequate workability, the slump of mixes containing silica fume should be increased to offset the “stickiness” or cohesiveness due to the abundance of fine particles. Mixes with silica fume also exhibit reduced bleeding characteristics which requires special considerations in curing such as proper fogging to avoid plastic shrinkage cracks.

2.1.5 Effect of Air Entraining Admixtures

Air-entraining admixtures entrain air in the concrete to provide an air void system for the movement of freezing water within the cement paste. An adequate well distributed air void system provides a relief space for expanding water which minimizes the amount of micro-cracking damage due to moist freeze-thaw cycles. The use of air entraining admixtures for HS/HPC mix designs is only desirable for components subjected to freeze-thaw cycles in excess of the critical saturation threshold (91.7 percent). Air entrainment is not recommended in other cases since entrained air can decrease a concrete's strength significantly at high dosages. The rule of thumb is that a five percent loss in strength may be anticipated for every one percent of air entrainment. Research by Ernzen (1992) and elsewhere has shown that a minimum of three percent air entrainment is required for HS/HPC as illustrated in Figure 2.4.

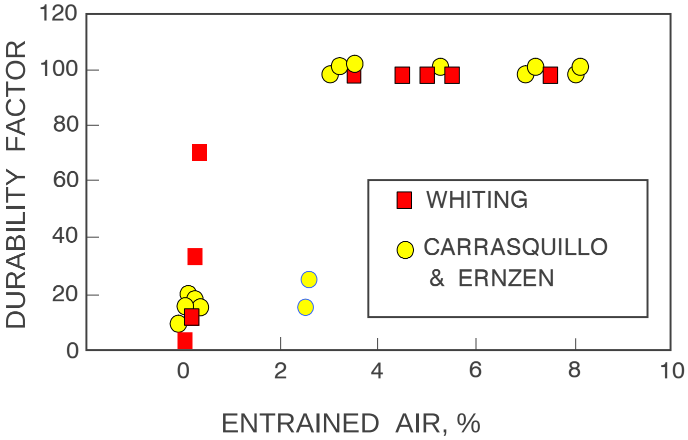

Figure 2.4: Durability performance of HS/HPC mixes with entrained air [Ernzen, 1992]

This is slightly lower than conventional mix designs due to the pore structure of HS/HPC with low w/cm ratios. HS/HPC mix designs are naturally more durable due to their higher strength, lower permeability, and decreased porosity. While research studies to date have not specifically investigated the levels of porosity and time-to-saturation for HS/HPC mix designs with low w/cm ratios, it is safe to assume that the reduced porosity of these mixes require a longer period of time to exceed the critical saturation threshold for a given moisture exposure. Air entrainment should only be used in HS/HPC where specifically required for exposure conditions and should always be tested under field conditions due to the high variability of air entrainments with other chemical and mineral admixtures.

2.1.6 Coarse Aggregates

In conventional concretes, w/cm ratio is the major factor controlling most mechanical properties including compressive strength. This is accomplished by altering the porosity of the cement paste. The aggregate plays a minor role in the performance of conventional concretes since the transition zone is typically the "weak link" as discussed in Section 2.1.2. However, the situation is quite different in HS/HPC with the enhanced transition zone properties. Two components, the aggregate and cement paste, behave more like a homogeneous material and share the stress associated with the load on the concrete. Under this situation, the aggregate can often be the limiting factor. Several parameters of coarse aggregate which affect the behavior of the concrete include its shape, surface texture, mineralogy, strength and elastic moduli. It has been well documented [Cetin, 1995] that a smaller aggregate size produces higher compressive strength at a given w/cm ratio where the effect is more pronounced at lower w/cm ratios and higher cementitious contents. This is due to a reduced unit bond stress resulting from an increased surface area from the smaller aggregate size. It should be noted that the increased surface area from the smaller aggregate size will require a higher paste content to maintain the same workability. In terms of the elastic modulus of the concrete, the elastic modulus appears to be independent of aggregate size for a given aggregate content based on research by Cetin [1995] and others.

While stiffer denser aggregates improve the elastic modulus of the concrete, they also can act as a stress riser resulting in stress concentrations at the transition zone and subsequent microcracking at the bond interfaces reducing the compressive strength of the concrete [Smadi, 1989; Baalbaki, 1991; Gia, 1992]. As a result, the compatibility of materials in producing high strength concrete is critical for microcrack development and compressive strength. To develop optimum strength characteristic out of a mix design, it is desirable to match the moduli of the aggregate with that of the mortar matrix. This will result in a more homogenous material. Since the aggregate type is largely responsible for the elastic modulus of the concrete, a higher aggregate content results in a higher elastic modulus. Therefore, the elastic modulus for HS/HPC may be “engineered” by selecting a specific aggregate type and content within a mix design.

Surface texture and particle shape of the coarse aggregate is responsible for the bond between the matrix and the aggregate due to mechanical interlocking. Crushed aggregates result in superior bond when compared to smooth, rounded gravel. The bond characteristics appear to be more pronounced at low w/cm ratios [Gia, 1992]. Additionally, tensile strengths are even more sensitive to the aggregate surface texture since the tensile strength is dependent on the aggregate-matrix bond strength [Zia, 1991].

Recent studies [Neville, 1996; Aitcin, 1990] also indicate that the aggregate type plays a role in the bond characteristic. In the case of limestone, dolomite, and siliceous aggregates, a chemical reaction between the rocks and cement matrix can enhance the bond characteristics for HS/HPC.

2.2 Mix Proportioning Guidelines for Optimization of HS/HPC

In the development of mix proportions for HS/HPC, there are basic guidelines, which can be applied to optimize each of the materials selected. The exact proportions are dependent on the chemical and physical properties of the constituents.

2.2.1 Required Concrete Strength

The initial step in the proportioning of a HS/HPC mix is to determine the required strength, the age at which the concrete strength should be achieved, and the manner in which the specimens will be tested.

2.2.1.1 Test Age. High strength concrete generally has a high early strength, as well as significant strength gain at later ages, particularly when mineral admixtures are used. Myers and Carrasquillo [1997] have shown that HS/HPC mix designs with a 35% Class C fly ash replacement can experience a fifteen percent strength gain from 28 to 56 days. Therefore, it is reasonable to specify a later age for acceptance such as 56 or 90 days unless construction loads require the design strength at an earlier time. Traditionally, a 28 day acceptance criteria for design strength is specified for both precast and cast-in-place (CIP) concrete by most design engineers. It is important to note that in many applications a later age acceptance criteria imposes no additional restrictions or detriment for a fabricator or contractor. Production and construction sequences can typically be adjusted such that a later test age does not impact or reduce productivity. Additionally, a later test age may be beneficial to the concrete producer in two ways. Firstly, a later test age may allow for more efficient use of materials and thereby result in reduced material and construction costs. Secondly, production concerns may be lessened regarding achieving higher end strengths which are typical for the primary load resisting elements such as columns, piers, and beams.

2.2.1.2 Laboratory Versus Field Test Results. Test results obtained from laboratory trial mixes are generally ten percent higher than those obtained in the field for identical mix proportions [Cook, 1980]. Therefore, if laboratory trial mixes are to be used for strength evaluation, the strength achieved by these mixes should be a minimum of ten percent higher than those desired in the field. A more accurate and cost effective approach is to investigate the actual strength loss associated with a mix design in the field prior to production. Once a mix design has been optimized in the laboratory, conduct a plant trial mix phase to investigate the concrete properties produced under field conditions. This process is schematically represented in Figure 2.5.

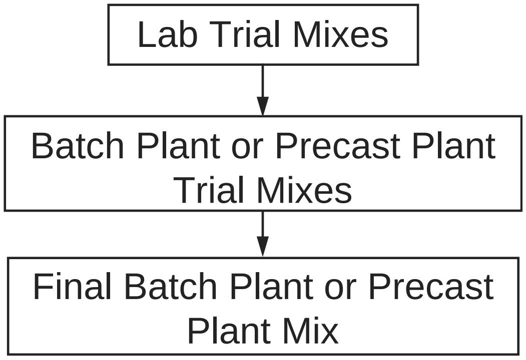

Figure 2.5: QC/QA mix design evolution

This process not only indicates what can be anticipated under field conditions, but also allows plant personnel the opportunity to gain experience with production of the mix design. This procedure also permits the opportunity to revise and re-batch mix designs in the laboratory if plant trial mixes are excessively high or low in strength.

2.2.1.3 Curing and Strength Development. The strength development with time is a function of the curing techniques and constituent materials. Curing may be defined as the process of maintaining a satisfactory moisture content and a favorable temperature in concrete during the hydration period of cementitious materials so that desired properties of the concrete can be developed [Mehta, 1983]. Primary curing methods include water curing and sealed curing. Water curing, either by ponding, spraying, or sprinkling, supplies additional moisture to the concrete surface and assists in preventing moisture loss. Sealed curing, either by plastic sheeting, waterproof paper, or curing membranes, is applied to solely prevent moisture loss from the concrete. Special curing situations may be required for hot-weather, cold-weather, and mass concrete. Precast/prestressed concrete may require curing at elevated temperatures through steam curing to satisfy release strengths. Table 2.1 illustrates the effect of limited moist curing on the development of compressive strength for a conventional concrete mix design at 180 days.

An adequate supply of moisture is necessary to ensure that hydration is sufficient to reduce porosity to a level such that a desired strength and durability can be attained.

Table 2.1: Influence of Moist Curing on Strength Development [Mindness, 1981]

Curing Condition of Specimen	**Relative Strength at 180 Days**
Continuous Moist Curing (Control Specimen)	1.00
28 Days Moist Curing followed by Lab Air Curing	0.91
14 Days Moist Curing followed by Lab Air Curing	0.85
7 Days Moist Curing followed by Lab Air Curing	0.71
3 Days Moist Curing followed by Lab Air Curing	0.62
Stored Continuous in Laboratory Air	0.43

In the case of HS/HPC mixes with low w/cm ratios, proper curing techniques play a very important role in strength development. There is enough water in concrete to ensure complete hydration without additional water being supplied if the w/cm ratio is 0.42 or greater [Mindness, 1981]. Below this value, self-desiccation occurs preventing further hydration unless water is supplied externally. This reduction of water stops hydration and arrests the strength development. Hydration cannot occur when the vapor pressure in the capillary pores fall below eighty percent relative humidity [Mehta, 1983]. As a result, moist curing is essential for strength development of concretes with low w/cm ratios while sealing is usually adequate for concretes with higher w/cm ratios due to the availability of water within the mix to develop complete hydration. According to Carrasquillo [1981], high strength concretes shows a larger reduction in compressive strength than conventional concretes when allowed to dry before completion of curing. Experts [Killoh, Vandewalle, Thomas (ACI SP)] generally agree that fly ash concretes are more sensitive to poor curing. This sensitivity increases with increasing fly ash content since the fly ash relies on the presence of CH for the pozzolanic reaction to occur. This is similar to cement hydration in that pozzolanic reaction requires a minimum vapor pressure of eighty percent relative humidity. Therefore, longer curing periods are needed for fly ash concrete to exhibit similar strength development to that of control mixes.

One area of construction in the United States in which inspection agencies and contractors have not placed a proper emphasis is in proper curing techniques particularly when strength requirements have been satisfied. Proper curing is one of the most inexpensive means in which not only the later age strength gain of all concretes can be improved, but more importantly can improve the long term durability and reduce the maintenance costs of a structure. Aitin [1994] and many others have concluded that the effect of moist curing is more pronounced on concretes with lower w/cm ratios. More attention must be paid to curing for HS/HPC including concrete, which is exposed to the environment where durability is an important consideration.

2.2.2 Water to Cementitious Ratio

The production of high strength /high performance concrete requires the use of low water to cementitious material ratios. In order to produce concrete with 28 day compressive strengths ranging from 41.4 MPa (6,000 psi) to 96.5 MPa (14,000 psi), a w/cm ratio in the range of 0.25 to 0.52 is required by weight. In addition, a HRWR is required when the very low w/cm ratios are used to produce HS/HPC.

2.2.3 Cement

The cement selected for the production of HS/HPC should have good strength producing properties. The fact that cements produced at different plants that meet the same ASTM specification for a given type of cement does not mean that concretes produced with each of the different brand cements will perform similarly. It is difficult to predict the interaction of a particular cement with other constituents within a mix design. As Figure 2.6 illustrates, concretes produced with different brands cements can have significantly different compressive strengths. For this reason, trial mixes varying locally available cements is suggested to investigate which cement produces optimum strength and thereby the most cost effective mix design.

An ASTM Type III cement should only be specified where early age strength gain is critical as is the case with many precast/prestressed elements. A Type III cement does not provide the same beneficial later age strength gain characteristics which is typical of Type I and II cements. Additionally, Type III cements generally experience higher concrete temperatures during hydration due to the higher blaine (fineness) of the cement particles. HS/HPC mixes in general develop higher concrete temperatures due to the high cement contents which typically vary from 390 to 558 kg/m^3 (658 to 940 lbs/cy). The use of coarser ground cements can help control the concrete temperature rise during hydration, but may also result in incomplete hydration due to the larger particle size. A good balance between these two concerns has been to use a mineral admixture such as a fly ash as a replacement material which can not only be used to reduce the concrete temperature during hydration but also benefit the ultimate strength capacity of the mix design.

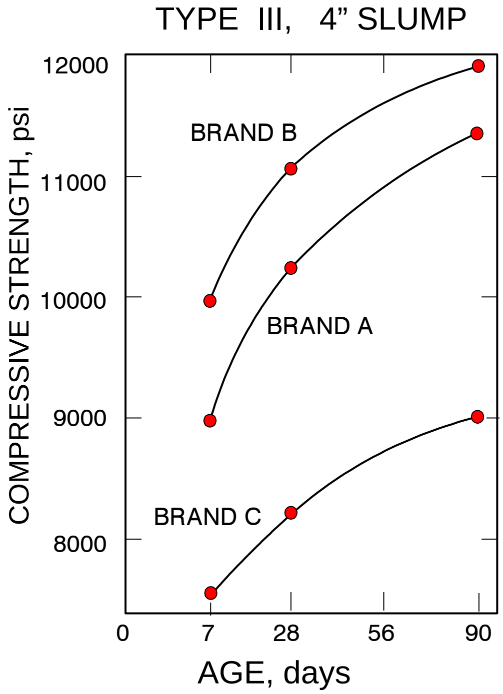

Figure 2.6: Cement brand variation versus compressive strength [Myers, 1998]

Trial mixes are required to determine the optimum cement content of a HS/HPC mix. The optimum cement content is the content in excess of which further addition of cement does not result in increased strength, and corresponds to the point at which all aggregates are completely surrounded by cement particles. Figure 2.7 illustrates this optimum cement content concept and how the aggregate type and surface texture might affect it. For example, the 13 mm (0.5 in) limestone aggregate has a rough surface texture and therefore a higher cement demand for a given aggregate content when compared to the smooth textured river gravel aggregate. In this case, the optimum cement content is higher for the limestone aggregate based on its surface texture, shape, and size.

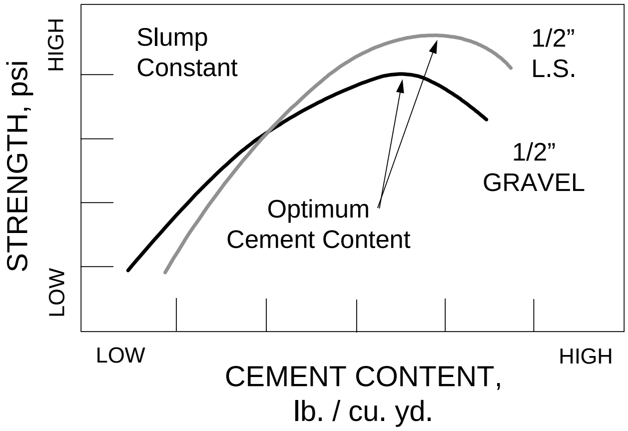

Figure 2.7: Optimum cement content for two aggregates [Myers, 1998]

2.2.4 Mineral Admixtures

The rates of addition of mineral admixtures are different for each type. ACI Committee 201 has established some guidelines for the replacement of Portland cement with other cementitious materials as illustrated in Table 2.2.

Table 2.2: ACI 211 Guidelines for Portland Cement Replacement

Other Cementitious Material	**Portland Cement Replacement** Percent by Weight
Fly Ash	
Class F	15 - 25
Class C	20 - 35
Blast Furnace Slag	30 - 50

Silica fume at additional rates in the range of 7 to 15 percent by weight of cement has been used in the production of high strength concrete. No specific guidelines or recommendations are given in terms of an optimum percentage of replacement material to use. This may be determined through trial mixes until specification requirements are satisfied.

2.2.5 Coarse Aggregate Type

Of great importance is the selection of coarse aggregates for the use in the production of HS/HPC. Recommended guidelines for the selection of aggregates include aggregates with a maximum gradation size less than 25 mm (1 in.) with good compactability. Furthermore, crushed aggregates are better than smooth as discussed in Section 2.1.6. Because of the effect of surface area on the water requirement, coarser gradations result in the achievement of higher compressive strengths as a result of being able to reduce the amount of mixing water as illustrated in Figure 2.8. In addition, the use of lower percent voids coarse aggregates results in the production of concrete of higher compressive strength due to a lower water demand for a given workability.

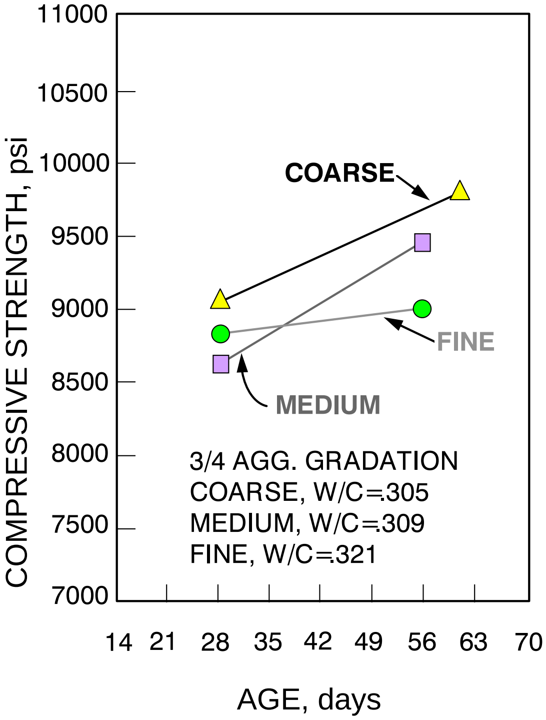

Figure 2.8: Aggregate gradation versus compressive strength [Myers, 1998]

2.2.6 Coarse Aggregate Content

Generally speaking, HS/HPC mixes contain a larger volume of coarse aggregate than conventional normal strength mixes. The higher aggregate content in HS/HPC mixes helps to reduce the water demand of the concrete and increase the elastic modulus of the concrete. Since many HS/HPC elements are thinner and have longer span lengths, the elastic modulus of the concrete becomes more critical in addressing serviceability requirements.

2.2.7 Fine Aggregate

Since HS/HPC mix designs have a high content of cementitious materials, the gradation of the fine aggregate is not so important as in conventional normal strength concrete. Recommendations for fine aggregates are those, which minimize the mixing water and provide good workability.

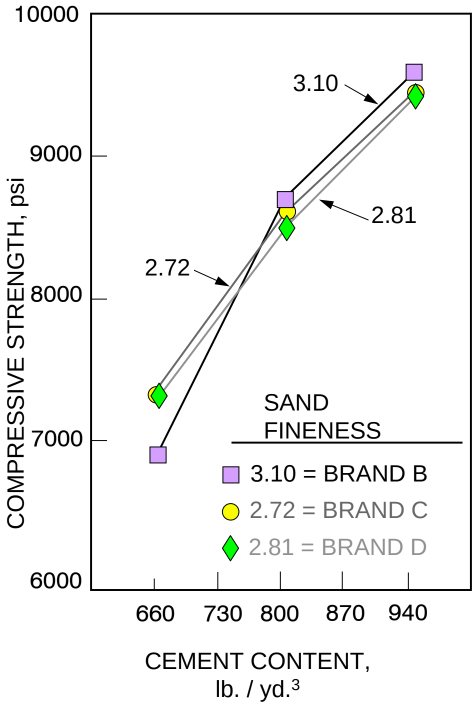

Figure 2.9: Fineness modulus variation versus compressive strength [Myers, 1998]

Generally sands meeting ASTM C-33 requirements and having a fineness modulus between 2.6 and 3.2 perform well in HS/HPC mixes. Figure 2.9 illustrates the low variability in compressive strength for sands with a moderate fineness modulus. Sands having a low fineness modulus may be too cohesive. Manufactured sands are generally not recommended for use in HS/HPC mixes due to their high absorption capacities. Fine aggregates with high absorption capacities makes it more difficult for a concrete producer to consistently produce a HS/HPC mix with a low standard deviation. This is caused by the variability of mixing water absorbed on a daily basis by the fine aggregate in conjunction with the low w/cm ratio.

2.2.8 Recommended Slump of Concrete

It is recommended that the slump of concrete produced without the addition of a mid-range water reducer or high range water reducer (HRWR) be 50 to 100 mm (2 to 4 in.). The minimum slump of concrete before the addition of a water reducer is recommended to be one inch. Requiring this one-inch slump prior to the addition of a water reducer ensures that the mix contains sufficient water to provide adequate workability. Satisfying this guideline will also reduce the potential of plastic shrinkage cracking. Furthermore, most HRWR manufacturers recommended that the slump of concrete after the addition of a HRWR be 200 to 250 mm (8 to 10 in.) as illustrated in Figure 2.10. This allows the HRWR to fully distribute the cement particles and maximize the strength potential of the concrete.

Before Addition of HRWR

After Addition of HRWR

Figure 2.10: Concrete slump before and after addition of HRWR [Myers, 1998]

2.2.9 Chemical Admixtures

In the production of HS/HPC, it is generally advantageous to use certain chemical admixtures such retarders, water reducers, and HRWRs. Dosage rate recommendations are provided in most cases by the manufacturer. However, the optimum dosage rate of any chemical admixture must be determined through field trial batches conducted under the expected job conditions. In general, the production of HPC will result in the use of higher than recommended dosages of chemical admixtures. As illustrated in Figure 2.11, the use of increasing dosages of chemical admixtures above the manufacturer recommended maximum dosage rate of 591 milliliters per 45.4 kilogram (20 oz. per 100 lb.) of cement resulted in higher concrete strengths without any detrimental effect on any of the performance characteristics of the concrete. This is based on research conducted at The University of Texas at Austin by Zakka and Carrasquillo [1989].

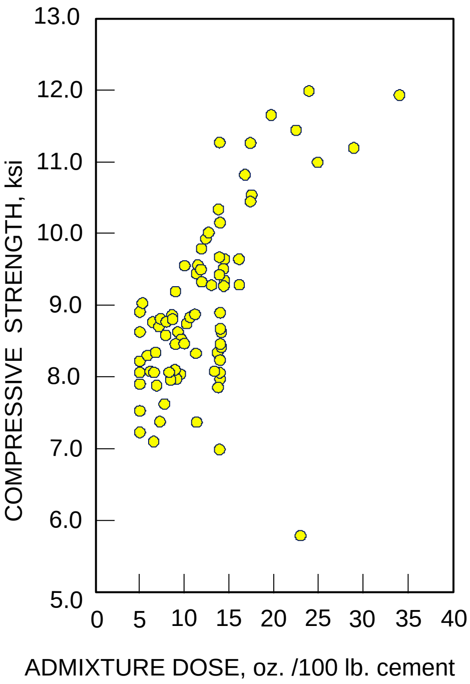

Figure 2.11: Dosage rate of HRWR effect on compressive strength [Zakka, 1989]

2.3 Durability of Concrete

Durability of concrete may be defined as the concretes ability to resist cracking and deterioration due to chemical and or physical attack. Concrete is inherently a durable material if properly designed and produced for the environment that it will be exposed to.

However, concrete is potentially vulnerable to attack in different exposures unless certain precautions are taken. Deterioration of concrete can be caused by the adverse performance of the aggregate, paste, or reinforcing due to chemical or physical attack. Although one particular environmental factor may initiate distress in a structure, other factors may contribute and aggravate the situation. One of the most difficult aspects of durability is predicting concrete behavior and performance decades into the future on the basis of short-term tests. Much of our understanding of durability has come through years of studies on actual field problems. First let us examine the primary causes of most durability related problems.

2.3.1 Damage and Deterioration of Concrete

The following section outlines several forms of chemical and physical attack including sulfate attack, freeze-thaw damage, alkali-aggregate attack, and corrosion of reinforcement.

2.3.1.1 Sulfate Attack. Sulfate attack is perhaps the most widespread form of chemical attack and is dependent on sulfates to occur. It is caused by the reaction of soluble sulfates with calcium hydroxide and calcium aluminate hydrate. The source of the soluble sulfates may include soils, seawater, groundwater, or materials selected and utilized in the production of cement and concrete. Sulfate attack is a complex process, which may involve a number of secondary processes although a correlation has been established between the C_3A content of a Portland cement and its susceptibility to sulfate attack. The major cause is sulfoaluminate corrosion [Hester, 1985] in which ettringite is formed from monosulfoaluminate as characterized by the following expression:

$$C_4ASH_{12} + 2CSH_2 + 16H \Rightarrow C_6AS_3H_{32} \quad \textbf{(2.5)}$$

This reaction is accompanied by a very large increase in solid volume which causes a volume expansion within the paste. The resulting internal stresses lead to cracking. Sulfoaluminate corrosion is initiated by a reaction described by gypsum corrosion. Only at high concentrations of sulfate ions (> 4,000 PPM) does gypsum corrosion directly contribute to concrete deterioration. Generally it exists at low levels and encourages the penetration of sulfate ions into the concrete and concentrates them into a form in which they can directly react with monosulfoaluminate. The use of mineral admixtures [Tikalsky, 1981] such as a Class F fly ash or blast furnace slag can improve sulfate resistance. Type II or V cements can also improve sulfate resistance by controlling the level of C_3A within the portland cement. HS/HPC's can also help control sulfate attack due to a reduced porosity resulting from the low w/cm ratio. It should be noted that this will only offset the initiation of damage and not prevent damage.

2.3.1.1.1 Delayed Ettringite Formation (Late Ettringite Formation). Delayed Ettringite Formation (DEF), often referred to as Late Ettringite Formation, is a form of sulfate attack, which is a recently discovered phenomenon. Within the last decade, DEF has been attributed to premature concrete deterioration in the United States and abroad. DEF involves the production of the compound ettringite in concrete months or years after casting. Ettringite naturally forms during the early hydration process of portland cement while the concrete is in the plastic state (See Section 2.1.1), but the natural reaction process of ettringite differs from that of DEF. DEF is characterized by the following reaction:

$$3CaO \cdot Al_2O_3 + 3(CaSO_4 \cdot 2H_2O) + 26H_2O \Rightarrow 3CaO \cdot Al_2O_3 \cdot 3CaSO_4 \cdot 32H_2O \quad \textbf{(2.6)}$$

The formation of ettringite, as illustrated in Figure 2.12, is an expansive reaction that can cause cracking when the concrete hardens or attains rigidity. Previous investigations of DEF have concluded that it may be caused by any of the following [Lawrence, Myers, and Carrasquillo, 1997; Hime, 1996]:

- Steam curing of the concrete at temperatures sufficient to decompose ettringite, which forms during the initial stages of the cement hydration.
- Heat developed in mass concrete above the decomposition temperature for ettringite generally considered to be above 71.1° Celsius (160° Fahrenheit). However, cases have been noted as low as 60° Celsius (140° Fahrenheit) Hime, 1996].
- Excessive amounts of sulfate in the clinker phase of Portland cement.
- Excessive amounts of sulfate in the cement.

Figure 2.12: Ettringite growth under SEM examination at X3000 magnification [Myers, 1998]

The term delayed or late ettringite formation is used to characterize that the ettringite has formed at a later stage when the concrete has hardened. As noted above, ettringite may decompose and reform at a later stage. This may occur due to excess sulfates in the cement composition. The development of DEF in the paste matrix proceeds in four stages.

1. Localized ettringite growth in situ or in nest.
2. A further growth of ettringite accompanied by characteristic crack patterns and formation of gaps around aggregate particles.
3. The further growth of ettringite or filling of ettringite within the developed cracks.

4. The further growth of ettringite or filling of ettringite within the developed gaps.

When the second stage of delayed ettringite formation is reached, severe cracking of the concrete may result. Severe concrete cracking, which was attributed to DEF, is illustrated in Figure 2.13. At this time, it is very difficult to address how large the problem of DEF could be. It has been suggested that previous cases of DEF attributed to ASR could have been misdiagnosed under low magnification petrography. Many designers such as TxDOT are just beginning to try to address in-service structures with this problem. Methods such as epoxy injection to seal any cracking are really not practical unless one can define the level of deterioration, which will take place. It certainly is not practical, if not impossible, to modify the exposure condition of a bridge structure to keep moisture away. To date, the industry has attempted to address this problem by some quality control measures such as recommending air entrainment for example.

Figure 2.13: Severe concrete cracking attributed to delayed ettringite formation [Myers, 1998]

Some contend [Hime, 1996] that the air voids provided by air-entraining can act as relief valves or reservoirs for ettringite to grow or expand into thereby reducing the concrete damage due to the expansive reaction. Figure 2.14 illustrates growth of ettringite in an air void. The use of air-entrained concrete might reduce damage due to DEF, however, it does little to prevent further concrete damage in severe exposures due to freeze-thaw. One of the conditions which has been reported to drastically influence the development of DEF is the curing temperature or conditions [Hime, 1996]. Reports throughout Europe recommended trying to maintain low curing temperatures without accelerated steam curing. In Germany, the specifications recommend concrete temperatures below 60°C (140°F). This may prevent “optimum” conditions for DEF to occur, but does not certainly guarantee that DEF will not develop as we have seen in several of the case studies [Lawrence, Myers, and Carrasquillo, 1997]

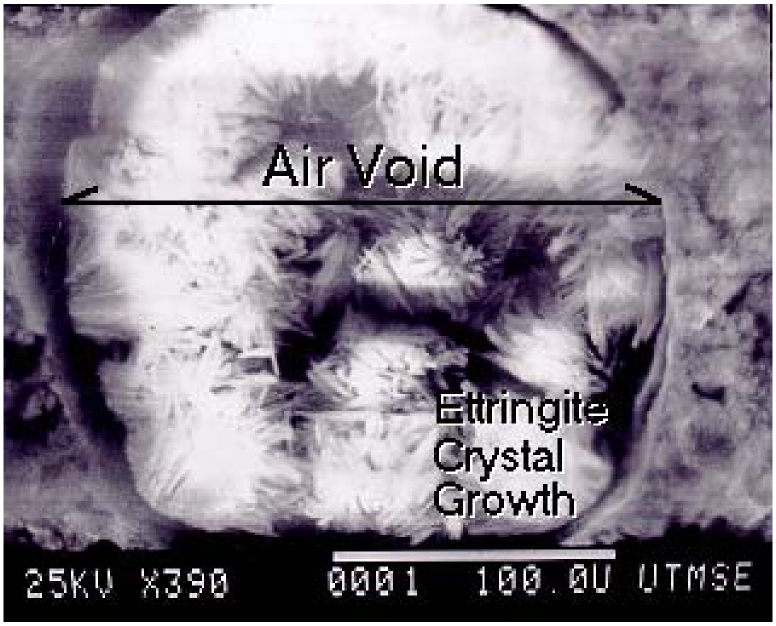

Figure 2.14: Ettringite growth in an air void at X390 magnification [Myers, 1998]

Naturally, one area, which we should closely monitor, is the sulfate contents in the clinker and cement. Currently, ASTM C150 limits the total sulfate content of the gypsum and clinker. However, the specification currently does not control the level of SO_3 within the clinker, which is critical in the development of DEF. Perhaps this is one area which should be more closely investigated.

2.3.1.2 Freeze-Thaw Damage. Frost damage to concrete is the result of successive freeze-thaw cycles of the cement paste and aggregate. Hardened cement paste is particularly susceptible to damage due to its high relative porosity. Fortunately, air entrainment, as discussed in Section 2.1.5, has proved to be an effective means of protecting concrete from frost attack. The number of freeze-thaw cycles to denote good performance has been defined by the measured change in length of a specimen at a specified number of cycles. ASTM C-666 *"Resistance of Concrete to Rapid Freezing and Thawing,"* has been used frequently to predict freeze-thaw performance in the field. Stark found a good correlation using a failure criterion of 0.035 percent length change at 350 cycles at 2 cycles per day [Stark, 1976]. Specimens, which have less than 0.035 percent dilation after 350 cycles generally, show good freeze-thaw performance in the field. However, it has been difficult to extrapolate the number of freeze thaw cycles in laboratory tests to the number of cycles in the field because the laboratory specimens are much smaller than actual field elements and do not experience similar cooling rates (gradients) to those in the field. Figure 2.15 illustrates the average number of freeze-thaw cycles per year in the State of Texas. In order for a freeze-thaw cycle to be detrimental to the concrete, the concrete must reach an internal temperature of at least -5°C (23°F) for a minimum of 6 hours and exceed a critical saturation threshold during this time period. An internal concrete temperature of -5°C (23°F) is equivalent to an ambient air temperature of -9°C (15°F) for concrete 75 mm (3 in.) below the surface. This is approximately the center of most bridge decks, which are 190 to 203 mm (7.5 to 8 in.) in thickness. Members, which are not subjected to becoming saturated above the critical saturation threshold of 91.7%, do not warrant air entrainment for freeze-thaw protection. These would include members such as beams, pier-caps or other substructure elements not subjected to a splash zone and protected from vertical saturation by a bridge deck or other element. In the context of a bridge, the only component, which generally warrants air entrainment are, the bridge decks themselves.

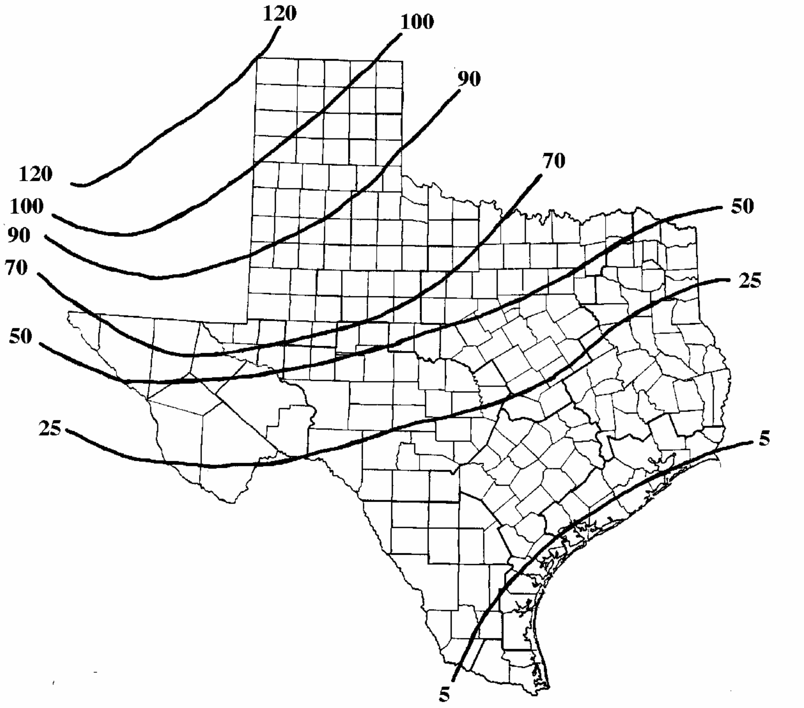

Figure 2.15: Number of freeze-thaw cycles per year [Visher, 1945]

Additionally, components such as a deck, which are open to air circulation on many sides generally, experience a higher number of freeze-thaw cycles. As an example, Figure 2.16 illustrates the number of moist freeze-thaw cycles below -9°C (15°F) ambient temperature in the State of Texas.

2.3.1.3 Alkali-Aggregate Reaction. The degradation of concrete due to alkali-aggregate reaction was identified for the first time in the United States in 1940 [Moranville-Regourd, 1992]. Disorders occur at various ages of structures from two to ten years or even at later-ages. The signs of distress may include the following [Moranville-Regourd, 1992]:

- Map cracking.
- Exudation of calcite and alkaline silicate gel.
- Pop-outs due to superficial reactive aggregates.
- Movements due to displacement of structures such as swelling of a dam crest.
- Coloration or Discoloration mainly along cracks.

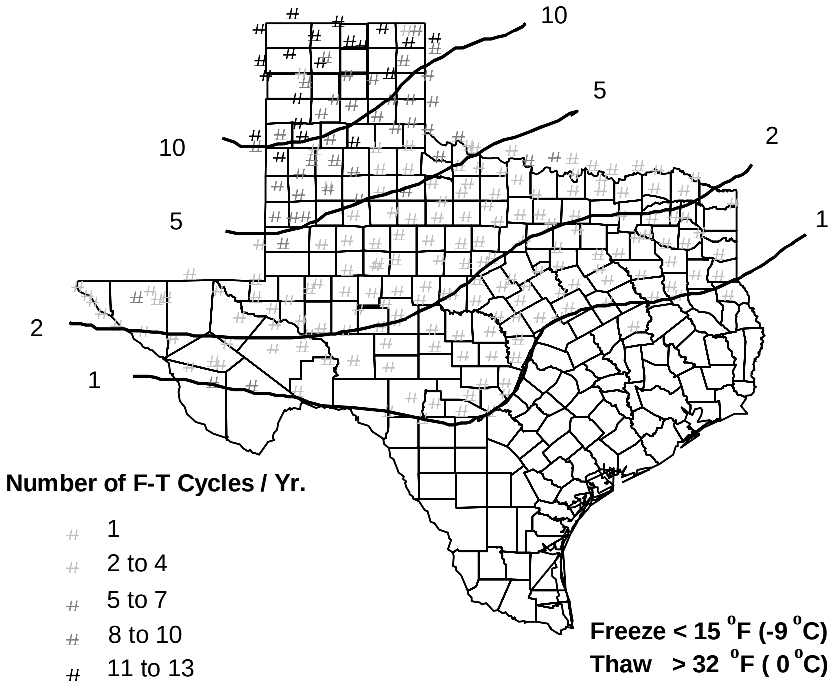

Figure 2.16: Effective freeze-thaw cycles per year [Watkins, 1997]

The main factors responsible for alkali-aggregate reactions are a humid environment, a high concentration of alkalis in the interstitial liquid phase of concrete, and alkali-reactive particles in the aggregates. Reactions, which are complex and heterogeneous, occur between the liquid localized in the capillary pores and solid particles irregularly distributed in the material. Chemical and physical processes interact in the formation of silicate gel which can swell and crack the concrete. The alkali-silica reaction is the most frequent case

2.3.1.3.1 Alkali-Silica Reaction. Alkali-silica Reaction (ASR) is a chemical reaction between the reactive siliceous components of an aggregate and the hydroxyl ions (OH^-) of the concrete pore solution. The product of this reaction, called alkali-silica gel (also referred to as ASR gel), can lead to expansion and cracking of the concrete. For ASR to occur the following preconditions must exist:

- The presence of Reactive Silica
- A High Alkalinity system composed of OH^- availability
- The presence of water or a relative humidity above 80%
- The presence of Calcium Hydroxide

Generally, silicas, which are poorly crystallized, or amorphous porous are the most reactive. However, case studies have shown that even dense crystalline silicas can cause ASR under unfavorable conditions of concrete production and use. The development of ASR is considered to occur in four stages [Mindness, 1981].

1. Initial alkaline depolymerization and dissolution of reactive silica
2. The formation of a hydrous alkali silicate gel
3. The attraction of water by the gel

4. The formation of a fluid sol (a dilute suspension of colloidal particles)

The comprehension of the factors affecting alkali-aggregate reaction can be used to control its effects in concrete. The following approaches can be used [Mindness, 1981]:

1. Control the pH in the concrete
2. Control of Alkali Concentrations
3. Control the amount of reactive silicas
4. Control of moisture
5. Alteration of alkali-silica gel

In addition, mineral admixtures are commonly known to control the expansions associated with alkali-aggregate reaction. Pozzolans react with the calcium hydroxide in the paste and thereby lowers the pH of the pore structure and concrete. Susceptible aggregates should be avoided based on service records and petrographic examinations. For exterior structures, it is impractical if not impossible to prevent moisture migration to a structure required for the reaction to precipitate and progress. However, low w/cm ratio concretes such as HS/HPC may help limit the supply of water needed to cause alkali-silica gel to swell due to very impermeable nature. Keep in mind, this approach will only slow down the reaction, not prevent it.

2.3.1.4 Corrosion of Reinforcement. The annual cost of corrosion in the United States has been estimated at $30 billion while corrosion of bridge decks alone has been estimated at $500 million [Fontana. 1986]. Corrosion not only represents a tremendous economic loss, but often times little is done to prevent or reduce it effects in concrete structures. By its very nature, concrete is a high alkaline environment, which protects and passivates the carbon steel reinforcement against corrosion. However, when concrete exists in an aggressive environment, this protection can be destroyed especially if the pH of the concrete reaches 11 or lower [Poston, 1985]. The passive iron oxide layer of the carbon steel reinforcement is destroyed when the pH is reduced below 11 causing the porous oxide layer (rust) to form during corrosion. The formation of this oxide layer (rust) on the surface of the carbon steel reinforcement exerts a force on the surrounding concrete initiating cracking and eventually spalling of the concrete. This critical reduction of pH occurs in the concrete when calcium hydroxide is converted to calcium carbonate (calcite) by atmospheric carbonation. The calcium hydroxide is responsible for maintaining the high pH in the cement paste and thereby the concrete. In well-cured concrete with a low w/cm ratio, the depth of the carbonated zone is unlikely to exceed 25 mm (1 in.), and therefore concrete cover of 25 to 40 mm (1 to 1.6 in.) over reinforcing bars should provide adequate protection from corrosion in most instances. Research studies have shown that low w/cm ratio concretes have an increased time to corrosion due to the reduced porosity over conventional concretes [Mindness, 1981].

Corrosion in concrete can take the form of a galvanic or an electrochemical reaction. For galvanic corrosion to occur, two dissimilar metals must come in electrical contact in the presence of oxygen and moisture to form an anode and cathode. Oxidation-reduction processes can then take place at the surface of the two metals, and under normal conditions iron becomes the anode and oxidation of the iron occurs. This anodic reaction is represented by the following reaction:

$$Fe \Rightarrow Fe^{++} + 2e^{-} \quad \textbf{(2.7)}$$

The electrons released by the anodic reaction are transported by either the steel rebars or the pore solution (electrolyte) to the cathode where an equivalent quantity of hydrogen ions forms a protective film around the steel. The destruction of the hydrogen film is achieved by the reduction of the oxygen. This cathodic reaction is represented by the following reaction:

$$O_2 + 2H_2O + 4e^- \Rightarrow 4OH^- \quad \textbf{(2.8)}$$

The hydroxide ions are carried back to the anode through the rebar where they will react with Fe^{++} to form ferrous hydroxide. In the presence of excess oxygen, the ferrous hydroxide is unstable and oxidizes further into ferric salt or red rust:

$$2Fe^{++} + 4OH^- \Rightarrow 2Fe(OH)_2 \quad \textbf{(2.9)}$$

$$2Fe(OH)_2 + \tfrac{1}{2}O_2 \Rightarrow H_2O\ Fe_2O_3 \bullet 2H_2O \quad \textbf{(2.10)}$$

This corrosion process in concrete is represented schematically in Figure 2.17.

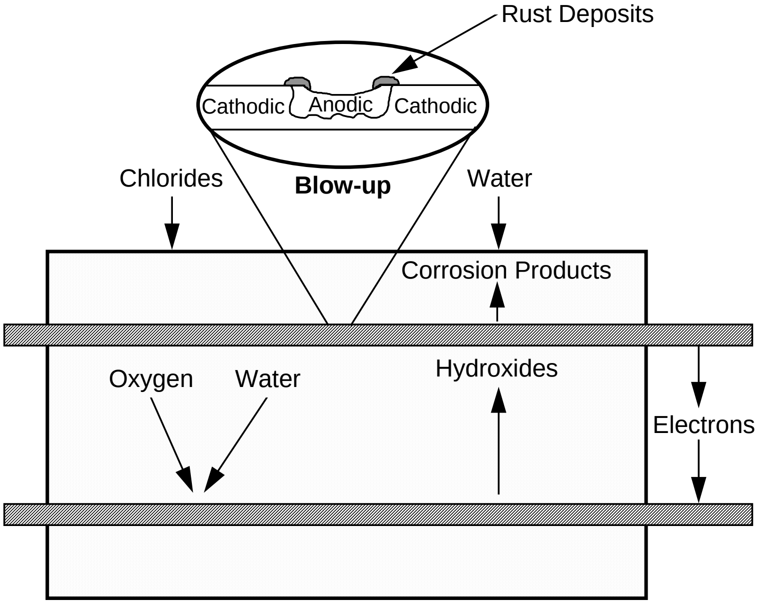

Figure 2.17: Schematic representation of the corrosion cell

In terms of corrosion protection, interruption of the chloride ions, oxygen, water, or electron flow will stop the entire corrosion process. The following corrosion protection systems approaches have been used to reduce or eliminate corrosion damage to the bridge reinforcing steel [Berke, 1988]:

1. Concrete Barrier System
2. Reinforcing Steel Coating
3. Chemical Stabilization
4. Surface Sealers
5. Electrochemical Systems

The most direct approach to preventing or reducing corrosion related damage is to prevent the chlorides in the concrete surface from reaching the reinforcing bars. This approach is represented by the use of overlay systems such as dense concrete, asphalt-based membranes, latex-modified, and polymer concrete overlays. Methods such as low w/cm ratio concretes, and mineral admixtures address the concrete in contact with the reinforcing while other methods include providing increased. Each of these methods have proven performance in the absence of surface cracking which allows for a more direct path for the chlorides to ingress toward the steel reinforcing.

The primary steel coating method specified over the last decade has been epoxy-coated reinforcing bars. Many studies have investigated epoxy-coated reinforcing [Babaei, 1989; Pfeifer, 1986; Sagues, 1990; Zayed, 1990; Clear, 1992] and have found the overall performance to be good. The major weakness of epoxy-coated bars is their susceptibility to surface coating damage. These problems are best avoided through care in fabrication and construction, repair of surface damage, and education for the installers. An estimated increase in 1 to 3 percent in the overall project costs can be anticipated when using epoxy-coated rebar.

Chemical stabilization additives such as calcium nitrite have been used to modify the environment within the concrete. Calcium nitrite, traditionally used as an accelerator, acts to stabilize the “passivating layer” that surrounds uncorroded steel in concrete. It does not influence the permeability of the concrete but rather it competes with the chloride to react with the steel and subsequently reduces the corrosion rate by “more than an order of magnitude” [60]. One of the drawbacks with calcium nitrite is that a retarder must be used in conjunction to offset its accelerating properties.

Sealer protection methods include silane and siloane sealers, high molecular weight methacrylates, and linseed oil. Successful sealers are those, which are “breathable” and allow water vapor to exit the concrete while preventing liquid water from penetrating. If water vapor cannot pass through a sealer to escape from the concrete, high vapor pressure can build up inside the concrete resulting in blistering and pealing of the sealer. These systems can be effective at preventing water and chloride migration, but often require re-application every three to five years increasing the maintenance costs of the structure.

Electrochemical systems such as cathodic protection have also been selected as a means of corrosion protection. Cathodic protection works by providing an external electric potential that opposes the “natural” corrosion cell [Sherman, 1993]. The electric potential established by the cathodic protection system prevents the flow of electrons associated with the reinforcement corrosion and thereby stops the corrosion process. Drawbacks of this system include the high initial expense and maintenance of the system, the additional dead load applied to the structure because of the system, the external power supply, which is required to operate the system, and the technical personnel, which are required to monitor the system. The system’s main merit is that it is the only corrosion protection method, which completely stops the corrosion process to date.

Perhaps the most cost effective system to combat corrosion in developing bridges for a 75 to 100 year design life is a combination of these systems. As described in subsequent sections of this dissertation, the long-term durability study of the North Concho River Overpass project will investigate the combination of epoxy-coated reinforcing with a low permeable low w/cm ratio HPC, and a surface sealer. This system will be compared to conventional concrete with and without epoxy-coated reinforcing.

2.3.2 Permeability of Concrete

Permeability has long been considered one of the most important aspects in durability performance since the permeability of the concrete controls the rate of entry of moisture that may contain aggressive chemicals and the movement of water during heating and freezing.

2.3.2.1 Mechanisms of Concrete Permeability. The permeability of concrete can be measured by determining the rate of flow through a concrete slab. The mechanisms involved in the permeability of concrete are dependent upon the penetrating solutions (water, fluids, gases, or ions), pressure head, temperature, and the initial state of the concrete. Whiting [1981] has listed seven stages to describe the movement of water through porous materials, which are as follows:

Stage 1: Absorption and Surface Diffusion.
Stage 2: Vapor Diffusion.
Stage 3: Film Transfer.
Stage 4: Surface Creep plus Vapor Diffusion.
Stage 5: Partially Saturated Liquid Flow.
Stage 6: Liquid Flow.
Stage 7: Ionic Diffusion.

The first two stages consist of initial surface absorption followed by water vapor movement which is diffusion controlled. Diffusion is mathematically expressed by Fick’s first law [Whiting, 1981] given in Equation 2.11:

$$J = -D\, dc/dx \quad \textbf{(2.11)}$$

where:
J = Flux ($g/cm^2 \cdot s$)
D = Diffusion coefficient (cm^2/s)
dc/dx = Concentration gradient ($g/cm^3/cm$)

As relative humidity increases, water begins to condense within the capillary spaces (Stage 3). Due to the pressure differential across the meniscus in the capillary, the resulting force induces a flow through the capillary, the rate of which is given by Washburn’s Equation [Whiting, 1981] as expressed in Equation 2.12:

$$v = (rV_L/4dn) \cos\theta \quad \textbf{(2.12)}$$

where:
v = Flow rate (cm/s)
r = Capillary radius (cm)
V_L = Surface tension (Pa•cm)
d = Depth of penetration (cm)
n = Fluid viscosity (Pa•s)
θ = Contact angle

Upon complete saturation of the pore system (Stage 6), water flows as a fluid governed by Darcy’s Law [Whiting, 1981] expressed in Equation 2.13:

$$Q = -KA\, \Delta h/L \quad \textbf{(2.13)}$$

where: Q = Volume outflow (cm^3/s)
A = Area (cm^2)
Δh = Fluid head (cm)
L = Path length (cm)
K = Permeability constant (cm/s)

Chloride ions and other ionic species can migrate through free water within the concrete pore structure. This phenomenon may occur due to diffusion at low velocity due to ionic interaction with the electric double layer on the cement paste surface during Stages 3 and 4 or more effectively during Stage 7 in the fully saturated state. The diffusion process of an ionic species into a porous material is altered when an electric potential is applied across an electrolytic solution [Touma, 1997]. Ions will migrate towards the opposing sign electrode with an ionic mobility (μ) given by the following expression:

$$\mu = x/t(dE/dx) \quad \textbf{(2.14)}$$

where: μ = Ionic mobility ($cm^2/V{\bullet}s$)
x = Distance (cm)
t = Time (s)
dE/dx = Electric field strength (V/cm)

2.3.2.2 Effect of W/Cm Ratio on Permeability. The single parameter, which has the largest influence on durability, is the water-to-cementitious ratio of the concrete [Mindness, 1981]. As the w/cm ratio is decreased, the porosity of the paste is decreased resulting in a more impermeable concrete. In fact the w/cm ratio plays a dual role in concrete durability. The resulting increase in strength due to a lower w/cm ratio also improves the concretes resistance to cracking from the internal stresses that may be generated by adverse reactions. The permeability coefficient, K, is dependent upon the w/cm ratio, the age of the paste, and the capillary porosity. According to Mindness [1981], the interconnecting network of capillary pores is what governs the permeability of the cement paste. As hydration proceeds, the formation of C-S-H breaks the capillary network and blocks the interconnected pores resulting in a decrease in K and in the concrete permeability. Table 2.3 illustrates the curing time required to produce a discontinuous system of capillaries. For a fixed w/cm ratio, the permeability coefficient, K, decreases and the capillary pores become more discontinuous as the cement paste age increases as illustrated in Table 2.4.

Table 2.3: Curing Time Required to
Produce a Discontinuous System of Capillaries [Mindness (1981)]

W/Cm Ratio	Curing Time (days)*
0.40	3
0.45	7
0.50	28
0.60	180
0.70	365
> 0.70	Not Possible

* Continuous Moist Curing

Table 2.4: Effect of Age of Cement Paste on
Its Permeability Coefficient (W/Cm = 0.51) [Mindness, 1981]

Age (days)	**Kp (m/s)**	
Fresh Paste	1E-05	Independent of W/Cm Ratio
1	1E-08	
3	1E-09	
4	1E-10	Capillary Pores Interconnected
7	1E-11	
14	1E-12	
28	1E-13	
100	1E-16	Capillary Pores Discontinuous
240	1E-18	

The capillary pores are the smallest at complete hydration (w/cm = 0.30) as illustrated previously in Figure 2.3. By their very nature, HS/HPC's are very durable concretes with generally very low permeability. The w/cm ratio selected (typically 0.27 to 0.40) to develop the high strengths are often very low resulting in discontinuous capillary systems at very early ages (less than 3 days). In fact, in precast / prestressed concrete where very high early strengths are required for release of the prestressing strands, a discontinuous capillary system occurs within the first 24 hours when the majority of the cement hydration occurs. This coupled with the prestressing forces applied which reduces any crack widths explains the excellent durability performance of precast/prestressed elements over the years. Neville [1996] also illustrates in Figure 2.18 how the permeability coefficient increases with an increase in the w/cm ratio. It may be inferred from this discussion that one of the most significant means to impact the durability performance of a mix design is the w/cm ratio.

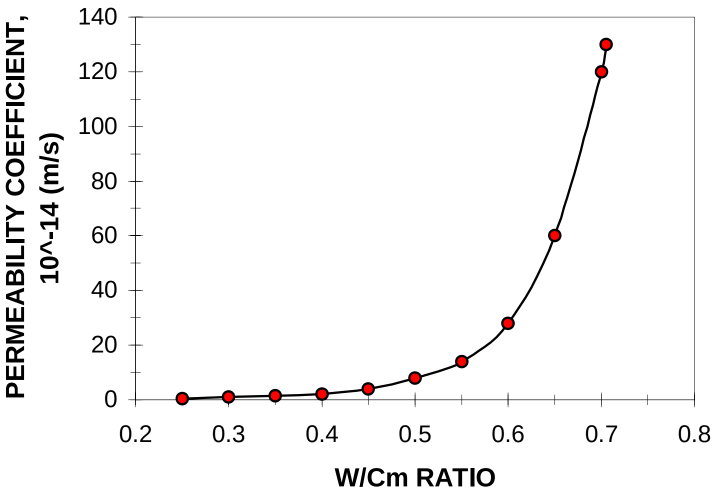

Figure 2.18: Effect of water-to-cement ratio
on the permeability of concrete [Neville, 1996]

2.3.2.3 Effect of Curing and Concrete Temperature on Permeability. Curing of concrete is a procedure used for promoting the hydration of cement and is not only used to control the temperature and moisture diffusion from and into concrete, but also to provide the necessary environment for complete hydration to occur. As previously discussed in Section 2.2.1.3, moist curing not only significantly influences the strength development, but also impacts the permeability of the concrete. The longer the moist curing period, the higher the strength development and the lower the permeability [63]. The curing temperature has also been reported to influence the pore size distribution of a cement paste. According to Young [1988], at higher curing temperatures there is an increase in the volume of large pores, which increases the permeability of the cement paste. The influence of moist curing and concrete temperatures on permeability is further investigated in Chapters Six and Eight of this dissertation.

2.3.2.4 Effect of Coarse Aggregates on Permeability. The selection of coarse aggregates also plays a role on the permeability of concrete. The use of highly porous aggregates will increase the permeability of the concrete because substances can flow more easily through the aggregate pores than through the smaller pores of the cement paste [Neville, 1996; Tia, 1992]. Many soft limestones, which are high in calcite, are generally considered porous. Many of these limestones can be found in south Texas and throughout parts of Mexico. Low permeable or non-porous hard dense aggregates such as river gravels will reduce the effective area over which substance flow can take place and therefore increase the effective flow path length. As a result, the permeability of a concrete will test lower when compared to a bulk cement paste with the same w/cm ratio and degree of maturity [Neville, 1996]. However, Metha [1986] indicated that in practice the permeability of concrete could exceed that of a cement paste with the same w/cm ratio due to the microstructure of the transition zones and the bleed water, which is trapped under the coarse aggregate particles. This bleed water can result in regions of locally high w/cm ratios resulting in additional calcium hydroxide crystal growth. The formation of new hydration products may result in microscopic transition zone cracking which can facilitate the formation of an interconnected capillary network increasing the permeability of the system [65]. As discussed in Section 2.1.2, the transition zones are quite different for HS/HPC when compared to conventional concretes. Microcracking in the transitions zones is often not an issue for HS/HPC's since the transition zones are not the "weak link" and microcracking does not occur at low to mid range stress levels which may be the case in conventional concretes. The selection of aggregates for a mix design is an important constituent where permeability is considered an important parameter of concrete performance.

2.3.2.5 Effect of Fly Ash on Permeability. Several studies have demonstrated that the incorporation of fly ash in the concrete matrix will reduce its total porosity and result in a finer pore structure compared to the matrix without any fly ash [68,69]. Other studies have suggested that the pozzolanic reaction of the fly ash has the tendency to break the interconnected pore system more readily [Marsh, 1985]. Hooton at the University of Toronto among others [Haque, 1992] contends that the fly ash binds a significant amount of the free chloride ions, which can ingress into the concrete from the surface. The binding of these chloride ions reduces the amount of free chloride ions, which are available to reach the level of the reinforcing steel to initiate corrosion.

Due to the strength gain characteristics with time of mix designs including fly ash, the permeability is greatly affected by the curing process. Studies at the University of Texas at Austin by Tikalsky [1989] have shown that the use of fly ashes increases the concrete permeability at early ages, but improves it at later ages. This is due to the slow process by which the pozzolanic reaction occurs.

2.3.2.6 Effect of Air Entrainment on Permeability. As discussed in Section 2.3.2.2, a continuous capillary system will result in a higher permeability, while a discontinuous system will prevent the diffusion of fluids into the concrete and result in a lower permeability. In conventional concretes, an adequately designed air entrained system will create discontinuities in the capillary pores within the paste and result in decreased permeability. However, research studies have shown [Ernzen, 1992;Touma 1997] that for HS/HPC's, the addition of air entrainment does not drastically affect the permeability of the concrete. HS/HPC's typically have a very low capillary porosity due to their low w/cm ratio as previously illustrated in Figure 2.3. Since a capillary pore system is very limited at best in HS/HPC's, the addition of an air void system does not create any new discontinuities within the system to reduce the permeability. It should also be noted that unless the air void system is properly distributed, it could result in creating a continuous system of voids, which will increase the permeability of the concrete. The presence of entrained air will also reduce bleeding water and increase the workability of the concrete due to its spherical shape. As a result, a lower w/cm ratio is allowed which results in a lower permeability [Neville, 1996].

2.3.2.7 Effect of HRWR on Permeability. The use of HRWRs has been shown to reduce the permeability of concrete by allowing the reduction in the w/cm ratio and the distribution of cement particles. The HRWR helps disperse the cement grains more uniformly within the paste resulting in a pore structure with fewer coarse pores. This results in a reduced permeability. However, research conducted at the University of Texas at Austin [Zakka, 1989] has shown that the use of a HRWR can increase the permeability of the concrete when compared to a control mix without a HRWR during hot weather concreting under certain conditions. The research was conducted on bridge decks, which were cast during both cold and hot weather. No associated increase was noted during the cold weather placement. The increase in permeability during the hot weather placement was attributed to difficulty in finishing. The problems associated with finishing the low w/cm ratio mix resulted in deep surface cracks and thereby a more permeable deck.

2.3.3 Freeze-Thaw Resistance of Concrete

Section 2.3.1.2 introduced and discussed the mechanism of freeze-thaw damage. To date, standard freeze-thaw tests using ASTM C666 / AASHTO T161 have been used to predict the freeze-thaw performance of concrete. A parameter known as the durability factor, DF, was introduced to characterize concrete performance. The DF is expressed in the following expression:

$$\mathrm{DF} = \frac{(\%\ \textbf{\textit{of Initial Modulus}})(\#\,\textbf{\textit{Cycles}})}{(\textbf{\textit{Duration of Test}})} \times 100 \quad \textbf{(2.15)}$$

The relative modulus is the dynamic modulus, determined using ASTM C215, at a given number of cycles divided by the original dynamic modulus of the specimen before testing. The duration of the test is typically 300 cycles.

2.3.3.1 Factors Affecting Freeze-Thaw Resistance. There are two conditions that must be present for freezing and thawing damage to be a concern as discussed in Section 2.3.1.2. Concrete must undergo sufficient freezing and thawing temperature cycles in the present of adequate moisture. If either of these two conditions are not met, no damage will occur. Moisture is present in concrete in one three forms or transitions of these forms. These include chemically bonded water, adsorbed water, or capillary pore water. The form of moisture within the concrete determines its freezing properties. Chemically bonded water or interlayer water is water that is chemically bonded to the C-S-H lattice. Adsorbed water is a film of non-freezable water adsorbed on the C-S-H particles which is physically bound on or between surfaces by adsorptive forces. Adsorbed water can become freezable if it desorbs to become capillary water. Capillary pore water is freezable water that is located in the capillary pores of the concrete between hydrated cement grains or in the capillary pores of the aggregate transition zones. It is free to move throughout the pore system and similar to bulk water. However, the freezing point and vapor pressure of the capillary pore water is affected by the size of the pore in which it is located and the concentration of alkalis.

De-icing chemicals are also an important criteria to consider since it has been known to greatly accelerate the amount of damage in concrete. The use of de-icing salts on exposed surfaces can create freeze-thaw effects by changing the freezing point of the water within the concrete. The de-icing agents cause the ice to melt at the surface of the concrete and thawed water to pond on the surface. The thawed water at the surface of the concrete can now saturate into the concrete which can create a depression in the freezing point to as low as -50°C (-58°F) [Watkins, 1997]. Damage caused from de-icing salts is typically in the form of popouts or scaling. The chlorides present in the de-icing chemicals can also lead to corrosion of the reinforcing which manifests itself as severe spalling and cracking of the concrete.

The size of the concrete mass and location in the structure affect how many times the element will freeze in a given winter. Elements with large dimensions and a large volume make it less susceptible to freeze-thaw cycles than concrete members with smaller properties due to the insulating properties of the larger sections. Concrete structures freeze from the outside to the inside. Structure which are open to air flow or circulation on many sides will generally experience a higher number of freeze thaw cycles. A faster rate of freezing will cause more damage since the pressure from the water freezing builds very quickly before expanding water can migrate to relief voids. The magnitude of hydraulic pressure in the paste is affected by the permeability of the paste, the distance to the nearest unfilled void, the rate of freezing, and the degree of saturation.

2.3.3.2 Recommendations for Freeze-Thaw Resistant Concrete In Texas. A recent research study undertaken by Watkins [1997] at the University of Texas provides recommendations for freeze-thaw resistant concrete based on exposure condition and member types. The results from the analysis of member exposure conditions based on the member's susceptibility to moisture, freeze-thaw cycles, and de-icing salts are presented in Table 2.5. The exposure conditions have been broken down into one of three exposures (mild, moderate, and severe) based on the previous criteria.

Similarly, Watkins [1997] has ranked the environmental conditions in Texas as severe, moderate, or mild based on the combined effects of freeze-thaw cycles, moisture, and de-icing chemicals. Taking into account both the environmental conditions and the member exposure, a recommendation on the amount of air entrainment required for freeze-thaw durability was developed in this study. Table 2.6 summarizes these recommendations based on environmental and member exposure conditions. Table 2.7 presents the total air requirement based on the maximum aggregate size of the mix design.

Table 2.5: Member Exposure Condition Ratings [Watkins, 1997]

Exposure Condition	**Member / Element**	
Mild Exposure	• Anchors • Back-up Walls • Culverts • Drilled Shafts • Driveways • Headwalls • Manholes • Prestressed Concrete Beams	• Prestressed Boxes • Prestressed Piling • Retards • Railroad Structures • Slurry Shafts • Road Signs & Anchors • Wing Walls
Moderate Exposure	• Bridge Piers* • Bridge Railing* • Bridge Substructure • Cast-in-place Traffic Barriers • Columns	• Drilled Shafts in Water* • Inlets • Precast Traffic Barriers* • Riprap
Severe Exposure	• Approach Slabs • Bents* • Bridge Slabs* • Concrete Overlay • Concrete Pavement* • Curbs	• Dense Concrete Overlay • Direct Traffic Culvert • Gutters • Seal Concrete • Sidewalks

* Indicates that these members are currently required by TxDOT to have air entrainment [73]

Table 2.6: Average Total Air Requirements Based on
Exposure Conditions [Watkins, 1997]

Member	**Environmental Exposure**		
Exposure	**Mild**	**Moderate**	**Severe**
Mild	None	None	None
Moderate	None	Medium Air 4.0% to 6.0%	Maximum Air 5.0% to 8.0%
Severe	None	Maximum Air 5.0% to 8.0%	Maximum Air 5.0% to 8.0%

Table 2.7: Recommended Average Total Air Content [Watkins, 1997]

Grade	**7 & 8**	**6**	**5**	**4**	**2 & 3**	**1**
Max Aggregate Size	3/8”	1/2”	3/4”	1”	1-1/2”	2”
Medium Air	6.0%	5.5%	5.0%	5.0%	4.5%	4.0%
Maximum Air	8.0%	7.0%	6.5%	6.0%	5.5%	5.0%

Conversion Factor: 1 inch = 25.4 mm

2.3.4 Abrasion Resistance of Concrete

Surface wear of concrete can take one of several forms. These forms of wear include cavitation, erosion, and abrasion. Both cavitation and erosion usually occur on dams, spillways, pipes, and tunnels where fluids are presents. Cavitation is caused by the sudden formation and collapse of low pressure bubbles in liquids flowing at high velocities [ACI 201.3R, 1982]. Erosion is caused by the action of abrasive materials carried by fluids. A third form of wear and most relevant to bridge decks is abrasion. Abrasion is the result of rubbing, scraping, skidding, or sliding of objects on concrete surfaces. Until the mid 1970’s, there was no specific standard test for determining the abrasion resistance of concrete. The American Society for Testing and Materials then adopted ASTM C779-93, *“Standard Test Method for Abrasion Resistance of Horizontal Concrete Surfaces.”* In 1980, ASTM C-944, *“Standard Test Method for Abrasion Resistance of Concrete or Motar Surfaces”* by the Rotating-Cutter Method was issued and has been successfully used as a quality control method for concrete used in highway structures subjected to traffic.

2.3.4.1 Factors Affecting Abrasion Resistance. The primary factors affecting the abrasion resistance of concrete are:

- Compressive Strength
- Aggregate Properties
- Surface Finishing
- Curing
- Use of Surface Hardeners or Toppings

Previous research has shown that the major factor influencing the abrasion resistance of concrete is the compressive strength. Air entrainment in concrete typically reduces the compressive strength and therefore the abrasion resistance. Backstrom and Witte [1951] investigated the effects of air entrainment on the abrasion resistance of concrete. Their test results revealed that for equal strengths, air entrainment concrete is as resistant as concrete without air entrainment. As the voids (water plus air) to cement ratio increases, both the compressive strength and abrasion resistance decreased as illustrated in Figure 2.20.

The abrasion resistance of aggregate is also important in determining the abrasion resistance of concrete [ACI 201.3R, 1982]. This is particularly true when an exposed aggregate surface is used. Aggregates, which are stiffer, are more wear resistance.

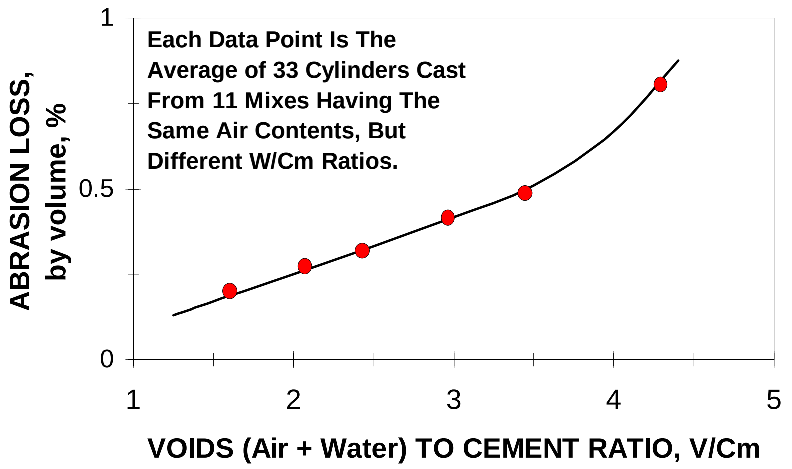

Figure 2.19: Void to cement ratio versus abrasion loss [37]

Proper finishing and curing significantly impact the abrasion resistance of concrete. In the case of conventional concrete, best results are obtained when finishing is delayed until all the bleed water has evaporated and the concrete has initially set. Fentress [Fentress, 1987] investigated the effect of finishing techniques and curing on the wear resistance of concrete from the same batch. Three finishing techniques were investigated including wood float, steel trowel, and hard steel trowel. The curing techniques included moist burlap, and curing compound at various stages. It can be seen from Figure 2.21 that when proper curing techniques are practiced in conjunction with a hardened finish, improved wear resistance results. Generally the longer wet mats and moist curing is specified, the better the wear resistance.

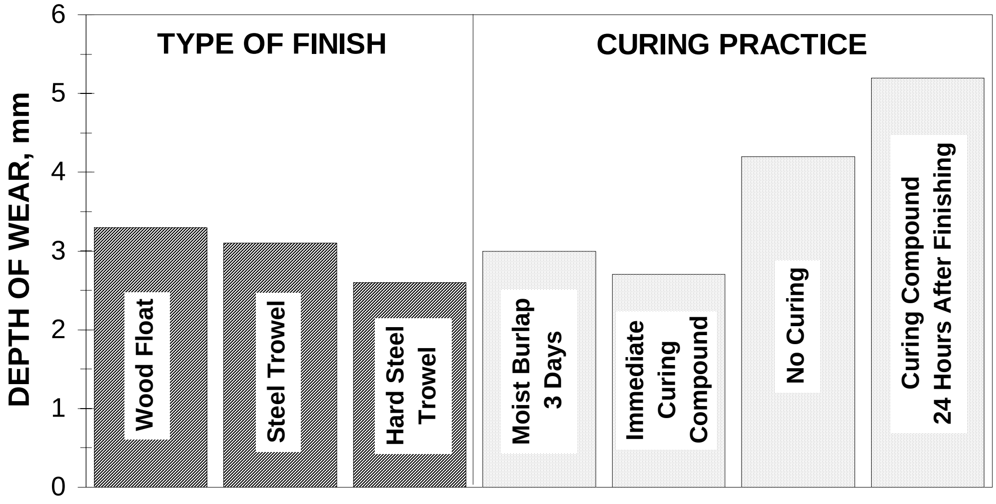

Figure 2.20: Influence of finish type and curing practice on wear resistance [Fentress, 1973]

The application of special toppings or the incorporation of fiber reinforcing has also been shown to improve the abrasion resistance of concrete [Hoff, 1987; Vondran, 1987]. Both Hoff and Vondran found that for concretes of equal strength, steel fiber reinforced concrete exhibited the most resistance to wear followed by polypropylene fiber reinforced concrete. Extensive research at The University of Texas at Austin [Hadchiti, 1981] has shown that the incorporation of fly ash replacement does not reduce or improve the wear resistance of the concrete. Concrete strength is the governing factor affecting the abrasion resistance of concrete rather than the material which makes up the cementitious fraction of the concrete as illustrated in Figure 2.22.

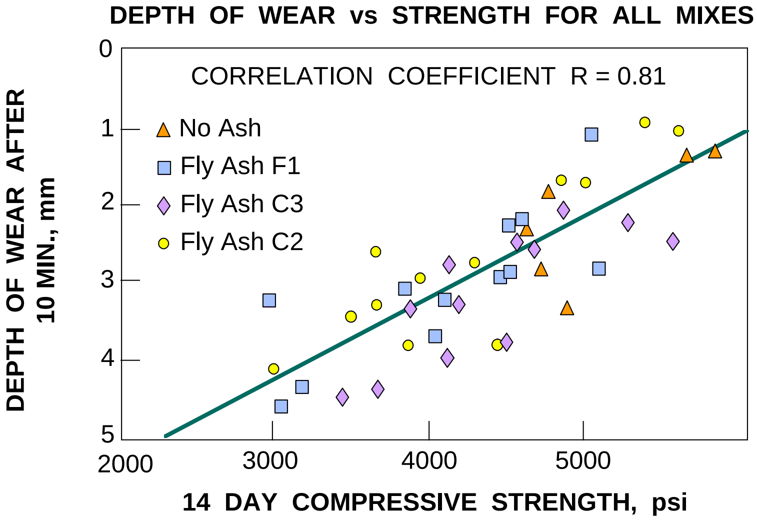

Figure 2.21: Depth of wear versus replacement type [Hadchiti, 1988]

One would expect that since the major factor influencing the abrasion resistance of concrete is the compressive strength, HS/HPCs would exhibit enhanced abrasion resistance over conventional concretes. This is indeed the case. High quality aggregates are traditionally used in HS/HPC mixes in order to develop the high strength characteristics which are desired. In addition, stiff aggregates are generally selected to satisfy elastic modulus requirements; all of which improve abrasion resistance. With respect to w/cm ratio and porosity, Almeida [1994] found that the abrasion resistance of HS/HPC varied inversely with w/cm ratio, cement paste volume, and porosity of concretes. He also showed that the use of a HRWR improved the abrasion resistance for a given mixture by 25 percent. Almeida concluded that the superplasticizing admixtures allowed a substantial reduction in the w/cm ratio and therefore a substantial improvement in the abrasion resistance of the concrete.

Following proper surface finishing and curing techniques can only improve the abrasion resistance of HS/HPC, just as the case with conventional concretes. However, there are some minor differences between the two types of concretes. Since bleed water is typically not a concern for low w/cm ratio concretes, the timing of surface finishing and techniques used are less critical when compared to conventional concretes. In fact some experts [44] feel that less finishing for HS/HPC's provides a reduced surface disruption and is actually better for the quality of the concrete.

Proper curing techniques are very critical for HS/HPC's. In climates such as Texas where environmental conditions with high temperatures, high winds, and low humidity often exist, surface moisture loss is always a concern. In this case, finishing should take place as soon as possible to avoid evaporation of surface moisture. Provisions for fogging should always be available when low w/cm ratio concretes are selected. According to Neville and Brooks [1987] HS/HPC should be exposed to curing earlier than conventional concrete, because surface hydration segments the pores preventing further benefit from prolonged curing. As curing water can not penetrate the concrete mass, it is not able to induce additional hydration. Moist curing of HS/HPC may not influence hydration as much as conventional concrete, but it does improve the quality of the concrete. It aids in keeping hydration temperatures down and thereby improving the long-term strength gain of the concrete.

2.3.4.2 Recommendations for Abrasion Resistant Concrete. To obtain abrasion resistance, the following measures should be followed for conventional concretes or high performance concretes with moderate w/cm ratios (0.40 to 0.50) [ACI 201.3R, 1982]:

1. The concrete should have adequate strength levels; 27.6 MPa (4,000 psi) minimum at time of exposure to services is recommended. This may be achieved through proper mix proportioning by keeping the w/cm ratio and air content low
2. The finishing operation of the concrete surface should be delayed until all the bleed water has evaporated and the concrete is stiff enough to withstand some pressure
3. Adequate curing should begin immediately after the finishing operation is completed and continued for a minimum of seven days

4. Where the concrete is likely to be subjected to excessive abrasion, the use of hard, tough aggregates or special topping may be recommended to lengthen the service life of the concrete

To obtain abrasion resistance, the following measures should be followed for high strength / high performance concretes with low w/cm ratios (< 0.40):

1. The concrete should have adequate strength levels; 27.6 MPa (4,000 psi) minimum at time of exposure to services is recommended
2. Proper fogging as required is recommended during concrete placement and finishing
3. The finishing operation of the concrete surface should occur as soon as possible. Excessive finishing is not recommended as it may adversely affect the top surface of the concrete
4. Adequate curing should begin immediately after the finishing operation is completed and continued for a minimum of ten days

2.3.5 Scaling Resistance of Concrete

Scaling occurs when the top surface of the concrete flakes or peels off. It is mainly caused by repeated freezing and thawing in the presence of deicing salts or chemicals. The scaling mechanism of concrete subjected to salt solution is very complex although there is a general consensus that the mechanism involved is mostly physical in nature rather than chemical. According to Mindness [1981], the consumption of heat required to melt ice when salt is applied causes a rapid drop in the temperature of the concrete just below the surface, which may cause damage either from the effects of rapid freezing or stress caused by differential thermal strains. The addition of free moisture now present at the surface of the concrete may encourage the growth of microscopic or macroscopic ice lenses near the surface, where ice formation can still occur. Osmosis pressure has also been suggested as a scaling mechanism [Hester, 1985]. When salt is used to melt ice, the salt solution slowly penetrates the concrete surface and fills the pores of the cement paste. The capillary pores which are filled much faster than the cement gel pores attain a higher salt concentration. Upon freezing, ice builds up in the capillary pore and the salt concentration of the unfrozen water is further increased. As the concentration of the solution keeps increasing, the capillary pores are transformed into osmotic pressure cells capable of attracting weaker solutions from the surrounding cement gel pores. This causes the capillaries to grow and exert pressures on the cement gel, which can eventually rupture. The larger the difference in concentration between the capillary pore solution and the cement gel pore solution, the greater the pressure exerted on the cement paste is. In the case of HS/HPC (w/cm ratio < 0.40), the capillary pore structure is discontinuous within three days after placement [Hester, 1985]. Since the capillary pore system is discontinuous at an early age and the differential in pore solutions would be reduced due to a lower porosity, HS/HPC's can be expected to demonstrate improved scaling resistance over conventional concretes when finished and cured under similar conditions.

Others such as Fagerlund [1975] suggest that deterioration by scaling could be the result of the combination of hydraulic and osmotic pressures. Upon cooling, ice formation takes first place in the coarser pores. This generates localized hydraulic pressures and triggers the pressures generated by both phenomena and it is influenced by the amounts of salts dissolved in the pore solution. The higher the salt concentration, the lower the amount of freezable water at a given temperature. The hydraulic pressure should therefore decrease with an increase in the salt concentration since less ice is formed while the osmotic pressures should increase with an increase in the salt concentration. While the imperfect understanding of mechanisms involved clearly underlines the very complex nature of the problem, many of the factors affecting scaling resistance are understood.

2.3.5.1 Factors Affecting Scaling Resistance. The primary factors affecting the scaling resistance of concrete are [Hadchiti, 1988; Marchand, 1994]:

- Materials.
- Mixture Characteristics.
- Curing and Curing Procedures.
- Use of Sealers.
- Aging Effects.
- Concentration of Salt Solution.
- Air Entrainment.

The materials selected for mix proportioning are essential in order to obtain proper scaling resistance. The use of good sound aggregates is necessary to ensure proper durability. The cement can also affect the scaling resistance. It has been found that the use of finer cements can improve the scaling resistance [48,49]. This can most likely be related to the reduction in the average size of the capillary pores that is observed from finer cements. Faster hydration rates due to finer hydration products or increased volume of cementitious materials also reduce the risks of surface damage. Fagerlund [49] also suggests that cements with low alkali / low C_3A contents exhibit reduced scaling. Fagerlund attributes this to the fact that high alkali / high C_3A cements can have detrimental effects on air entrainment. They can result in larger spacing factors for the entrained air bubbles. Air entrainment has proven to enhance the scaling resistance of concrete since it acts as a pressure relief point and provides a path for water osmosis. A tighter spacing factor can be expected to result in reduced damage. This is not to say that air entrainment by itself will always effectively prevent scaling. The best protection against scaling is reduced porosity [Hadchiti, 1988].

The most fundamental characteristic of any concrete mixture is the w/cm ratio. The ratio influences the porosity of the paste and thus many of the concrete properties including most notably the strength and durability. Most field and laboratory data show for normal strength concrete that as the w/cm ratio decreases, the scaling resistance increases [49]. Since HS/HPC generally have w/cm ratios in the 0.35 to 0.25 range, improved scaling resistance over traditional concretes can be expected. As the w/cm ratio decreases, so does the freezable water content. At a certain critical w/cm value for a given cement, air entrainment is not required for protection against freezing in the presence of deicer salts [Marchand, 1994].

2.3.5.2 Recommendations for Scaling Resistant Concrete. To obtain scaling resistance, the following measures should be followed for conventional concretes or high performance concretes:

1. Selection of good sound aggregates which have a documented proven performance. Generally, the selection of aggregates for HS/HPC mix designs is not as critical as conventional mix designs since good quality aggregates are required to meet the mechanical property requirements such as compressive strength
2. Proper and timely curing of the concrete will result in improved scaling resistance. Excessive finishing is not recommended as it may adversely affect the top surface of the concrete
3. Use of sealers or surface hardeners where applicable
4. The specification of air entrainment for conventional mix designs where strength gain is not critical

CHAPTER 3: RESEARCH PROGRAM

3.1 Experimental Program

3.1.1 Introduction

Two groups of concrete matrices were investigated. First group is designed to be high strength concrete (HSC) for bridge girder/deck applications, whereas the second was the representative of high performance concrete (HPC), which is mostly utilized in deck constructions. It is noteworthy to mention the concept of active and passive concrete for better understanding the preference of usage of HPC/HSC. Active concrete is concrete that will be exposed to and function in aggressive environments and the performance is measured by its potential for long-term durability; whereas the passive concrete is subject to mainly structural loads in a protected environment and the performance is primarily based on strength [Shilstone, 1993].

The matrix constituents used in this investigation included cementitious binder of Type I Portland cement, fine aggregate, coarse aggregate, tap water, ground granulated blast-furnace slag (GGBS), mineral admixture as Class F fly ash (FA), and chemical admixtures of HRWR and air entrainer. All of the materials used in this research consistent with those used by the local suppliers and approved by MODOT for use of Missouri Highway construction. The laboratory test involved around various mechanical tests, and durability tests. Since the durability of concrete including abrasion resistance, freezing & thawing resistance, and other forms of physical attack are largely influenced by the aggregate source, the aggregate type has been primary focus of this study along with the cementitious content and the air content. A representative HRWR meeting ASTM C494 has been selected for low w/c ratio concrete.

3.1.2 Materials

The course and fine aggregate were obtained from the local available sources. Representative samples from locally available aggregate sources as outlined in Table 3.1, have been selected for this study.

Table 3.1. Current Locally Available Missouri Aggregate Sources

	Aggregate Based Source	
Limestone	Dolomite Source	River Gravel Source
Bethany Falls LS	Bonne Terra Dolomite	Crowley Ridge Gravel
Burlington LS	Citter-Powell Dolomite	Osage River Gravel
Cedar Valley LS	Gasconade Dolomite	Meramec River Gravel
Plattin LS		
St. Louis LS		
Warsaw Limestone		

Aggregates that are similar in mineral and physical composition within a source have not been duplicated within the study. The locally available coarse aggregates had a maximum aggregate size of ¾ inches. The fineless module and the SSD specific gravities were 6.22, 6.43, and 6.47; 2.45, 2.73, and 2.63 lb/ft^3 for the Limestone, Dolomite, and

River (Missouri Creek) Gravel sources, respectively. The absorption rates of the aggregates sources of Limestone, Dolomite and River Gravel were 3.80%, 1.91%, and 0.41%, respectively.

The locally available fine aggregate is sand that has a fineness modulus of 2.11 and absorption percent of 2.58 with a SSD specific gravity of 2.54. The size distribution of the coarse and fine aggregates is shown in Table 3.2. The absorption tests were run according to the ASTM C127 and ASTM C128.

Table 3.2. Aggregate Grading

Sieve	**Coarse Aggregate**			**Fine Aggregate**
Size	Limestone	Dolomite	River Gravel	Sand
1 in.	100.00	100.00	100.00	100.00
3/4 in.	100.00	100.00	100.00	100.00
3/8 in.	61.00	44.50	37.50	100.00
#4	10.60	3.20	6.45	99.10
#8	3.00	2.25	2.90	90.90
#16	1.65	2.10	2.05	84.40
#30	1.25	2.00	1.75	75.50
#50	0.65	1.85	1.50	27.70
#100	0.35	1.70	1.20	1.30
Pan	0.00	0.00	0.00	0.00

The cementitious binder consists of hydraulic cement, Class C fly ash, and ground granulated blast-furnace slag. The hydraulic cement meets the specifications of ASTM C1157 for Type GU cement and ASTM C150 for Type I cement. The physical and chemical properties of cementitious binders are shown in Table 3.3, and 3.4, respectively. This Portland cement is also MODOT approved.

Table 3.3. Physical Properties of Type I Portland Cement and Class C Fly Ash

Physical Tests	**Type I PC**	**Class C Fly Ash**
Autoclave Expansion, %	0.13	N/A
Specific Surface Blain, cm^2/gr	3730	N/A
Time of setting:		
Vicat, Initial, min	86	-
Vicat, Final, min	183	-
Comp. Strength, psi (MPa)		
3 days	3350 (23.1)	-
7 days	4550 (31.3	-
Air Content, %	7	N/A
Specific Gravity	N/A	2.5
No. 325 sieve Fineless, %	N/A	16.40
Water Requirement, %	N/A	95.9
7-Day Strength Activity Index	N/A	77.0

Note: N/A= Not Applicable

Table 3.4. Chemical Properties of Type I Portland Cement and Class C Fly Ash

Chemical Composition	**Type I PC (%)**	**Class C Fly Ash (%)**
Silicon Dioxide(SiO_2)	20.8	50.45
Aluminum Oxide (AL_2O_3)	4.9	19.26
Ferric Oxide (Fe_2O_3)	2.1	17.82
Calcium Oxide (CaO)	64.4	4.77
Magnesium Oxide (MgO)	3.5	0.94
Sulfur Oxide (SO_3)	2.5	1.59
Loss on Ignition	1.4	1.14
Insoluble Residues	0.19	N/A
Tricalcium Silicate (C_3S)	61	N/A
Dicalcium Silicate (C_2S)	14	N/A
Tricalcium Alimunate (C_3A)	9	N/A
Tetracalcium Alumino-Ferite (C_4AF)	6	N/A
Na_2O equivalent	0.49	N/A
Available Alkalis as Na_2O	N/A	0.81
Free Moisture	N/A	0.10
Total K_2O	N/A	2.38

Note: N/A= Not Applicable

The ground granulated blast-furnace slag meets the requirement of ASTM C989 specifications for Grade 100 ground blast-furnace slag. The GGBS used in this research has a Blaine fineless of 5650 cm^2/gr, air content of 5%. The 7-day, and 28-day compressive strengths of GGBS were 4340 psi (30 MPa), and 5390 psi (37 MPa), respectively.

In terms of the concrete costs, it was assumed that the cement and cementitious materials are the dominating factors. For the cost comparison of the cementitious material, the following cost data was used to calculate the cost effectiveness of the mix designs: Type I Cement: $70.00 per short (2000 lbs) ton, Class F fly ash: $20 per short (2000 lbs) ton, GGBS: $60 per short (2000 lbs) ton. Hence, replacement of cement by fly ash reduced the price by almost 1/3 of the cementitious material cost. Moreover, the increase in workability by utilizing fly ash could also cause a slight decrease in labor cost. However, a significant reduction in cost cannot be mentioned for GGBS replacement.

3.1.3 Mix Proportion Design

Optimization of mix proportions have been accomplished though trial batching series investigating the interaction of various materials in the production of HSC/HPC. The initial set of mix proportions was formulated from the guidelines of ACI 211. Three coarse aggregate sources as Limestone, River Gravel, and Trap Rock used in HPC, whereas HSC produced by a single source of Limestone.

The mix design matrix developed for HSC is shown in Table 3.5 and in Appendix A. The water/cement ratios of 0.25, 0.3, and 0.35 were used with mixes containing 100% Type I cement, 30% fly ash replaced with 30% cement, and 25% fly ash and 5% ground granulated blast-furnace slag replaced with 30% cement. The slump was targeted as 8 to 10 inches, which was obtained by the use of HRWR. The aimed amount of air entrainment was also a factor that was under investigation. Air entrainments of 0, 1.5, 3.0, and 4.5% were aimed for in this study. The air content was determined using the procedure set forth by ASTM C 231 “Air Content of Freshly Mixed Concrete by the Pressure Method”. The air measurements were done after the aimed slump was achieved. The number of the concrete batches was 36.

Table 3.5. Mix Proportion Design of HSC

Aggregate Source	w/c	Cementitious Materials	Air (%)
Limestone	0.25	100% P. Cement	0.0
	0.30		1.5
	0.35		3.0
			4.5
	0.25	70% P. Cement 30% Fly Ash (F-Class)	0.0
	0.30		1.5
	0.35		3.0
			4.5
	0.25	70% P. Cement 25% Fly Ash (F-Class) 5% GGBS	0.0
	0.30		1.5
	0.35		3.0
			4.5

The HPC mix design, which is presented in Table 3.6, contained same cement & cementitious materials with respect to HSC mixtures. However, since bridge deck applications aimed for this group, the w/c ratio defined as 0.40, and 0.45 for workability and finishability purposes. No air entrainer used. The total number of mixtures was 18. The mix design matrix developed for HPC is shown in Table 3.6 and in Appendix A.

Table 3.6. Mix Proportion Design of HPC

Aggregate Source	w/c	Cementitious Materials	Air (%)
River Gravel Trap Rock Limestone	0.4	100% P. Cement	0.0
	0.45		
	0.40	70% P. Cement 30% Fly Ash (F-Class)	0.0
	0.45		
	0.4	70% P. Cement 25% Fly Ash (F-Class) 5% GGBS	0.0
	0.45		

3.1.4 Test Methods & Procedures

The unconfined-compression test followed the procedure of ASTM C 39 “Standard test Method for Cylindrical Concrete Specimens”. The load was applied according to this standard with an average loading rate of 26,250 lb/min. and the failure load recorded. The test involved the use of 4 inches (101.6 mm) diameter, 8 inches (203.2 mm) in height specimens; and the samples were tested after 7, 28, and 56 curing days.

The static modulus of elasticity is determined according to the procedure defined by ASTM C 469 “Standard Test Method for Static modulus of Elasticity and Poisson’s Ratio of Concrete in Compression”. A compressometer was used to obtain the compressive modulus of elasticity via measuring the axial deformation. Figure 3.1 illustrates the uniaxial compression test and MOE test.

Figure 3.1. Uniaxial compression and MOE tests

The resistance of concrete samples to external chloride attack was determined by using AASHTO Designation: T 259-80I “Resistance of Concrete to Chloride Ion Penetration”. The concrete samples were exposed to chloride solutions for three months according to the above-mentioned standard with a modification of increased chloride percent from 3 to 7.5. One sample from each group left unexposed as a control sample. The dimensions of the test samples were 6x6x3.5 inches (152.4x152.4x89 mm). Each specimen was air-dried for 14 days before ponding with Chloride ion solution according to AASHTO recommendation. Figure 3.2 presents the test set-up for sample ponding with chloride solution.

After three months, powder samples collected from each concrete sample by using a drill. The powder samples are taken from three different depths: 0.5 inch, 1 inch, and 1.5 inches. Each concrete sample drilled five times for each depth to get minimum 20 grams of powder. Then, 3-gram of test samples have been weighed from each 20 grams and put into vials. Figure 3.3 shows the drilling and sampling process.

The Building Research Establishment suggested that a total (acid-soluble) chloride content of less than 0.4 (% by weight) produces low risk of corrosion, between 0.4% and 1.0% produces a medium risk, and greater than 1.0% produces a high risk [Arya, 1990; Haque, 1995].

Figure 3.2. Concrete samples exposed to chloride solution

3-gram test samples have been determined in acid and chloride content by percent of weight determined by using the apparatus shown in Figure 3.4.

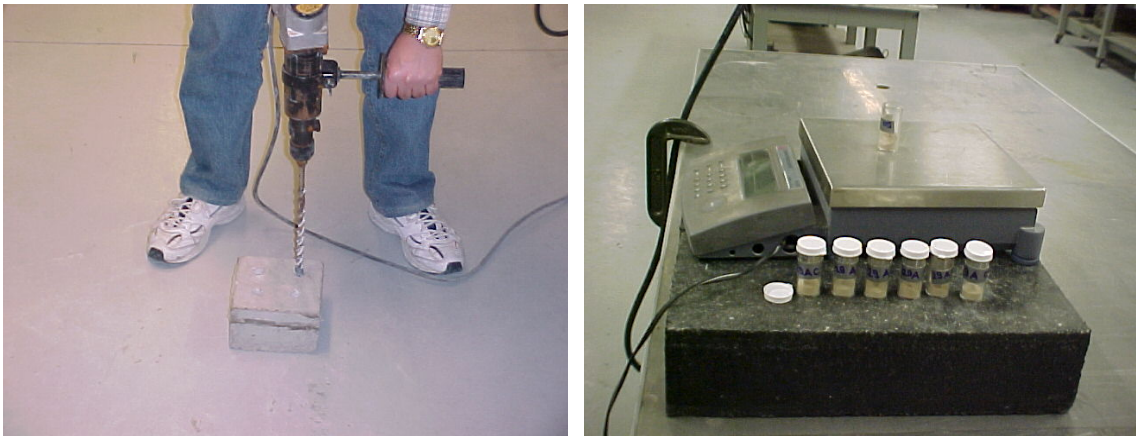

Figure 3.3. Drilling and sampling for chloride permeability test.

Figure 3.4. Chloride content (percent by weight) measurements

The abrasion test was performed to evaluate the surface resistance of high strength & high performance concrete. The test was conducted by using ASTM C 944 "Standard Test Method for Abrasion Resistance of Concrete or Mortar Surfaces by the Rotating-Cutter Method". Concrete specimens measuring 3x3.5x16 inches (72.6x89x406 mm) were cast. The top part of the surface of the specimen was divided into three equal areas. The test was performed three times on each sample and average depth of wear was measured. The rotation of abrading cutter was at a speed of 380 r/min and exerting a force of normal load of 22 lbs (98 N). The each test was continued for one minute. Figures 3.5, and 3.6 illustrate the test set-up and wear path of several paving blocks, respectively.

Figure 3.5. Abrasion test by rotating-cutter method

The rapid freezing and thawing test was conducted as per ASTM C 666 "Standard test Method for Resistance of Concrete to Rapid Freezing and Thawing". The specimens with the dimensions of 3x3x16 inches (76x76x406 mm) placed into stainless steel containers which's are already in the freeze-thaw machine with a strip heater between every container. The temperature was lowered form 40 ^{o}F to 0 ^{o}F for freezing, and rose from 0 ^{o}F to 40 ^{o}F for thawing not more than 5 hours, nor less than 2 hours (ASTM C 666). The mass loss and the length change of the each specimen measured according to the ASTM C 666. Figures 3.7, and 3.8 present the freezing & thawing test machine and test samples.

Figure 3.6. Concrete test samples after abrasion test

Figure 3.7 Freezing & thawing test set-up

Figure 3.8 Freezing & thawing test set-up

CHAPTER 4 TEST RESULTS & DISCUSSION

The aim of this chapter is to present the mechanical and durability characteristics of HSC/HPC. The discussions consist of a detailed analysis of how the matrix constituents impact the properties of the hardened products.

The hardened properties discussed in this chapter include compressive strength, modulus of elasticity, freezing & thawing resistance, abrasion resistance, and chloride permeability.

4.1 Concrete Mixtures for HSC Applications

4.1.1 Unconfined compressive strength

Concrete strength is often expressed with its compressive strength, which is defined as the ultimate uniaxial load carrying capacity of a concrete, and is presented in load per unit area, psi or MPa. The gain in compressive strength, or compressive strength development, is mainly a function of hydration of the cement paste, in which cement reacts with water to form calcium silicate gel.

HSC samples compressive strength development is under investigation in this section. In general, mixtures showed a compressive strength in Psi ranging from 4400 to 11000. Figure 4.1 presents the compressive strength of all moist cured HSC samples at the age of 56-day versus water per cement ratio. HPC samples test results, which were produced with 0.40 and 0.45 w/c ratios and with same respective curing time, are also presented herein for comparison purposes. As it can be seen, the plot followed a well-known pattern, which is the compressive strength of all mixtures decreased with the increase in w/c ratio with a coefficient of determination (R^2) of 0.61. The reason that the plot yielded to a smaller R^2 value can be speculated to the fact that each group formed by different mixtures, and mineral admixtures such as fly ash and g. g. blast-furnace slag utilized in some of them.

When the strength of fly ash and FA-GGBS substituted mixtures compared with that of the control mixtures (100% P. cement mixtures), as shown in Figure 4.2, the effect of mineral admixtures can be clearly seen. All mixtures represented in the plot have same air content of 4%, except the control sample with 0.35 w/c ratio, in which the air content measured as 3%. All the mixtures showed same strength development trend; as the w/c ratio decreased, the compressive strength got higher. It is noteworthy to mention that all the control samples displayed higher values at 7, 28, and 56-day curing periods, ranging from 8900 Psi to 8100 Psi, compared to the mineral admixture substituted samples. The average 56-day compressive strength of control mixtures was 25%, and 30% higher than FA-GGBS and FA substituted samples, respectively. It is also noted that, even though the FA-GGBS samples exhibited 2.5% lower compressive strength values compared to FA samples at 28-day, they showed 4% higher results compared to fly ash substituted samples at the end of the 56-day curing. This can be noticed if the trends of FA-GGBS substituted samples and fly ash substituted samples are compared at Figure 4.2.

Within the groups, the effect of w/c ratio was clear. As the w/c ratio decreased, the strength increased in all mixtures except the control sample with 0.35 w/c, which can be explained by having relatively lower air content.

The complete results of compression tests are listed as a table in Appendix A.

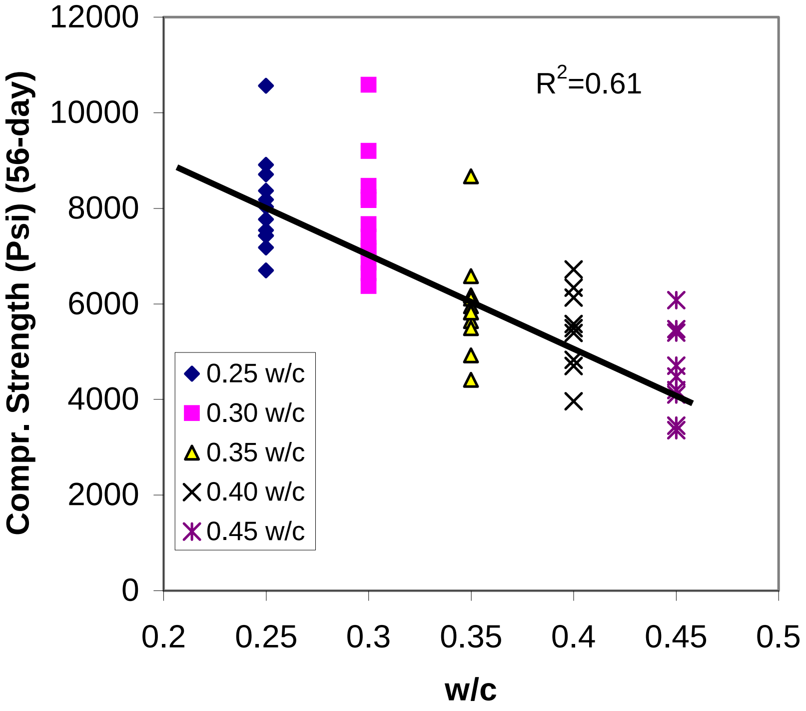

Figure 4.1. Compressive strength (Psi) at 56-Day vs. w/c ratio

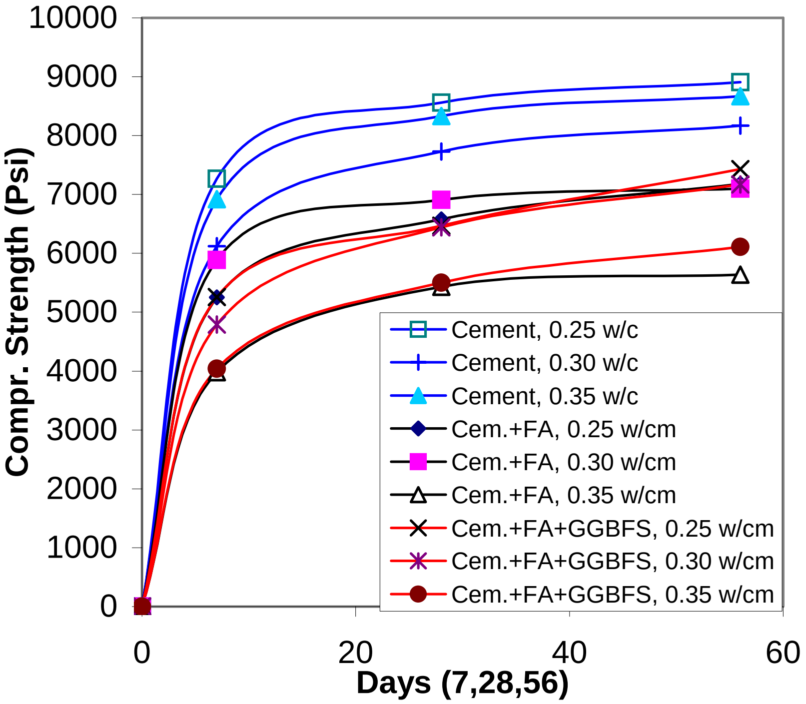

Figure 4.2. Strength development of HSC samples with similar air contents

4.1.2 Compressive strength versus modulus of elasticity (MOE) comparisons

The static modulus of elasticity (MOE) can be defined as the ratio between the applied stress and instantaneous strain within an assumed proportional limit (Mehta 1986). This is a material property, which represents the stiffness of the material and is often used in calculating the deflections and stresses caused by strains. Since only a segment of the stress-strain curve of concrete is linear, the calculation of modulus of elasticity is more complex than homogeneous materials like steel. In general three methods are used to calculate the MOE: the initial tangent modulus, the secant modulus, and the chord modulus. In this section, the static secant modulus of the concrete samples was studied. The MOE is obtained in this method by calculating the slope of a line drawn from the origin to a point beyond the proportional limit on the stress-strain diagram. This stress value has been suggested by the ASTM C 464 to be 40% of the ultimate compressive strength.

In the design of concrete structures, the modulus of elasticity is determined by the equation given by ACI 318 (Building Code Requirements for Structural Concrete), which is an estimated value for use in situations where the actual data is not available. This equation has been updated by ACI 363R (State-of-the-Art Report on High Strength Concrete, 1992) for high strength concrete. These equations are shown as following:

According to ACI 318 (for normal weight concrete)

$$E = 57 * \sqrt{f_c^{'}} \quad \text{(ksi)} \qquad (4.1)$$

According to ACI 363R

$$E = (40 * \sqrt{f_c^{'}}) + 1000 \text{ (ksi)} \qquad (4.2)$$

In this section, the relation between static modulus of elasticity, and the 56-day cured compressive strength of concrete has been studied. Figure 4.3 through Figure 4.5 represents the plots between static modulus of elasticity versus square root of 56-day compressive strength of HSC mixtures. As it can be seen from these graphs that all the mixtures verified the ACI 318 recommended equation, whereas the equation proposed by ACI 363R presented lower values.

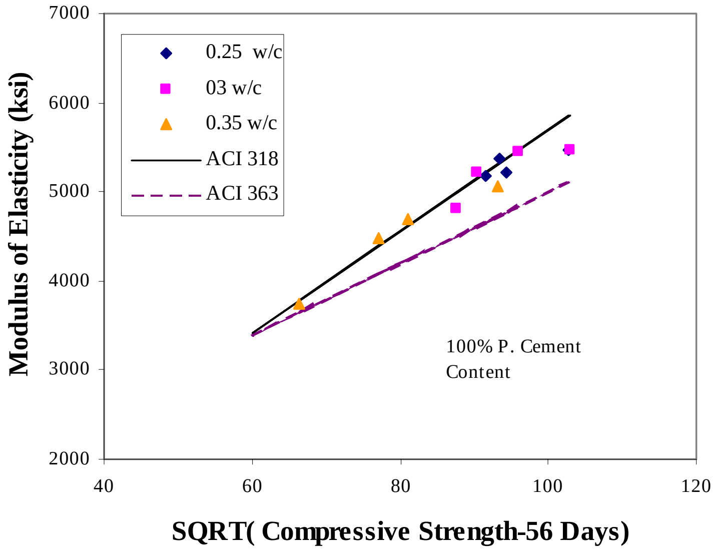

Figure 4.3. Modulus of Elasticity comparisons for HSC mixtures with 100% P. cement

In addition, the plots exhibited a clear identification between the mixtures with 0.25 w/c, 0.30 w/c, and 0.35 w/c ratios. As water per cement ratios increased, a decrease in MOE has been observed. The overall decrease in MOE when w/c ratio changed from 0.25 to 0.30, and 0.30 to 0.35 was 2% and 16%, 0.3% and 5%, and 3% and 9% for the mixtures with 100% P. Cement, 70% P. cement + 30% fly ash, and 70% P. cement + 25 % FA + 5% GGBS, respectively. This can be speculated by the reduction in the paste porosity as the w/c ratio decreased, which increased the MOE of the matrix.

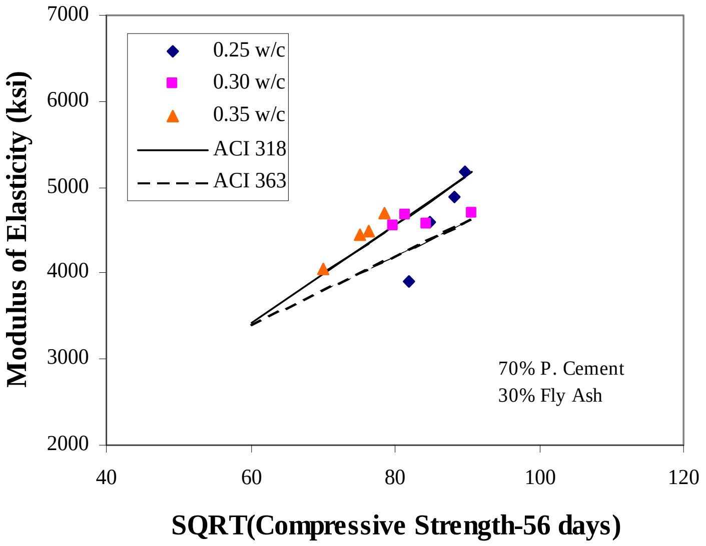

Figure 4.4. Modulus of Elasticity comparisons for HSC mixtures with 70% P. cement and 30% fly ash

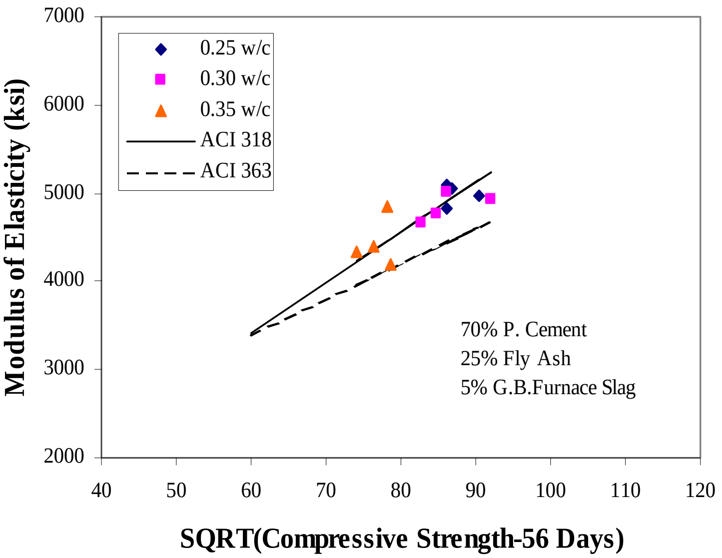

Figure 4.5. Modulus of Elasticity comparisons for HSC mixtures with 70% P. cement, 25% fly ash, and 5% GGBS.

Another observation that can be made from these plots is the substitution of mineral admixtures has an adverse effect on MOE. The decrease in MOE was more significant for the mixtures in which 30% fly ash replaced with same amount of P. cement than the mixtures in which 30% P. cement replaced with 25% fly ash and 5% GGBS. The average decrease in MOE for the 30% fly ash substituted mixtures relative to 100% P. cement was 9.6%, whereas this number was 5% for mixtures in which 25% fly ash and 5% GGBS used.

4.1.3 Freezing & thawing resistance of HSC mixtures

The deterioration of concrete due to freezing and thawing cycles is a typical occurrence in cold climates. The main action in freeze-thaw deterioration is the freezing and thawing of water inside the capillary pores of the hardened matrix. The density of water is 62.4 lb/ft^3; the density of ice is 57.4 lb/ft^3. Hence, when a unit volume of water freezes, the volume gets 8.7% bigger. This increase in volume exerts pressure on the surroundings. If subsequent thawing is followed by refreezing, additional stress will take place. This repetitive freezing and thawing action will have a cumulative effect, which may yield to cracking and spalling of concrete. This situation may end up failure of hardened product, especially in case the pressure created by volume change of water exceeds the tensile capacity of the surrounding paste.

The resistance of concrete to freezing and thawing action can be improved by several parameters. First one is to produce air bubbles by air entrainment, which can help frozen water to find a passageway to escape without creating additional tensile forces inside of concrete. Tensile strength seems very important factor, because any damage will not happen unless it is surpassed; however, non-air-entrained concretes with higher strength than air –entrained concretes observed to have lover resistance (Mehta, 1986).

The degree of saturation also plays an important role, since the increase in water volume after getting frozen is close to 9%, concrete whose pores are less than 91% saturated will have resistance to freezing and thawing damage.

In this section, the resistance of HSC samples to freezing and thawing cycles examined. The specimens have been cured for 56 days and then soaked in curing tank for 48 hours before placing them into freeze-thaw machine. The specimens weighed every 20 cycles of freezing and thawing and the percent mass loss calculated. The test samples were planned to be removed from freeze-thaw machine either when they are broken because of substantial mass loss or after each one completes 300 cycles. It was seen at the end of the tests that none of the test sample reached to the failure point, however some minor mass loss, mostly in the form of spalling, was observed.

18 test samples have been selected for this test. The main criterion in selection of samples was to test two samples from each cementitious group, one with no air entrainment, and one with the highest air entrainment by percent.

Figure 4.6 shows the percent mass loss versus freezing-thawing cycles. The cycles continued up to 300, and the mass of the samples weighed every 20 cycles. All the mixtures analyzed herein completed 300 cycles with the highest mass loss of 4.15%. The mixtures with 0.25 w/c ratio and no air-entrainment performed relatively poor after 300 cycles. The mass loss at the end was 4.15%, 3.15% and 2.53% for the no-air-entrained mixtures with 100% P. cement, 30% fly ash substitution, and 25% fly ash-5% GGBS substitution, respectively. Except these three mixtures, two other mixtures with 0.35 w/c, one with 30% fly ash substitution and 1.5% air entrainment, and the other with 25% fly ash-5% GGBS substitution and 0% air entrainment presented mass loss of 1.3%, and 0.60%, respectively. All other samples exhibited increase in mass due to absorption through 100th cycle and stabilized after that. These samples did not show a substantial mass loss. The pictures of some selected test samples after 300 cycles are presented in Appendix B. The surface scaling records and pictures of samples are presented in Appendix A. The pictures of two samples of 30% fly ash substituted mixtures, one with zero air entrainment, second one with 4% air entrainment are shown in Figures 4.7, and 4.8, respectively.

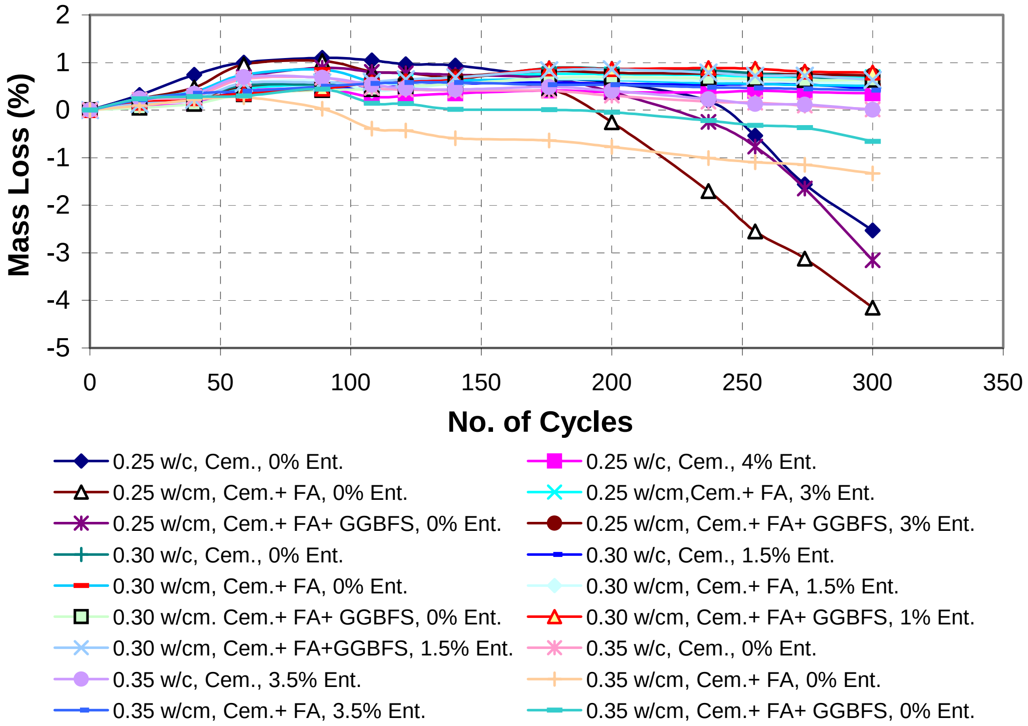

Figure 4.6. Freezing & thawing cycles of HSC mixtures

Figure 4.7. 30% fly ash substituted mixture with 0.25 w/c ratio, 0% air entrainment, after 300 freezing & thawing cycles

Figure 4.8. 30% fly ash substituted mixture with 0.25 w/c ratio, 4% air entrainment, after 300 freezing & thawing cycles

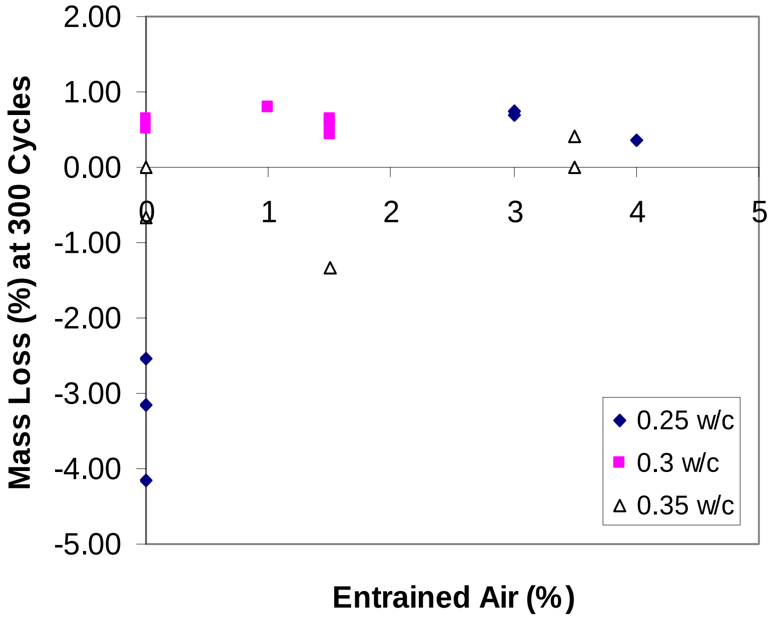

Figure 4.9. Freezing & thawing mass loss (%) of HSC versus entrained air (%)

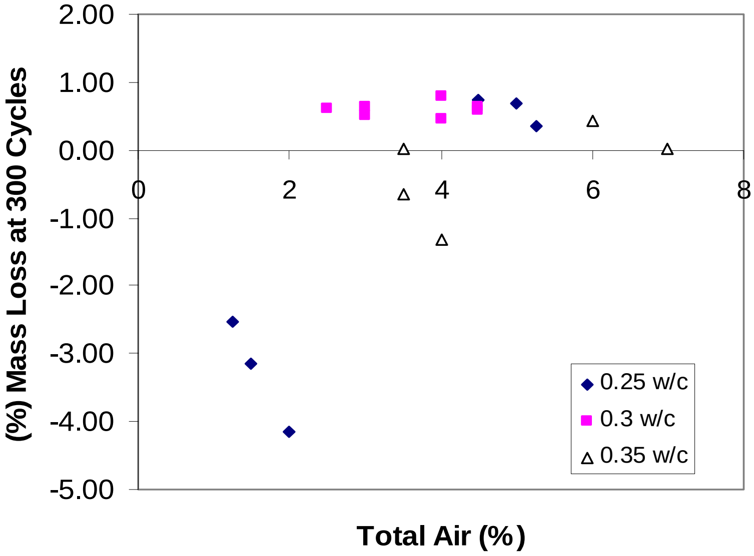

Figure 4.10. Freezing & thawing mass loss (%) of HSC versus total air content (%)

Figures 4.9 and 4.10 present the percent mass loss at the end of 300 cycles versus percent-entrained air and percent total air content of mixtures tested, respectively. These plots clearly identified the importance of air content of concrete to provide adequate resistance to freezing & thawing cycles, as well as water per cement ratio. The poor performance of some mixtures with 0.25 w/c ratio can be speculated to lower air content, and some of the 0.35 w/c ratio mixtures are related to the high water content.

The percent mass loss at 300 cycles versus compressive strength of test samples is illustrated in Figure 4.11. As it was previously mentioned, the effect of compressive strength on resistance to freezing and thawing is not as important as the air content of concrete, since some relatively high strength samples with lower air content displayed high mass loss. A 95% confidence interval lines added to Figures 4.9, 4.10, and 4.11. The related figures are presented in Appendix-A. The pictures of samples after 300 freezing and thawing cycles presented in Appendix B.

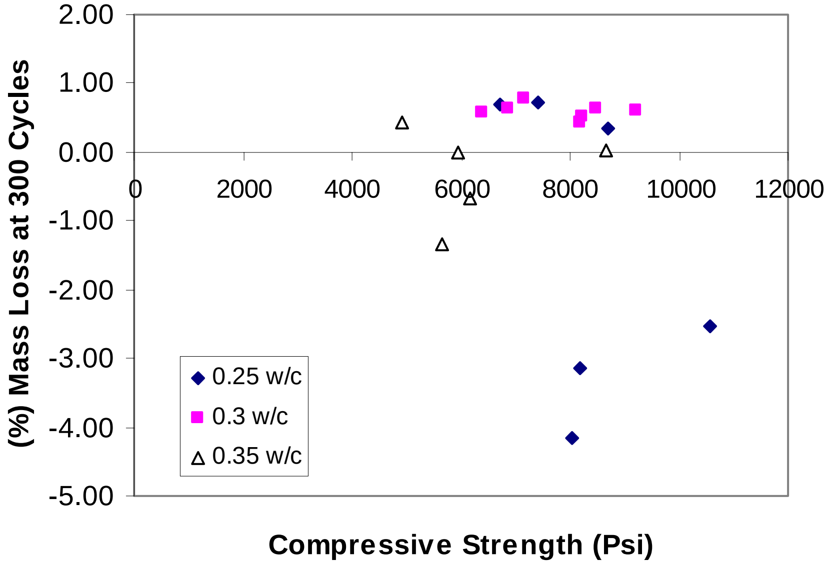

Figure 4.11. Freezing & thawing mass loss (%) of HSC versus compressive strength

4.1.4 Abrasion resistance of HSC mixtures

Abrasion is a progressive loss of mass from a concrete surface because of vehicular traffic or environmental effects. It was reported by researchers that the main factors effecting abrasion resistance of concrete are cement content, air content, slump, surface finish, curing types and regimes (Mehta, 1986). Since these factors also affect the concrete strength, there is a tendency to accept compressive strength as a criterion for abrasive resistance evaluation. Water per cement ratio has also impact on surface durability. Decreased w/c ratio causes less bleeding and segregation and improvement in surface layer characteristics.

In this section, accelerated laboratory abrasion tests have been aimed to perform. The primary goal was to evaluate the quality of concrete surface, comparing the types of the mixtures, and appraising the effects of compressive strength and air content. Test methods for abrasion resistance are not suitable for exact simulation of real life conditions give definitive values for service life; however, they provide sufficient data to compare the mixtures with respect to changes in material type or properties. The tests have been performed herein are according to the ASTM C 944, which is “rotating-cutter method”. Each sample has been separated into three zones and tested three times under the constant pressure of 22 lbs (98 kN). The rotation of abrading cutter was at a speed of 380 r/min. The samples were air dried for 14 days before testing.

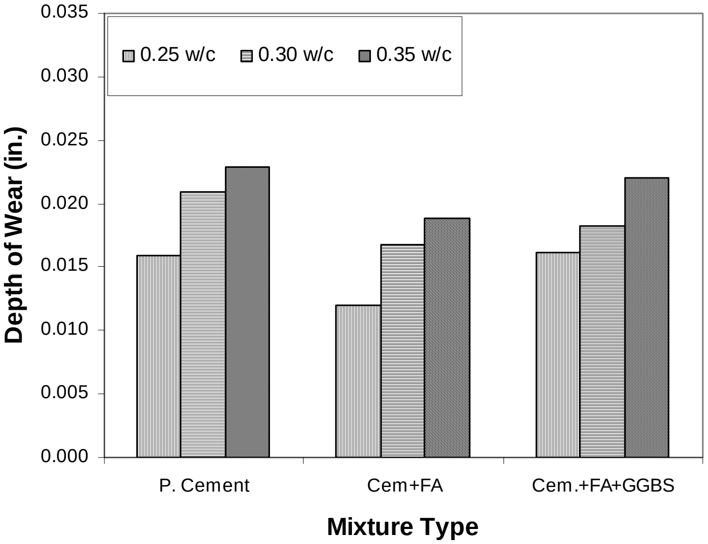

Figure 4.12. Depth of wear (in.) of HSC samples

The values of depth of wear of HSC samples are illustrated in Figure 4.12. The values are calculated by taking the average of samples with 4 different air entrainments of every cementitious group. As it can be seen from Figure 4.12, there is a tendency to decrease the depth of wear as the w/c ratio decreases. The average decreases for all samples when the w/c ratio decreases from 0.35 to 0.30, and from 0.30 to 0.25 were 8% and 23% for control samples, 10%, and 30% for fly ash substituted samples, and 21% and 11% for fly ash – GGBS substituted samples, respectively. As it can also seen by the figure that the control samples and fly ash – GGBS substituted mixtures yielded to very close numbers, however the fly ash substituted samples performed on average of 24%, 20%, and 21% lower than the other samples with respect to 0.35 w/c, 0.30 w/c, and 0.25 w/c ratios.

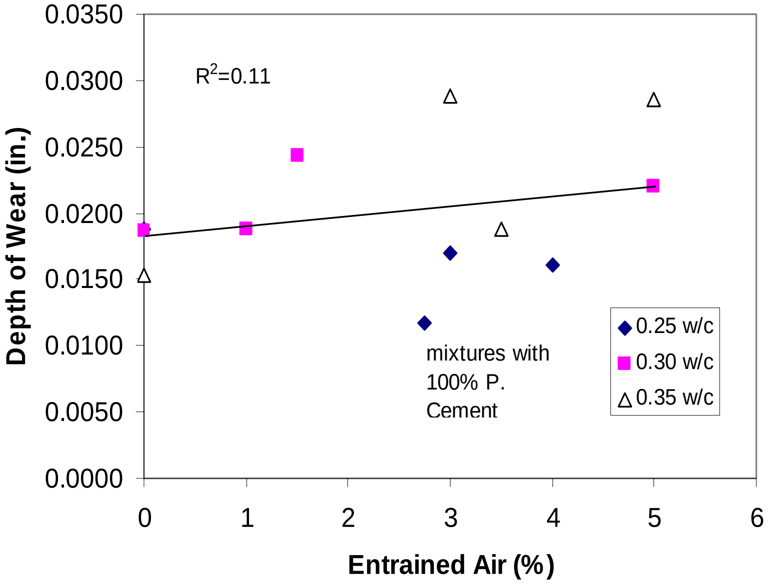

Figure 4.13. Depth of wear (in.) of HSC control samples versus entrained air (%)

Figures 4.13 through 4.15 illustrate the relation between depth of wear of test samples in inches versus entrained air in percent. Air-entrained mixtures, which have adverse effect on strength, believed to reduce the resistance of concrete to abrasion. The diagrams presented below show an increase in depth of wear as the entrained air goes up. Since the coefficients of determinations are 0.11, 0.02,and 0.09 for the control mixtures, 30% fly ash substituted mixtures, and 25% fly ash + 5% GGBS substituted mixtures, respectively, a strong relation can not be mentioned.

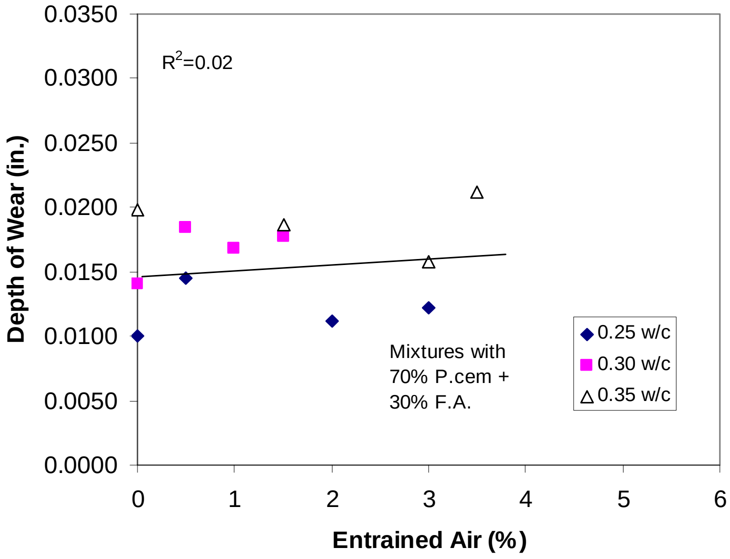

Figure 4.14. Depth of wear (in.) of HSC with 30% fly ash substitution versus entrained air (%)

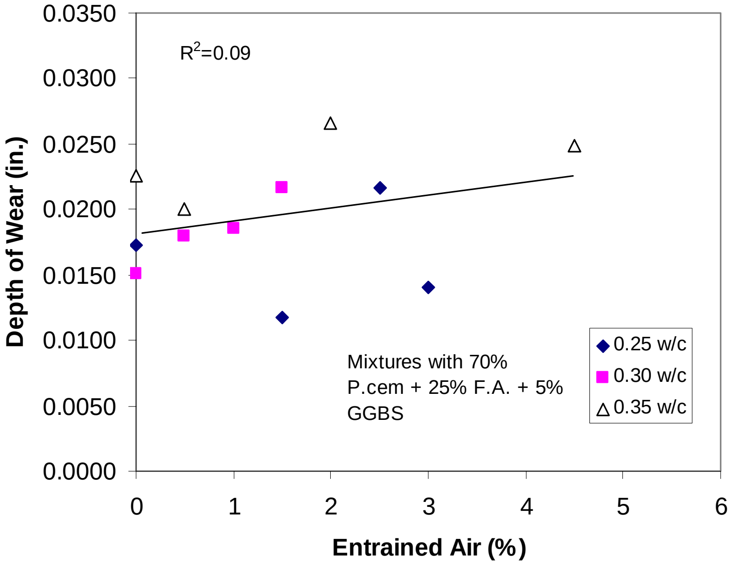

Figure 4.15. Depth of wear (in.) of HSC with 25% fly ash and 5% GGBS substitution versus entrained air (%)

The effect of total air content on the abrasion resistance presented by the Figures of 4.16, 4.17, and 4.18 for the control mixture, 30% fly ash substituted mixtures, 25% fly ash and 5% GGBS substituted mixtures, respectively. Since the coefficients of determinations are higher relative to the diagrams of abrasion resistance versus entrained air, we can speculate a better relation. The beneficial effect of low w/c ratio was clear in all the diagrams including the previous ones of Figures 4.15 through 4.17.

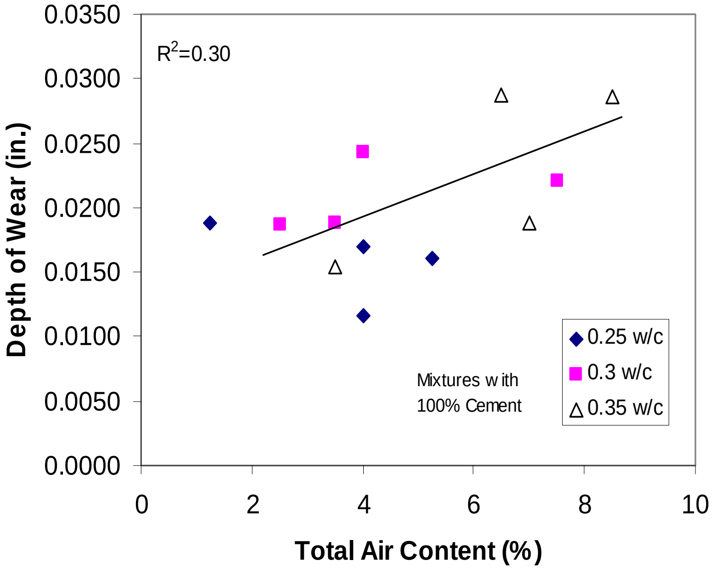

Figure 4.16. Depth of wear (in.) HSC control samples versus total air (%)

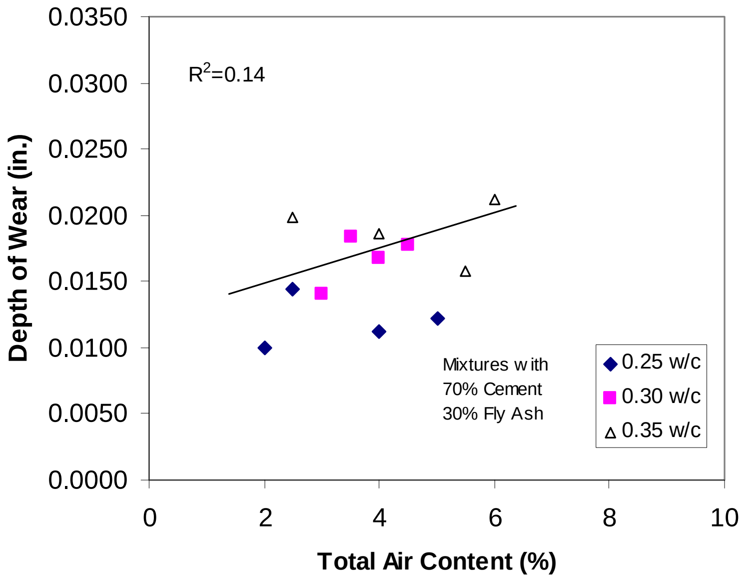

Figure 4.17. Depth of wear (in.) of HSC with 30% fly ash substitution versus total air (%)

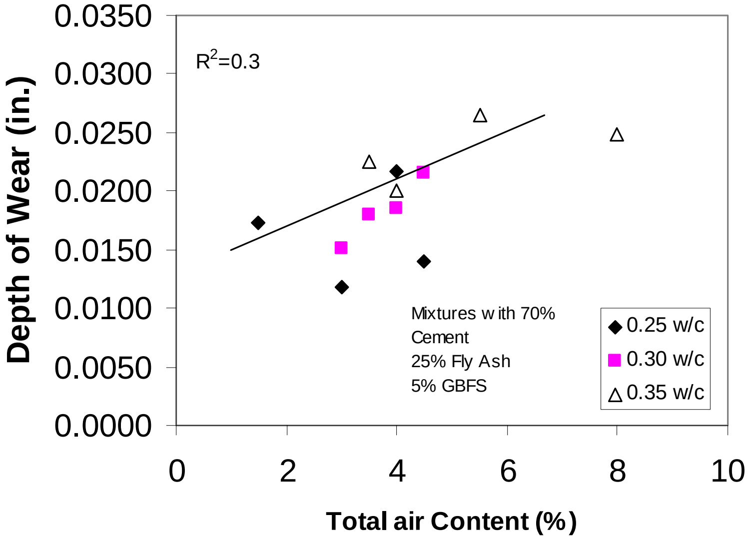

Figure 4.18. Depth of wear (in.) of HSC with 25% fly ash and 5% G.G.B.S. substitution versus Total Air (%)

The effect of compressive strength at 56-day to the resistance of abrasion are shown in Figures 4.19, 4.20, and 4.21. It can clearly be seen that the increase in compressive strength caused a decrease in depth of wear. The coefficients of determination as 0.35, 0.56, and 0.60 for control samples, fly ash substituted samples and fly ash – GGBS substituted samples, respectively, are the proof of a stronger relation compared to effect of air content. In these diagrams, the effect of w/c ratio can also be well identified. An increase can be observed in depth of wear as the w/c ratio increased.

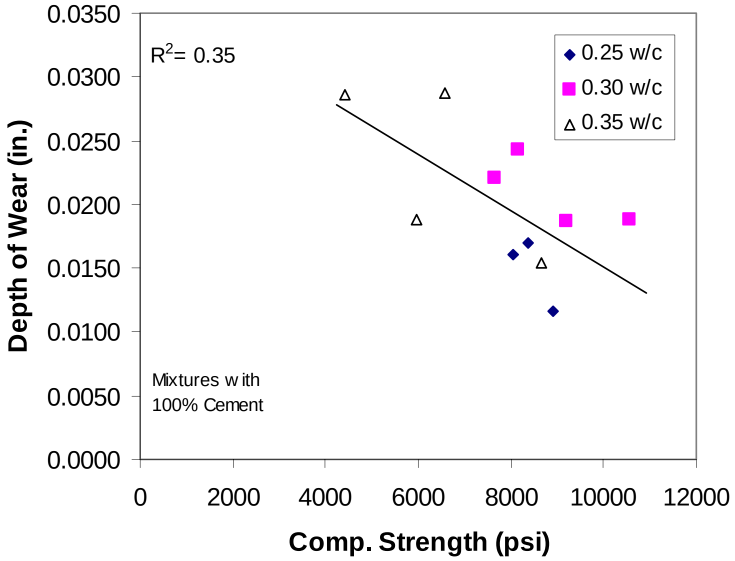

Figure 4.19. Depth of wear (in.) of HSC control samples versus compressive strength (Psi)

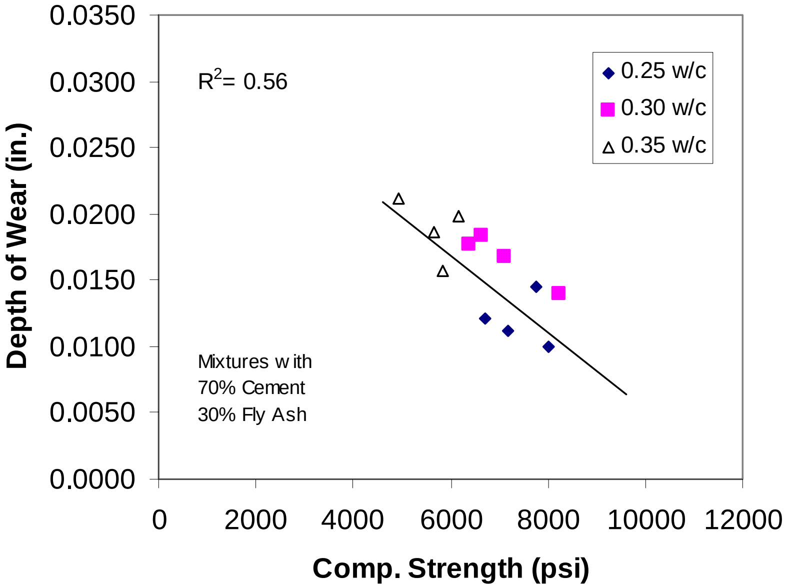

Figure 4.20. Depth of Wear (in.) of HSC with 30% fly ash substitution versus compressive strength (Psi)

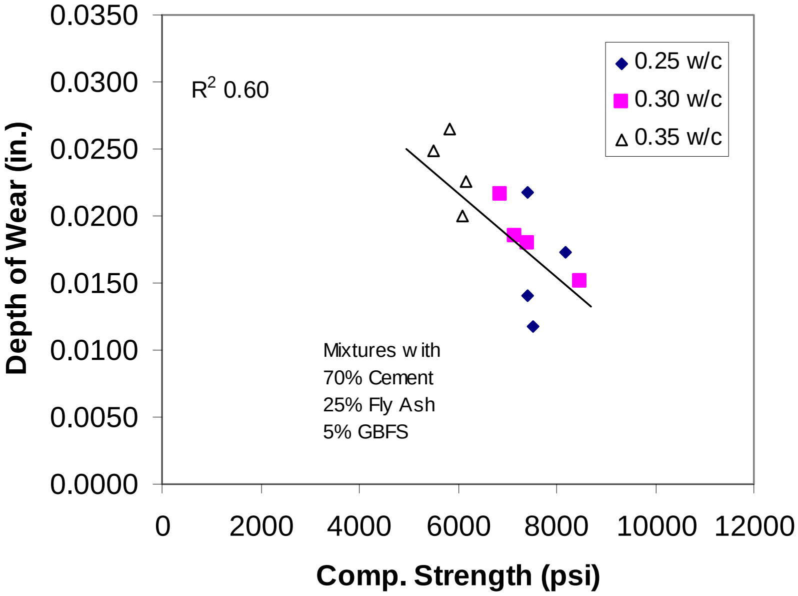

Figure 4.21. Depth of wear (in.) of HSC with 25% fly ash and 5% GGBS substitution versus compressive strength (Psi)

4.1.5 Chloride permeability of HSC mixtures

The use of chloride based materials for the purpose of de-icing over bridge decks and pavements may cause permeation of these ions into concrete. Such permeation of chloride can destroy the passivity layer formed around the reinforcement bars by the high alkalinity of concrete, and causes the corrosion of reinforcement. Hence the permeability of concrete is the key issue in deterioration of reinforcement due to chloride attack. Many factors effect the permeability of concrete, however, the primary factor is the water per cement ratio; the reduction in w/c ratio yields to more dense material, less porous and, consequently, less permeable.

In this section, chloride permeability test have been performed according to the AASHTO Designation: T 259-80I “Resistance of Concrete to Chloride Ion Penetration”. One sample from 6 groups ponded with 7.5% calcium chloride solution and the samples kept in this condition for three months. Three different depths, 0.5 in., 1 in., 1.5 in., have been drilled on each sample after 3 months and three grams of test powder have been taken. The powder samples solved in acid and chloride content by weight measured. The Building Research Establishment suggested that a total (acid-soluble) chloride content of less than 0.4 (% by weight) produces low risk of corrosion, between 0.4% and 1.0% produces a medium risk, and greater than 1.0% produces a high risk. [Arya, 1990; Haque, 1995]. As for comparison, the concrete samples produced by Myers, Touma, and Carrasquillo with 100% Portland cement, 25% fly ash replacement, and 35% fly ash replacement were ponded with 3% sodium chloride for 90 days and tested according to AASHTO T 259; test samples exhibited a chloride content (% by weight) ranging between 0.08 (0.35% fly ash replacement) and 0.32 (no fly ash) at a depth of 0.5 inch (12.7 mm) [Myers, 1997].

Figure 22 shows the percent chloride content by weight of HSC mixtures versus depth of concrete. As expected, there is a clear-cut difference between the mixtures with 0.25 w/c ratio and 0.35 w/c ratio. The reason that the 0.25 w/c ratio performed better than the mixtures with w/c ratio of 0.35 can be the more dense paste of 0.25 w/c ratio samples because of the reduction in water amount. It can also be noticed from the graph that the chloride content of all tested mixtures at the depth of 1.5”, this is the minimum cover depth for RC structures, was almost zero.

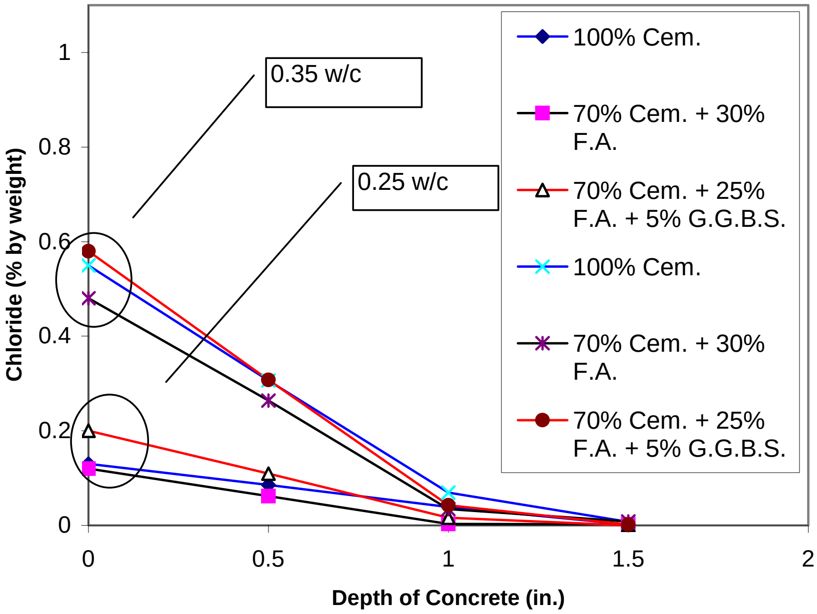

Figure 4.22. Chloride content of HSC samples versus depth of concrete

Between all the mixtures, it is noteworthy to mention the outstanding performance of fly ash substituted mixtures. At the depth of 0.5 inch, the 30% fly ash substituted mixtures with 0.25 w/c ratio performed 38%, and 76% lower chloride content than 100% P. cement and 25% fly ash+5% GGBS substituted mixtures, respectively. The reduction in chloride content for the 0.35 w/c mixtures was 16% and 18%, with same respect. This can be speculated by the increase in CSH gels and the decrease in $Ca(OH)_2$ in the capillary pores of concrete. In the fly ash substituted mixtures, the formation of CSH gels were not enough to give a strength increase compared to control mixtures, however, they were enough to block the capillary pores and reduce the diffusion rate of chemical penetration into concrete. The poor performance of slag-substituted mixtures can be explained by the slow reaction capacity, long-term test can be conducted for better understanding of their behavior. The complete results of chloride permeability tests are listed as a table in Appendix A.

As for information, the chloride content of concrete samples at the depth of 0.5-inch depth versus compressive strength at 56-day, and compressive strength development are displayed in the diagrams of Figure 4.23, and Figure 4.24, respectively. The effect of w/c ratio can be clearly seen for strength increase as well as the permeability issues. If the groups are individually examined according to the constant w/c ratio, it can be seen that the chloride content of concrete does not completely related to compressive strength of concrete. This is supporting the approached that was mentioned previously as CSH gels produced by mineral admixtures are blocking the passages of concrete and positively affecting the resistance to chloride permeability.

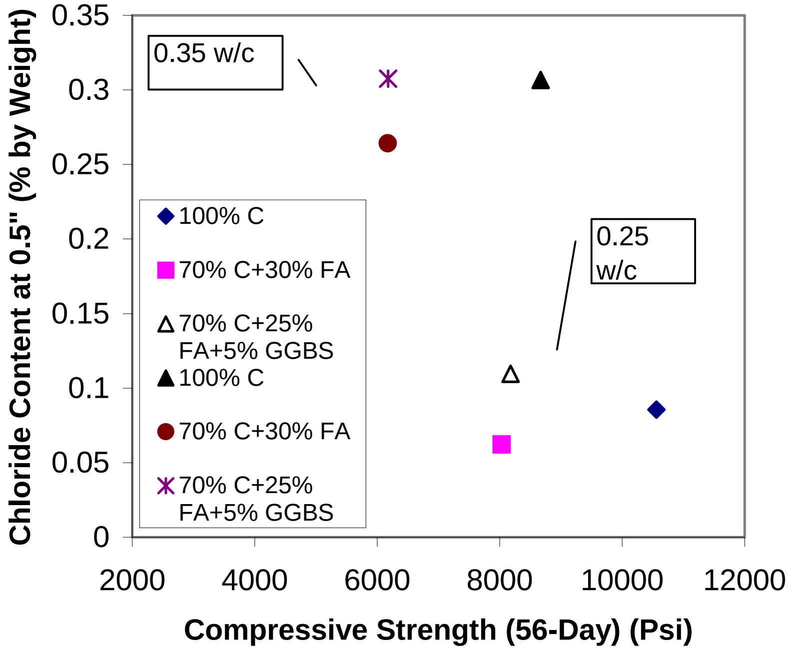

Figure 4.23. Chloride content of HSC at 0.5-inch depth versus compressive strength

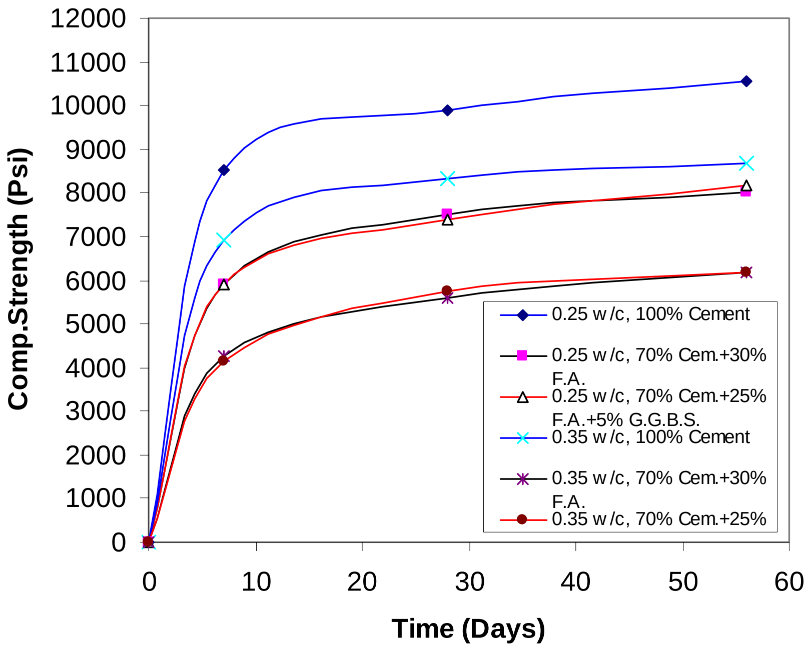

Figure 4.24. Compressive strength development of samples tested for chloride permeability

4.2 Concrete Mixtures for HPC Applications

4.2.1 Unconfined compressive strength

In this section, the compressive strength of HPC designs was under investigation. The mix design of HPC is briefly explained at Section 3.3, and Table 3.6. The information about compressive strength tests was mentioned at the Sections 3.4 and 4.1.1. As a reminder, three different coarse aggregate sources were used in mix designs: Limestone, Trap Rock, and River Gravel. The complete results of compression tests are listed as a table in Appendix A.

The strength development of each material is compared in Figure 4.25. All the coarse aggregate sources were provided by local companies of the state of Missouri. The mixtures presented a compressive strength distribution ranged from 3400 Psi up to 6700 Psi. As shown in the figure, the strength development of limestone mixtures was superior to all other mixtures produced by River Rock and Trap Rock. Within the mixtures prepared with 0.40 w/c ratio, the average of the compressive strength of Limestone samples were 21%, and 36% higher than the River Gravel samples and Trap Rock samples, respectively. The 0.45 w/c ratio samples showed the same trend. The limestone mixtures presented 34% and 45% higher results compared to River Gravel and Trap Rock mixtures, respectively. The increase in compressive strength when the w/c ratio decreased from 0.45 to 0.40 were 13%, 25%, and 21% for the mixtures with Limestone, River Gravel, and Trap Rock, respectively.

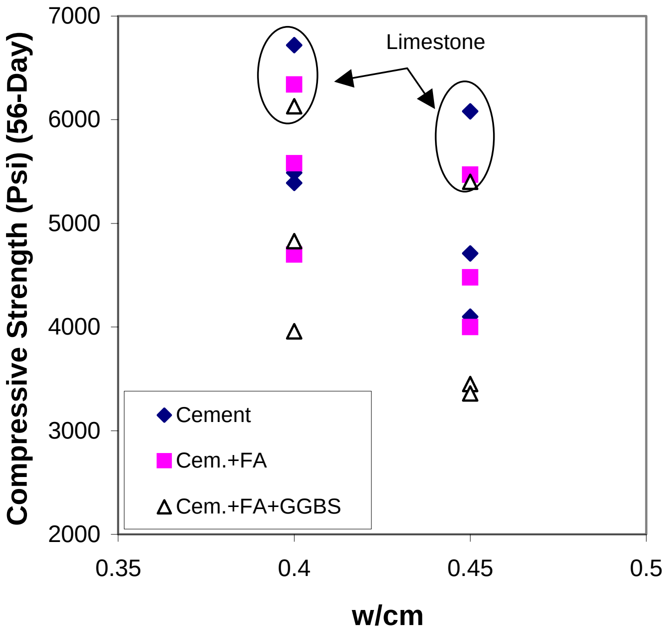

Figure 4.25. Compressive strength of HPC mixtures at 56-day versus w/c ratio

The strength developments of HPC samples grouped according to the coarse aggregate sources are presented in Figures 4.26 through 4.28. A well-known pattern is also repeated in these compressive strength-curing time diagrams; as the water-cement ratio of a concrete mixture, having a constant cement content, is increased, a corresponding decrease in compressive strength is observed. At 56-day, all the mixtures exhibited the same trend, the control samples performed better than fly ash substituted samples (except the mixture produced with river gravel and 0.40 w/c ratio which showed higher results), and fly ash substituted samples showed better performance than fly ash-GGBS substituted samples. Results can be interpreted that the 30% substitution of fly ash did not provide same amount of calcium-silica gel as 30% cement. The slower reaction ability of ground granulated blast-furnace slag did not contribute strength development as much as cement or fly ash, hence they yielded lower strength values compared to control mixtures and fly ash substituted mixtures.

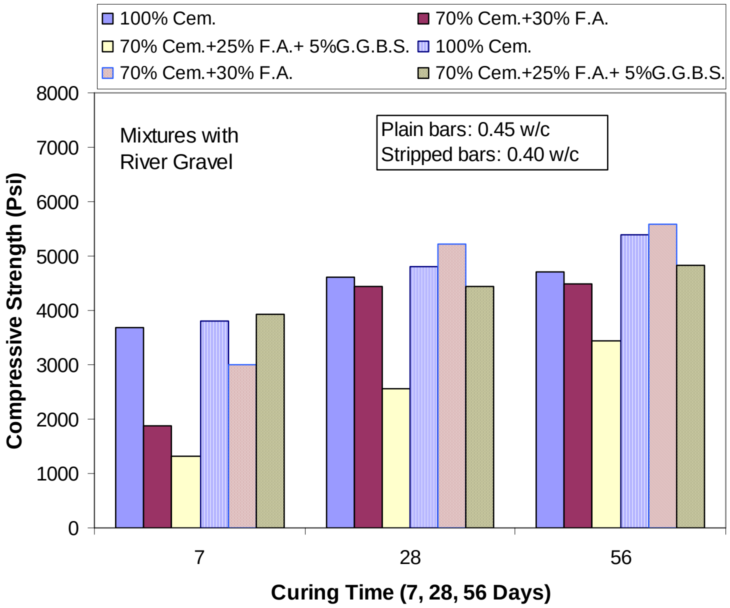

Figure 4.26. Compressive strength development of River Gravel utilized HPC mixtures

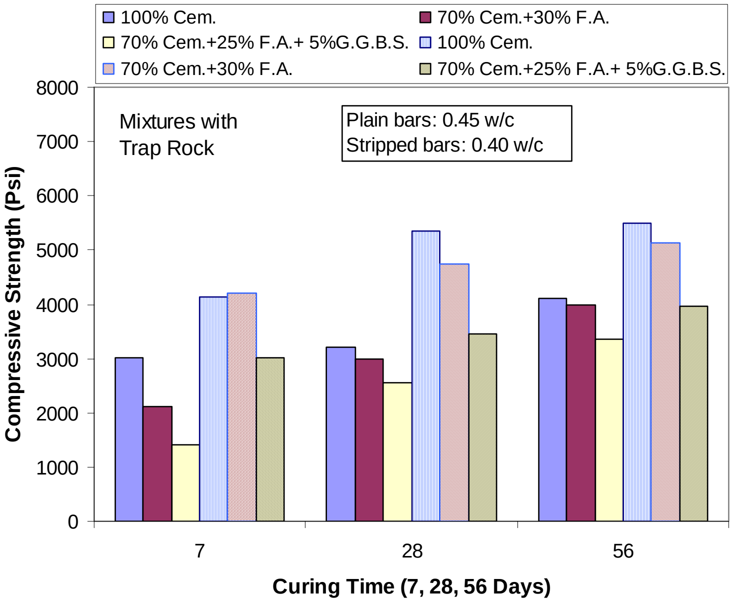

Figure 4.27. Compressive strength development of Trap Rock utilized HPC mixtures

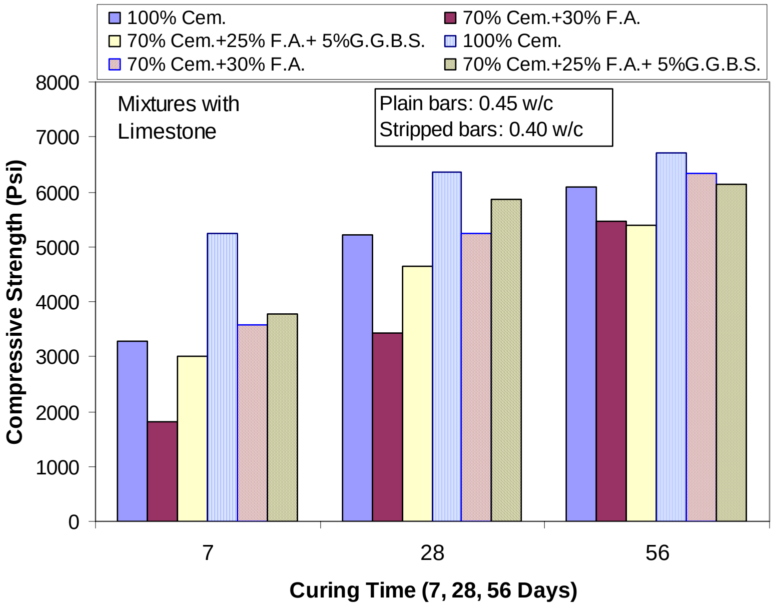

Figure 4.28. Compressive strength development of Limestone utilized HPC mixtures

4.2.2 Compressive strength versus modulus of elasticity (MOE) comparisons

The concept of modulus of elasticity and application of test procedures were briefly discussed in the Sections of 3.4 and 4.1.2. In determination of modulus of elasticity of HPC mixtures, the same procedure is followed as in HSC tests according to ASTM C 469, in which the secant modulus of elasticity corresponding to forty percent of the ultimate strength is calculated.

The modulus of elasticity as a function of square root of compressive strength are presented in Figures 4.29, 4.30, and 4.31 for the coarse aggregate sources of River Rock, Trap Rock, and Limestone, respectively. From these diagrams, the detrimental effect of a high water cement ratio can be clearly seen. The MOE of HPC mixtures yielded to a range between 3750 ksi and 6250 ksi. The highest values obtained from the mixtures in which Limestone coarse aggregate utilized. The results suggested that the HPC mix design of this research yielded to higher values than the recommended values by ACI 318 and ACI 363.

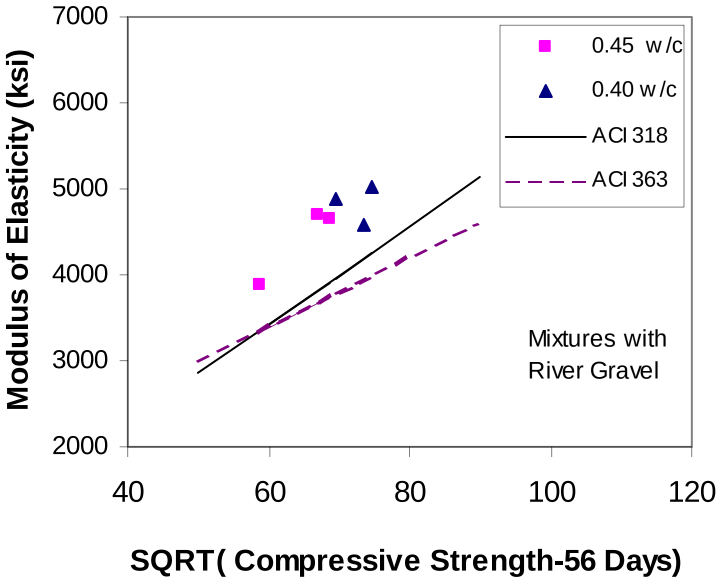

Figure 4.29. Modulus of Elasticity comparisons for HPC mixtures with River Gravel

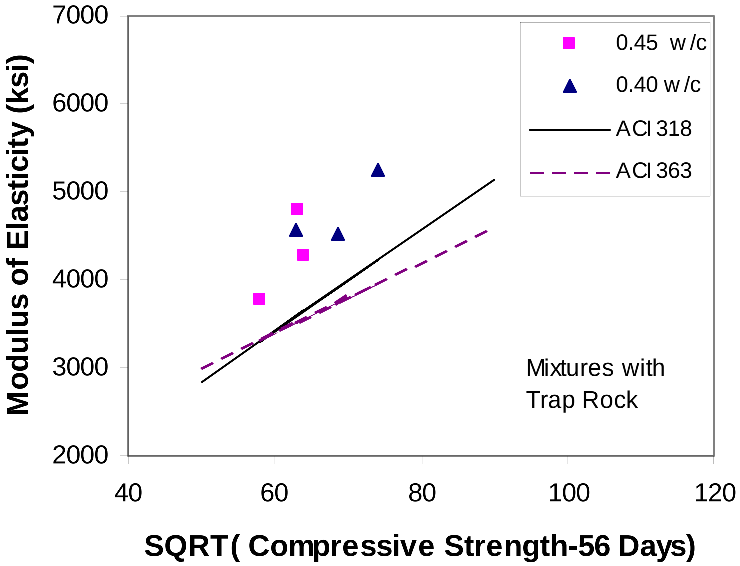

Figure 4.30. Modulus of Elasticity comparisons for HPC mixtures with Trap Rock

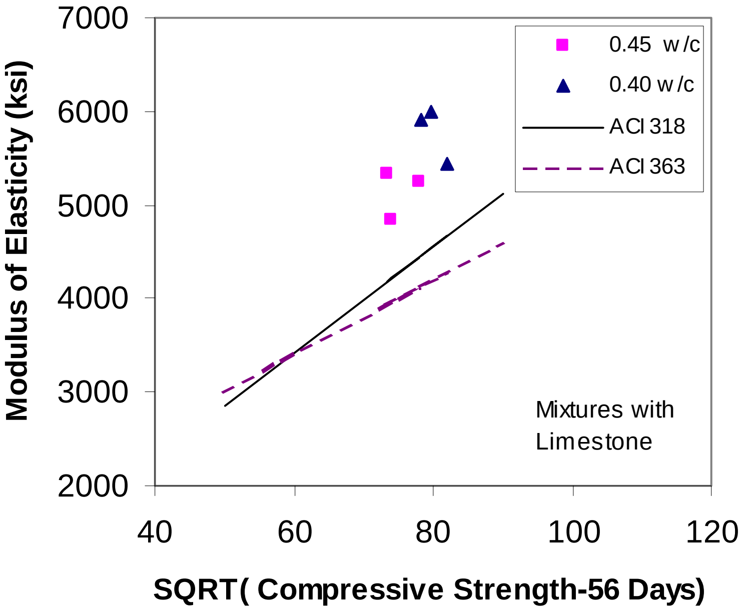

Figure 4.31. Modulus of Elasticity comparisons for HPC mixtures with Limestone

4.2.3 Freezing & thawing resistance of HPC mixtures

High Performance Concrete samples have also subjected to freezing and thawing cycles. The procedure applied for this test is based on ASTM C 666 and explained in details in the Sections of 3.4, and 4.1.3. The test continued for 300 cycles. At the end of the 300 cycles, none of test sample terminated because of substantial mass loss. The test stopped when every single specimen completed the aimed 300 cycles. The pictures of some selected test samples after 300 cycles are presented in Appendix B. The surface scaling records are presented in Appendix A.

Figures 4.32 through 4.34 display the percent mass loss as a function of number of freezing & thawing cycles for the HPC mixtures. The percent mass loss of the specimen increased with respect to freezing & thawing cycles.

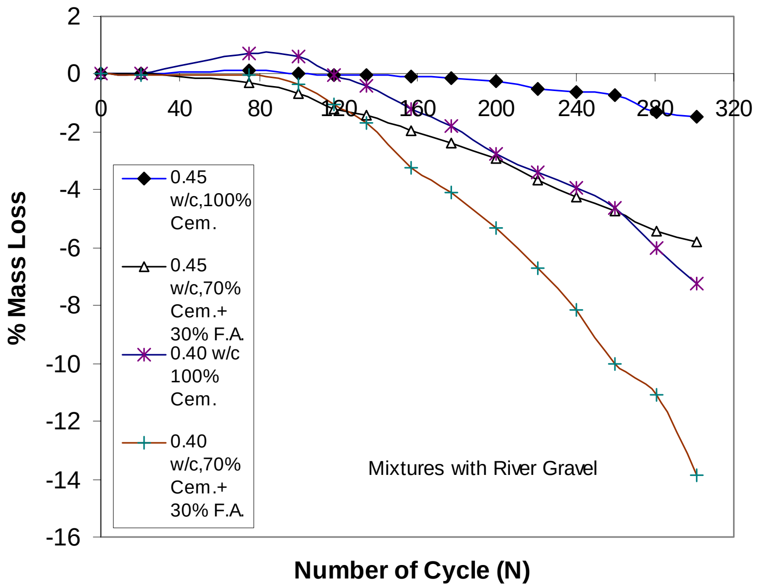

Figure 4.32. Freezing & thawing cycles of HPC mixtures with River Gravel

As it can be seen at Figure 4.32, the control samples with 0.45 w/c ratio, even though it has lower compressive strength relative to 0.40 w/c ratio control mixture and similar total air content, performed better than any other mixture in this category with a mass loss of 1.45%. The 30% fly ash substituted mixture and control mixture with 0.40 w/c ratio showed mass loss and air content of 13.8%, and 4.5; 7.22%, and 4.7, respectively. The 30% fly ash substituted mixture with 0.45 w/c ratio, which had the highest air content of 5.7%, exhibited a mass loss of 5.7%. The reasons that fly ash substituted mixture with 0.40 w/c ratio exhibited significant mass loss did not fully understand. Repeatability of testing these samples is possible.

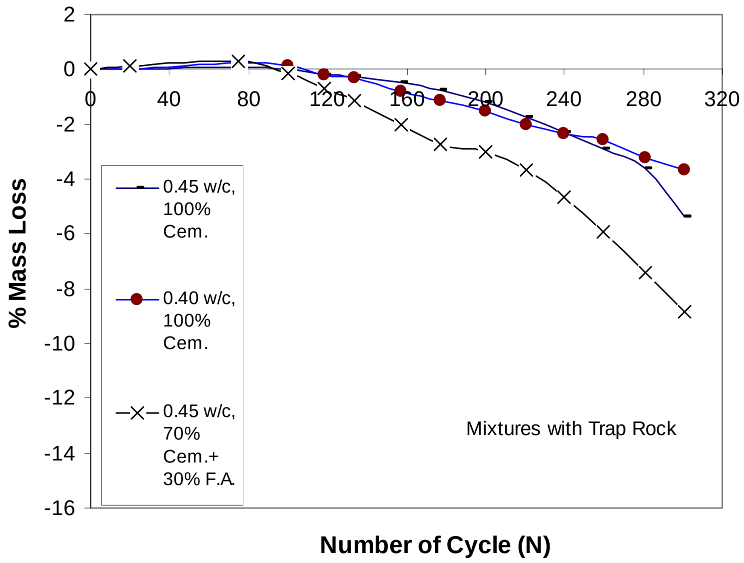

Figure 4.33. Freezing & thawing cycles of HPC mixtures with Trap Rock

Because of limited capacity of freezing and thawing machine, reduced number of samples had to be tested for the mixture group produced by Trap Rock coarse aggregate (Figure 4.33). The control mixtures with 0.40, and 0.45 w/c ratio exhibited mass loss of 3.67% and 5.36%, respectively. They had a compressive strength and air content of 5490, and 4.5%; 4100, and 5.5%, respectively. Fly ash substituted sample performed poor with 8.89% mass loss, which was 50% higher than the similar mixture produced with River Gravel. The poor performance can be speculated by the relatively lower air content of 2.75%.

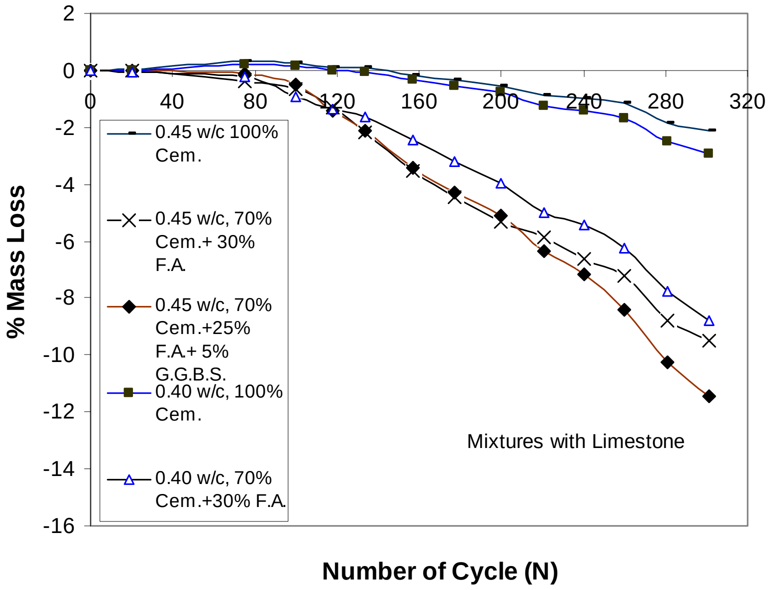

Figure 4.34. Freezing & thawing cycles of HPC mixtures with Limestone

The tests for the mixtures with Limestone coarse aggregate (Figure 4.34) also proved the well-known relation between freezing& thawing resistance, compressive strength, and air content. The mixtures performed from excellent to poor after 300 cycles in the order of: control mixtures with w/c ratio of 0.40 and 0.45 (2.09% and 2.9% mass loss, respectively), fly ash substituted mixtures with w/c ratio of 0.40 and 0.45 (8.7% and 9.5% mass loss, respectively), and finally GGBS substituted mixture with 0.45 w/c ratio (11.4% mass loss). Except 0.40 w/c ratio fly ash substituted mixture, which has 2.5% air content, all others had a total air content between 4.5% and 5%. The lowest compressive strength exhibited by slag substituted mixtures, which was 19 percent less than control sample with 0.40 w/c. Fly ash substituted mixtures with Limestone also displayed 63% less than the similar mixture produced with River Gravel, which can also be explained by lower air content.

The pictures of test samples after 300 cycles are presented in Appendix B. As an example, the pictures of two River Gravel utilized samples after 300 cycles, one with 100% cement and with 0.45 w/c, the other one with 0.40 w/c ratio and 0.40 w/c ratio are presented herein in the Figures of 4.35, and 4.36, respectively.

Figure 4.35. River Gravel used control mixture with 0.45 w/c ratio, after 300 freezing & thawing cycles

Figure 4.36. 30% fly ash substituted, River Gravel used mixture with 0.40 w/c ratio, after 300 freezing & thawing cycles

4.2.4 Abrasion resistance of HPC mixtures

In this section, the abrasion resistance of high performance concrete mixtures was under investigation. The general information about abrasion resistance of concrete is briefly mentioned in the Section 4.1.4. The test procedure was described in the Section 3.4, as well as 4.1.4.

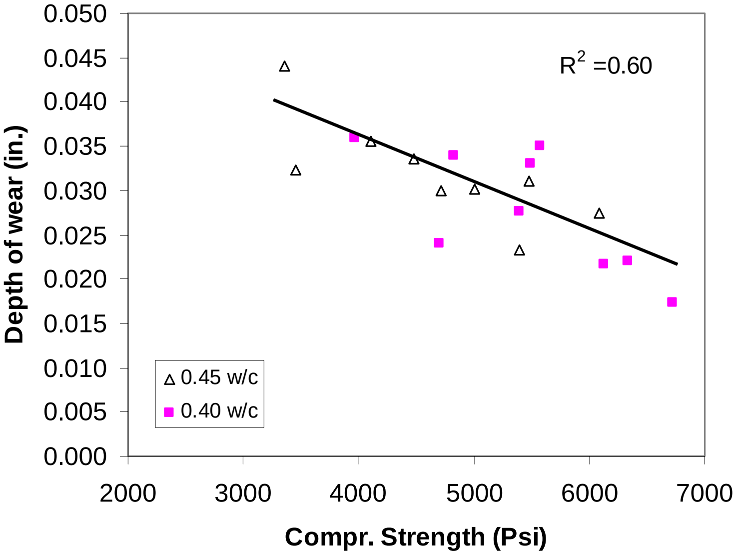

Figure 4.37. Depth of wear (in.) of HPC samples versus compressive strength (Psi)

The depth of wear of HPC samples as a function of compressive strength is presented in Figure 4.37. The coefficient of determination of 0.60 is an indication that the compressive strength has significant influence on abrasion resistance of concrete.

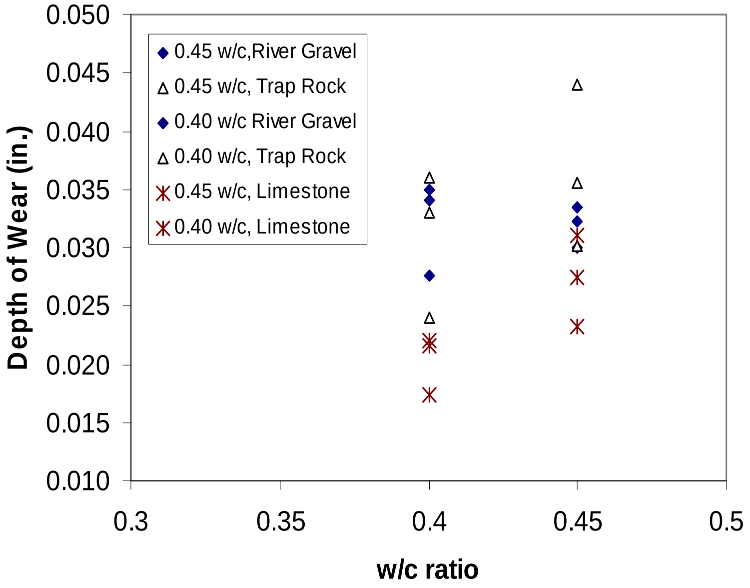

Figure 4.38. Depth of wear (in.) of HPC samples versus w/c ratio

Figure 4.38 illustrates the relation between depth of wear of HPC samples as a function of w/c ratio. A clear-cut difference can be seen between 0.40 and 0.45 w/c ratio mixtures. As the water per cement ratio reduced, the abrasion resistance increased. Figure 4.38 also presents that the mixtures produced by Limestone performed outstanding relative to other mixtures. On average, the Limestone utilized mixtures with 0.40 w/c ratio performed less depth of wear with 35%, and 37% compared to mixtures with Trap Rock, and River Gravel, respectively. Limestone mixtures with 0.45 w/c ratio were also superior to other coarse aggregate utilized mixtures. Limestone mixtures exhibited 14%, and 26% more resistance than that of River Gravel and Trap Rock, respectively. This can be speculated by the high compressive strength development displayed by Limestone utilized mixtures relative to others.

4.2.5 Chloride permeability of HPC mixtures

One of the most common forms of chemical attack is the effect of chloride on concrete. The chloride permeability test was performed on HPC samples according to the AASHTO Designation: T 259-80I “Resistance of Concrete to Chloride Ion Penetration”. The test procedure was described in the Section 3.4, as well as 4.1.5.

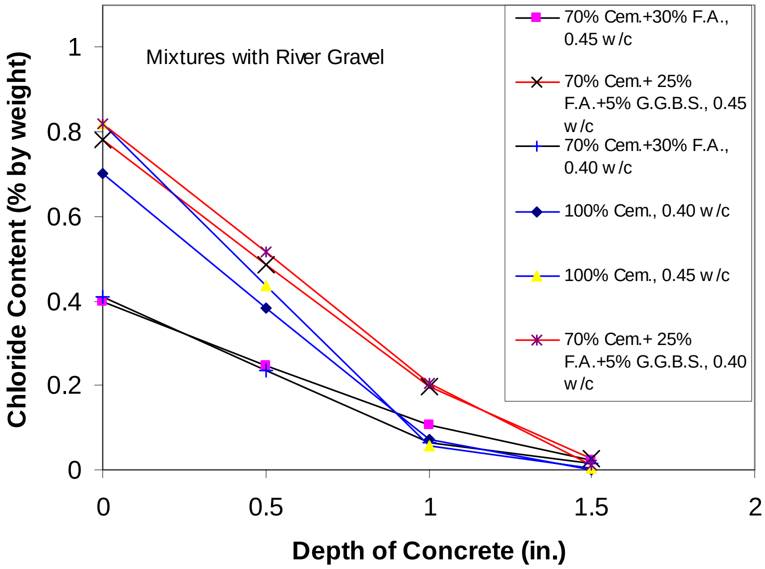

Figure 4.39. Chloride content of HPC with River Gravel samples versus depth of concrete

Chloride permeability of HPC samples were presented in the Figures of 4.39, 4.40, and 4.41, which show the percent chloride content by weight for River Gravel, Trap Rock, and Limestone, respectively. As expected, the increase in w/c ratio caused an increase in the chloride content. The 0.45 water-cement ratio resulted in a greater permeability than that of the mixtures produced with 0.40 water-cement ratio. All of the diagrams clearly stated the superior performance of 30% fly ash substituted mixtures over the control and 25% fly ash-5% GGBS substituted mixtures. As a comparison, the fly ash substituted samples with 0.45 w/c ratio of all groups presented very low chloride content at the depth of 0.5 inch in a range from 0.18% to 0.25% by weight. The highest content was exhibited by River Gravel utilized mixtures, which was 15%, and 37% higher than the samples produced with Trap Rock and Limestone, respectively.

As for comparison, the HPC concrete samples produced by Myers, Touma, and Carrasquillo with 100% Portland cement, 25% fly ash replacement, and 35% fly ash replacement were ponded with 3% sodium chloride for 90 days and tested according to AASHTO T 259; test samples exhibited a chloride content (% by weight) ranging between 0.08 (0.35% fly ash replacement) and 0.32 (no fly ash) at a depth of 0.5 inch (12.7 mm) [Myers, 1997].

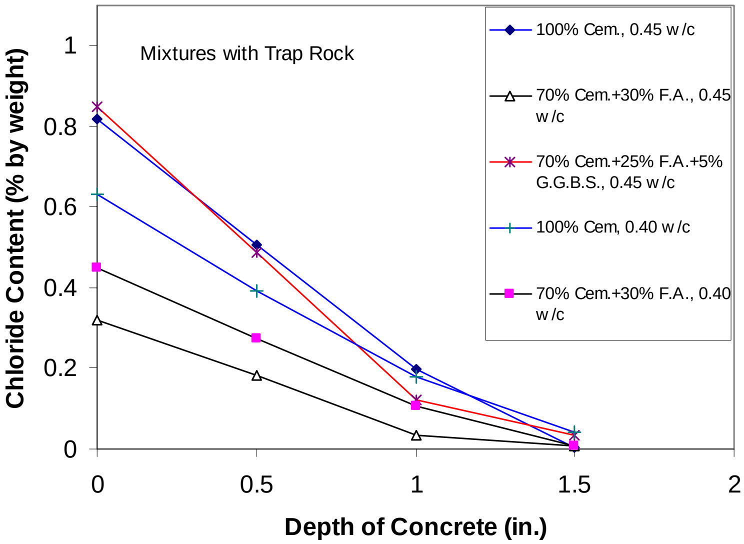

Figure 4.40. Chloride content of HPC with Trap Rock samples versus depth of concrete

As for the mixtures produced with River Gravel (Figure 4.39), the average chloride content of fly ash substituted samples with 0.40 and 0.45 w/c ratio exhibited 41% and 52% less chloride content than the average of control samples and fly ash-GGBS substituted samples at the depth of 0.5 inch, respectively. A similar trend can also be seen in Figure 4.40. The 0.45 w/c ratio control sample and fly ash-GGBS sample yielded high chloride contents as 0.5%, and 0.49% by weight, respectively. The average chloride content of fly ash substituted mixtures with 0.40 and 0.45 w/c ratio showed 41%, 53%, and 55% less chloride content than the 0.40 w/c ratio control mixture, 5% slag substituted mixture and 0.45 w/c ratio control mixture, respectively.

The mixtures prepared by Limestone coarse aggregate illustrated in Figure 4.41. The lowest values are presented by the fly ash substituted samples with 0.44 and 0.45 w/c ratios as 0.18%, and 0.22% by weight, respectively. The average value presented by fly ash substituted mixtures showed 33%, 65%, and 68% less permeability of chloride ions than the fly ash-GGBS substituted samples with 0.40 w/c ratio, the average value of control sample with 0.40 w/c ratio and fly ash-GGBS substituted samples with 0.45 w/c ratio (which were very close to each other by the values of 0.57% and 0.58% by weight), and control sample with 0.45 w/c ratio, respectively.

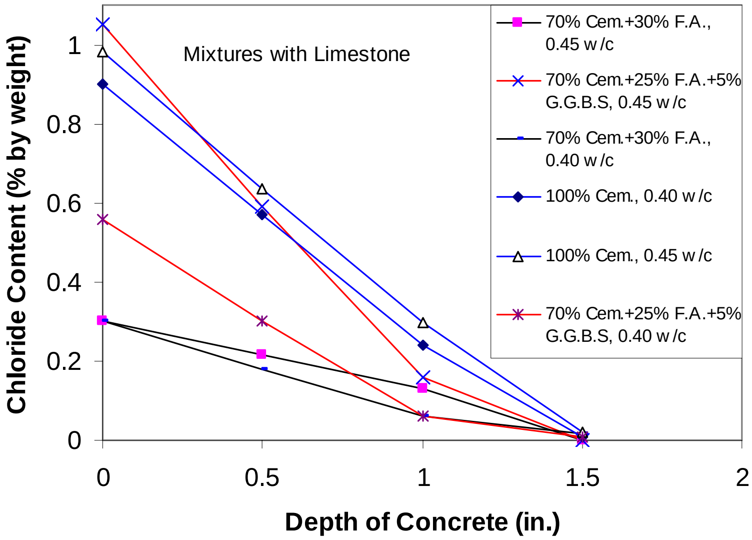

Figure 4.41. Chloride content of HPC with Limestone samples versus depth of concrete

CHAPTER 5 CONCLUSIONS / RECOMMENDATIONS

Based on the research study undertaken using the locally available materials obtained in Missouri, the following conclusions were drawn for the mix designs investigated:

1. The control mixtures (100% Portland cement) for the high strength concrete (HSC) series and high performance concrete (HPC) series displayed higher strength development at the end of 56-day compared to the mixtures in which a Class F fly ash and fly ash-GGBS blend was utilized as a cement replacement material. This is attributed to the slow reaction capability of ground granulated blast-furnace slag, which started contributing to the strength development after 56-day; and the low CaO content of Class F fly ash, which yielded to lesser amount of CSH gel production with respect to control samples.
2. For the HPC series, the compression strength development of the mixtures produced with locally available Limestone at the end of 56-day curing performed superior compared to the mixtures prepared with River Gravel and Trap Rock. Substitution of GGBFS reduced the strength gain compared to the mixes with fly ash at 56 days.
3. The detrimental effect of w/c ratio was clear in all applications. The decrease in w/c ratio caused a reduction in the paste porosity, which caused an improvement in the mechanical properties, as well as in impermeability. Implicit on the abrasion tests results is the idea that w/c ratio has also effect on surface durability.
4. The modulus of elasticity results of HSC samples mostly conformed the ACI 318 empirical equation, however the ACI 363R recommendation underestimated the test results. The HPC mix design yielded higher results than both of the ACI recommendations.
5. The effect of air-entrainment was clear on freezing & thawing resistance of concrete. The air-entrained HSC mixtures performed outstanding compared to mixtures without air-entrainment for HSC. This suggests that a minimal level of air entrainment (2-3%) is warranted for HSC to ensure extremely high F-T resistance for mixes in the 0.25-0.35 w/cm ratio range. If the structural element is not subjected to possible saturation above the critical saturation level of 91.7%, no air-entrainment is warranted.
6. For the HPC series, the fly ash and fly ash-GGBFS blend mix resulted in lower freeze-thaw resistance compared to the control mixes without replacement materials. The associated mass loss for the mixes without replacement materials would be expected to translate into a durability factor (DF) above 85 which is representative of highly freeze-thaw resistant concrete. The samples in which GGBFS was utilized would be considerably lower and not recommended for use where high F-T durability is required.
7. In terms of chloride permeability of HSC and HPC mixtures, a similar trend was obtained in both series; the Class F fly ash replacement mixtures performed superior to control and fly ash-GGBFS replacement mixtures. The lower performance of fly ash-GGBFS replacement samples compared to the

control mixes is explained by the relatively slower reaction speed of GGBFS and being a kind of hydraulic cement, not a pozzolan. All the HSC and HPC mixtures showed practically 0% chloride concentration at the depth of 1.5 inches (38.1 mm), which is often recommended as a minimum cover depth for reinforced concrete structures. The w/cm ratio was clearly the dominant factor to reduce the level of chloride content close to the surface of the concrete.

REFERENCES

1. Aitcin, P.C., Miao, B., Cook, W.D., Mitchell, D., “Effects of Size and Curing on Cylinder Compressive Strength of Normal and High Strength Concretes,” ACI Materials Journal, July-August 1994, pp. 349-354.
2. Aitcin, P.C., Mehta, P.K., “Effect of Coarse Aggregate Characteristics on Mechanical Properties of High Strength Concrete,” ACI Materials Journal, March-April 1990, pp. 103-107.
3. Alampalli, S., Owens F. “In Service Performance of High-Performance Concrete Bridge Decks”, Transportation Research Record – Journal of the Transportation Research Board, Washington D.C., No. 1696, Vol. 2, Publication 5B0121, 2000, pp. 193-196.
4. Almeida, I.R., “Abrasion Resistance of High Strength Concrete with Chemical and Mineral Admixtures,” SP 145-60 Durability of Concrete, Third International Conference Proceedings, Nice, France, 1994, pp. 1099-1113.
5. American Concrete Institute, “Building Code Requirements for Structural Concrete”, ACI Committee 318, Farmington Hills, MI.
6. American Concrete Institute, “State-of-the-Art Report on High Strength Concrete”, ACI Committee 363R, Farmington Hills, MI.
7. American Conceret Institute, “Specifications for Structural Concrete for Buildings”, ACI Committee 301, Farmington Hills, MI, 1999
8. American Concrete Institute, “Guide to Durable Concrete,” ACI Committee 201 Report, ACI Committee 201.3R, 1982.
9. Annual book of ASTM Standards: 4.02. ASTM. Philadelphia, PA. 2002
10. AASHTO T 259. Resistance of Concrete to Chloride Ion Penetration. 1980.
11. Arya, C; "Problem of predicting risk of corrosion of steel in chloride contaminated concrete", Proc. Instn Civ. Engrs, part 1, 88, 1990, pp. 875-888.
12. Baalbaki, W., Benmokrane, B., Chaallal, O., Aitcin, P.C., “Influence of Coarse Aggregate on Elastic Properties of High Performance Concrete,” ACI Materials Journal, September-October 1991, pp. 499-503.
13. Berke, N.S., Pfeifer, D.W., Weil, T.G., “Protection against Chloride-Induced Corrosion,” Concrete International, Vol. 10, No. 12, Dec. 1988, pp. 45-55.
14. Carrasquillo, R.L., Slate, A.H., Nilson, F.O., “Properties of High Strength Concrete Subjected to Short-Term Loading,” ACI Journal, May-June 1981, pp. 171-178.
15. Cetin, A., “Effect of Accelerated Heat Curing and Mix Characteristics on the Heat Development and Mechanical Properties of High Performance Concrete,” The University of Texas at Austin, Department of Civil Engineering, Dissertation, December 1995.
16. Cook, J.E., “A Ready Mix Concrete Company’s Experience with Fly Ash,” Paper Presented at the 1980 Fly Ash Conference, Texas A & M University, May, 21 1980.
17. Diamond, S., Lopez-Flores, F., “Comparative Studies of the Effect of Lignitic and Bituminous Fly Ashes in Hydrated Cement Systems,” Proceedings, Symposium on Fly Ashes Incorporation in Cement and Concrete, Materials Research Society, 1981, pp. 112-123.

18. Ernzen, J.J., Carrasquillo, R.L., “Resistance of High Strength Concrete to Cold Weather Environments,” Center for Transportation Research, The University of Texas at Austin, Research Report 481-7, July 1992.
19. Fagerlund, G., “Studies of the Destruction Mechanisms at Freezing of Porous Materials,” Proceedings of the Sixth International Congress on the Problems Raised by Frost Action, LeHarve, France, 1975, pp. 166-196.
20. Federal Highway Administration Report. High Performance Concrete for Bridges. 1997, www.ota.fhwa.dot.gov. Accessed April 2002.
21. Fentress, B., “Slab Construction Practice Compared Wear Tests,” ACI Journal, No. 7, July 1973, pp. 486-491.
22. Fisher, G.L., Prentice, B.A., Silberman, D., Ordov, J.M., Bierman, A.H., Ragaini, R.C., McFarland, A.R., “Physical and Morphological Studies of Size-Classified Coal Fly Ash,” Environmental Science and Technology, Vol. 12, No. 4, April 1978, pp. 447-451.
23. Fontana, M.G., “Corrosion Engineering,” McGraw-Hill Inc., Third Edition, 1986.
24. Gia, G., Rocco, C., Violini, D., Zappitelli, J., Zerbino, R., “High Strength Concrete Incorporating Different Coarse Aggregates,” ACI Materials Journal, My-June 1992, pp. 242-246.
25. Hadchiti, K.M., Carrasquillo, R.L., “Abrasion Resistance and Scaling Resistance of Concrete Containing Fly Ash,” Center for Transportation Research, The University of Texas at Austin, Research Report 481-3, August 1988.
26. Haque, M.N., Kayyali, O.A., Gopalan, M.K., “Fly Ash Reduces Harmful Chloride Ions in Concrete,” ACI Materials Journal, Vol. 89, No. 3, May-June 1992, pp. 238-241.
27. Hester, W.T., “Microstructure as a Tool for Proportioning High Strength Concrete Mixes,” Materials Research Society Proceedings, Vol. 42, Very High Strength Cement-Based Materials, Materials Research Society, 1985, pp. 193-200.
28. Hime, W.G., “Delayed Ettringite Formation - A Concern for Precast Concrete ?,” PCI Journal, July-August 1996, pp.26-30.
29. Hogan, F.J., Meusel, J.W., “Evaluation for Durability and Strength Development of a Ground Granulated Blast Furnace Slag,” Cement, Concrete, and Aggregates, Vol. 3, No. 1, Summer 1981, pp. 40-52.
30. Hoff, G. “Durability of Fiber Reinforced Concrete in a Severe Marine Environment,” SP-100-55, Concrete Durability, Katherine and Bryant Mather International Conference, Vol. 1, 1987, pp. 1012.
31. Killoh, D.C., Parrott, L.J., Patel, R.G., “Influence of Curing at Different Relative Humidities on the Hydration and Porosity of a Portland / Fly Ash Cement Paste,” 1989 Trondheim Conference, SP 114-7, American Concrete Institute, pp. 157-174.
32. Lauf, R.J., “Microstructure of Coal Fly Ash Particles,” Ceramic Bulletin, Vol. 61, No. 4, April 1982, pp. 487-490.
33. Lawrence, L., Myers, J.J., Carrasquillo, R.L., “Premature Concrete Deterioration in Texas Department of Transportation Precast Elements,” Proceedings for ACI Spring Meeting, Seattle, Washington, March 1997.
34. Malhotra, V. M., Mehta, P. K. “Pozzolanic and Cementitious Materials”, Overseas Publishers Association, 1996

35. Marchand, J., Sellevold, E.J., Pigeon, M., “The Deicer Salt Scaling Deterioration of Concrete - An Overview,” SP 145-1 Durability of Concrete, Third International Conference Proceedings, Nice, France, 1994, pp. 1-46.
36. Marsh, B.K., Day, R.L., Bonner, D.G., “Pore Structure Characteristics Affecting the Permeability of Cement Paste Containing Fly Ash,” Cement and Concrete Research, Vol. 15, No. 6, November 1985, pp. 1027-1038.
37. Mehta, P K; “Concrete: Structure, Properties, and Materials”, Prentice Hall Inc. Englewood Cliffs, N.J., Prentice-Hall, 1986.
38. Mehta, P.K., “Pozzolanic and Cementitious By-Products as Mineral Admixtures for Concrete - A Critical Review,” Special Publication SP-79, Fly Ash, Silica Fume, Slag, and Other Mineral By-Products in Concrete, Vol. 1, American Concrete Institute, Detroit, 1983, pp. 1-46.
39. Mehta, P K; “Durability- Critical Issue For the Future”, V 19, n 7, pp. 27-32, July 1997
40. Mehta, P.K., “Concrete, Structures, Properties, and Materials,” Prentice Hall Inc., Englewood Cliffs, New Jersey, 1986, Chapter 5.
41. Mindness, S., “Relationships Between Strength and Microstructure for Cement-Based Materials: An Overview,” Materials Research Society Symposia Proceedings, Vol. 42, Very High Strength Cement-Based Materials, Materials Research Society, 1985, pp. 53-68.
42. Mindness, S., Young, J.F., “Concrete,” Prentice Hall Inc., Englewood Cliffs, 1981.
43. Myers, J.J. “The Production and Quality Control of High Performance Concrete in Texas Bridge Structures,” The University of Texas at Austin, PhD Dissertation, December 1998.
44. Myers, J.J., Carrasquillo, R.L., “Influence of Hydration Temperature on the Durability and Mechanical Property Performance of HPC Prestressed / Precast Beams,” National Research Council, Transportation Research Record – Journal of the Transportation Research Board, Washington D.C., No. 1696, Vol. 1, Publication 5B0038, April 2000, pp. 131-142.
45. Myers, J.J., Carrasquillo, R.L., “Quality Control & Quality Assurance Program for Precast Plant Produced High Performance Concrete U-Beams,” Advanced Concrete Solutions for Bridges and Transportation Structures, PCI/FHWA International Syposium on High Performance Concrete, New Orleans 1997, pp. 368-682.
46. Myers, J.J., Touma, W., Carrasquillo, R.L., “Permeability of High Performance Concrete: Rapid Chloride Ion Test vs. Chloride Ponding Test,” Proceedings for the PCI/FHWA International Symposium on High Performance Concrete, Advanced Concrete Solutions for Bridges and Transportation Structures, New Orleans, Louisiana, October 1997, pp. 268-282.
47. Moranville-Regourd, M., “Durability of High Performance Concretes: Alkali-Aggregate Reaction and Carbonation,” High Performance Concrete: From Material to Structure, E & FN Spon, London SE1 8HN, 1992, pp. 225-233.
48. Neville, A; “Properties of Concrete”, John Wiley & Sons, N.Y, 1996.
49. Neville, A.M., Brooks, J.J., “Concrete Technology,” Longman, Essex (U.K.), 1987, pp. 438.

50. Philleo, R.E., “Freeze-Thaw Resistance of High Strength Concretes,” NCHRP Synthesis of Highway Practice 129, Transportation Research Board, Washington D.C., December 1986, 31 pp.
51. Poston, R.W., Carrasquillo, R.L., Breen, J.E., “Durability of Prestressed Bridge Decks,” Center for Transportation Research, The University of Texas at Austin, Research Report 316-1, July 1985.
52. Sarkar, S.L., Aitcin, P.C., “Comparative Study of the Microstructures of Normal and Very High Strength Concrete,” Cement, Concrete, and Aggregates, CCAGDP, Vol. 9, No. 2, Winter 1987, pp.57-64.
53. Skalny, J., Roberts, L.R., “High Strength Concrete,” Unpublished Draft.
54. Shah, S. P., Ahmad, S. H.; “High Performance Concrete: Properties and Applications”, McGraw-Hill, N.Y., 1994.
55. Sherman, M.R., Carrasquillo, R.L., Fowler, D.W., “Field Evaluation of Bridge Corrosion Protection Measures,” Center for Transportation Research, The University of Texas at Austin, Research Report 1300-1, March 1993.
56. Shilstone, J. M. Sr, Shilstone J. M. Jr.; “High Performance Concrete Mixtures for Durability”, SP 140-14, American Concrete Institute, Detroit, 1993.
57. Smadi, M.M., Slate, F.O., “Microcracking of High and Normal Strength Concretes under Short and Long-Term Loadings,” ACI Materials Journal, March-April 1989, pp. 117-127.
58. Stark, D., “Characteristics and Utilization of Coarse Aggregates Associated with D-Cracking,” Living with Marginal Aggregates, ASTM STP 597, American Society of Testing and Materials, 1976, pp. 45-57.
59. Swamy, R.N., “The Nature of the Strength of Concrete,” Unpublished Draft.
60. Tia, M. et al., “Extensive Study of Field and Laboratory Study of Modulus of Rupture and Permeability of Structural Concrete in Florida for Development of a Concrete Performance Specification,” Final Report, DOT # FL/DOT/RMC/0384-3366, The University of Florida, Department of Civil Engineering, December 1992.
61. Tikalsky, P.J., Carrasquillo, R.L., “The Effect of Fly Ash on the Sulfate Resistance of Concrete,” Center for Transportation Research, The University of Texas at Austin, Research Report 481-5, August 1989.
62. Touma, W.E., “Permeability of High Performance Concrete: Rapid Chloride Ion Test vs. Chloride Ponding Test,” The University of Texas at Austin, Department of Civil Engineering, Master’s Thesis, August, 1997.
63. Thomas, M.D.A., Matthews, J.D., Haynes, C.A., “The Effect of Curing on the Strength and Permeability of PFA Concrete,” SP 114-9, American Concrete Institute, Detroit, pp. 192-217.
64. Vandewalle, L., Mortelmans, F., “The Effect of Curing on the Strength Development of Mortar Containing High Volumes of Fly Ash,” 1992 Istanbul Conference, SP 132-4, American Concrete Institute, Detroit, pp. 53-63.
65. Visher, S.S., “Climatic Maps of Geological Interest,” Geological Society of America Bulletin, July-December 1945, Vol. 56, No. 7, pp. 713-736.
66. Vondran, G., “Making More Durable Concrete With Polymeric Fibers,” SP-100-23, Concrete Durability, Katherine and Bryant Mather International Conference, Vol. 1, 1987, pp. 377-396.

67. Watkins, D.A., “Specification of Air Entrainment for Freezing and Thawing Environments,” The University of Texas at Austin, Master’s Thesis, August 1997.
68. Witte, L.P., Backstrom, J.E., “Some properties Affecting the Abrasion Resistance of Air-Entrained Concrete,” ASTM, Proceedings, Vol. 51, 1951, pp. 1141-1155.
69. Whiting, D., “Rapid Determination of the Chloride Permeability of Concrete,” Final Report No. FHWA/RD-81/119, Federal Highway Administration, August 1981.
70. Young, J.F., “A Review of the Pore Structure of Cement Paste and Concrete and Its Influence on Permeability,” Permeability of Concrete, ACI SP-108, 1988, pp.1-18.
71. Zakka, Z.A., “Effects of High Range Water Reducers on the Properties of Fresh and Hardened Concrete,” The University of Texas at Austin, Department of Civil Engineering, Master’s Thesis, October 1989.
72. Zia, P.; “High Performance Concrete in Severe Environments”, SP-140, American Concrete Institute, Detroit, 1993.
73. Zia, P., Leming, M.L., Ahmad, S.H., “High Performance Concrete, A State-of-the-Art Report,” SHRP-C/FR-91-103, Strategic Highway Research Program, National Research Council, Washington D.C., 1991.

Appendices

Appendix A

TABLE A.1 Mix Design for HSC Mixtures

Mix	**w/cm ratio**	**%**	**Replacement**	**Cement**	**Coarse Aggr.**[1]	**Fine Aggr.**	**HRWR**	**AEA**
No		FA	GGBFS	(lbs)	(lbs/yd^3)	(lbs/yd^3)	(oz/cwt)	(oz/cwt)
1	0.25	0	0	987	1918	1029	27	0.0
2	0.25	0	0	987	1918	1029	25	1.7
3	0.25	0	0	987	1918	1029	27	1.3
4	0.25	0	0	987	1918	1029	30	2.7
5	0.25	30	0	691	1918	1029	36	0.0
6	0.25	30	0	691	1918	1029	48	1.3
7	0.25	30	0	691	1918	1029	43	2.6
8	0.25	30	0	691	1918	1029	43	2.6
9	0.25	25	5	691	1918	1029	43	0.0
10	0.25	25	5	691	1918	1029	43	1.7
11	0.25	25	5	691	1918	1029	41	3.0
12	0.25	25	5	691	1918	1029	41	4.4
13	0.30	0	0	820	1811	1302	31	0.0
14	0.30	0	0	820	1811	1302	39	1.1
15	0.30	0	0	820	1811	1302	39	0.6
16	0.30	0	0	820	1811	1302	24	0.8
17	0.30	30	0	574	1811	1302	50	0.0
18	0.30	30	0	574	1811	1302	49	0.7
19	0.30	30	0	574	1811	1302	36	1.0
20	0.30	30	0	574	1811	1302	36	1.8
21	0.30	25	5	574	1811	1302	49	0.0
22	0.30	25	5	574	1811	1302	39	0.9
23	0.30	25	5	574	1811	1302	30	1.5
24	0.30	25	5	574	1811	1302	32	2.1
25	0.35	0	0	694	1811	1302	35	0.0
26	0.35	0	0	694	1811	1302	46	4.6
27	0.35	0	0	694	1811	1302	20	2.1
28	0.35	0	0	694	1811	1302	31	1.2
29	0.35	30	0	486	1811	1302	46	0.0
30	0.35	30	0	486	1811	1302	38	1.2
31	0.35	30	0	486	1811	1302	37	1.5
32	0.35	30	0	486	1811	1302	43	2.2
33	0.35	25	5	486	1811	1302	46	0.0
34	0.35	25	5	486	1811	1302	38	1.2
35	0.35	25	5	486	1811	1302	37	1.5
36	0.35	25	5	486	1811	1302	37	1.7

Note: Limestone was utilized as coarse aggregate. Slump was kept constant as 8± 2 inches (200±50 mm)

Conversions factors: 1 lbs = 0.454 kg; 1 lbs/yd ^{3}= 0.594 kg/m

Table A.2 The Summary of Fresh & Hardened Properties of HSC

Mix	**1**	**2**	**3**	**4**	**5**	**6**	**7**	**8**	**9**	**10**	**11**	**12**
Slump-Before (in)	0.25	0.5	0.5	0.5	0.5	0.5	0.25	0.25	0.25	0.5	0.25	0.25
HRWR (ml)	82	75	81	91	85	100	100	100	100	100	95	95
Slump-After (in)	9.25	9	8.75	8.75	8	9	9	8.75	9	9	8.75	9.25
Air Entrainment (ml)	0	5	3.1	8	0	3	6	9	0	4	7	10.2
Entrained Air (%)	0	3	2.75	4	0	0.5	2	3	0	1.5	2.5	3
Total Air (%)	1.25	4	4	5.25	2	2.5	4	5	1.5	3	4	4.5
Unit Weight (lbs/ft^3)	147.4	143.4	143.2	140.9	144.3	143.0	140.9	139.8	145.2	143.4	141.9	141.4
f'c (7-Day) Avg (psi)	8540	6890	7270	7420	5900	5800	5250	4960	5900	5620	5260	5210
MOE (7-Day) Avg (ksi)	5110	4620	4910	4750	4370	4410	4300	4060	4540	4330	4050	4080
f'c (28-Day) Avg (psi)	9900	8270	8560	8400	7490	7390	6580	5910	7370	7210	6470	6580
MOE (28-Day) Avg (ksi)	5500	5040	5130	5150	4810	4770	4480	4280	5060	4890	4670	4780
f'c (56-Day) Avg (psi)	10560	8370	8910	8710	8030	7770	7180	6700	8180	7540	7430	7430
MOE (56-Day) Avg (ksi)	5470	5180	5210	5370	5170	4880	4590	3910	4970	5060	4830	5100

Conversions factors: 1 lbs = 0.454 kg; 1 lbs/yd^3 = 0.594 kg/m^3.

Table A.2 The Summary of Fresh & Hardened Properties of HSC

Mix	**13**	**14**	**15**	**16**	**17**	**18**	**19**	**20**	**21**	**22**	**23**	**24**
Slump-Before (in)	0.5	0.5	0.5	0.5	0.5	0.5	0.75	0.75	0.5	0.5	0.5	0.5
HRWR (ml)	115	141	140	87	141	135	100	100	136	110	82	88
Slump-After (in)	8.5	9	9	9	8	9	9.25	9.25	8.5	9	9.25	9
Air Entrainment (ml)	0	4	2	3	0	2	3	5	0	2.4	4	6
Entrained Air (%)	0	5	1	1.5	0	1	0.5	1.5	0	0.5	1	1.5
Total Air (%)	2.5	7.5	3.5	4	3	4	3.5	4.5	3	3.5	4	4.5
Unit Weight (lbs/ft^3)	145.8	138.6	145	143.4	144	142	143.2	141.2	144.4	145.4	143.8	141.2
f'c (7-Day) Avg (psi)	7750	6660	7990	6120	5870	5890	4740	4420	6700	5140	4790	4440
MOE (7-Day) Avg (ksi)	4870	4320	5290	4470	4330	4730	4020	3990	5120	4270	4360	4190
f'c (28-Day) Avg (psi)	8860	7510	9840	7730	7170	6910	6300	5830	7610	6680	6440	6240
MOE (28-Day) Avg (ksi)	5470	4440	5680	5040	4950	4670	4710	4470	4860	4930	4460	4590
f'c (56-Day) Avg (psi)	9200	7670	10580	8170	8230	7100	6640	6370	8470	7410	7170	6860
MOE (56-Day) Avg (ksi)	5450	4810	5470	5210	4690	4580	4680	4550	4940	5020	4760	4670

Conversions factors: 1 lbs = 0.454 kg; 1 lbs/yd^3 = 0.594 kg/m^3.

Table A.2 The Summary of Fresh & Hardened Properties of HSC

Mix	**25**	**26**	**27**	**28**	**29**	**30**	**31**	**32**	**33**	**34**	**35**	**36**
Slump-Before (in)	0.5	1	0.5	0.5	0.5	0.5	0.5	0.5	1	0.5	0.5	0.5
HRWR (ml)	150	150	86	130	150	125	120	108	150	125	123	120
Slump-After (in)	8	8	8.5	9	8	8	8.5	8.5	8	8	8	8.5
Air Entrainment (ml)	0	15	9	5	0	4	4.8	7	0	4	7	5.5
Entrained Air (%)	0	5	3.5	3	0	1.5	3	3.5	0	0.5	4.5	2
Total Air (%)	3.5	8.5	7	6.5	2.5	4	5.5	6	3.5	4	8	5.5
Unit Weight (lbs/ft^3)	143	134.6	139.2	139.2	143.4	142.4	140.4	139.4	140.6	142.4	137	141.2
f'c (7-Day) Avg (psi)	6920	3510	4560	5220	4270	3980	4050	3450	4140	4040	3800	3920
MOE (7-Day) Avg (ksi)	4540	3480	4160	4020	4020	3930	3940	3610	3910	3740	3800	4230
f'c (28-Day) Avg (psi)	8330	4100	5530	5910	5600	5430	5310	4310	5760	5500	5190	5620
MOE (28-Day) Avg (ksi)	5120	4200	4280	4450	3990	4240	4300	4070	4450	4510	3970	4280
f'c (56-Day) Avg (psi)	8670	4410	5950	6580	6170	5640	5830	4920	6180	6110	5490	5820
MOE (56-Day) Avg (ksi)	5060	3750	4480	4690	4690	4440	4480	4050	4200	4850	4340	4390

Conversions factors: 1 lbs = 0.454 kg; 1 lbs/yd^3 = 0.594 kg/m^3.

TABLE A.3 Mix Design for HPC Mixtures

Mix No	w/cm ratio c.m	% FA	Replacement GGBFS	Cement lbs.	CA Type Type	Coarse Aggr. lbs/yd^3	Fine Aggr. lbs/yd^3	Slump (in.)
1	0.45	0	0	611	River Gravel	1811	1440	4.00
2	0.45	0	0	611	Trap Rock	1811	1440	3.75
3	0.45	30	0	428	River Gravel	1811	1440	4.25
4	0.45	30	0	428	Trap Rock	1811	1440	6.50
5	0.45	25	5	428	River Gravel	1811	1440	6.75
6	0.45	25	5	428	Trap Rock	1811	1440	5.00
7	0.40	0	0	687	River Gravel	1811	1440	5.00
8	0.40	0	0	687	Trap Rock	1811	1440	5.00
9	0.40	30	0	481	River Gravel	1811	1440	6.00
10	0.40	30	0	481	Trap Rock	1811	1440	5.25
11	0.40	25	5	481	River Gravel	1811	1440	5.00
12	0.40	25	5	481	Trap Rock	1811	1440	6.00
13	0.45	0	0	611	Limestone	1811	1440	5.50
14	0.45	30	0	428	Limestone	1811	1440	6.00
15	0.45	25	5	428	Limestone	1811	1440	5.00
16	0.40	0	0	687	Limestone	1811	1440	3.00
17	0.40	30	0	481	Limestone	1811	1440	6.50
18	0.40	25	5	481	Limestone	1811	1440	3.50

Note: A constant air-entrainment admixture of 3 oz/cwt was used in all mixtures.

Conversions factors: 1 lbs = 0.454 kg; 1 lbs/yd^3 = 0.594 kg/m^3.

TABLE A.4 Compressive Test Results (56-Day) of HPC samples

	Compressive Strength at 56-days Psi (MPa)		
Mix Description	**River Gravel**	**Trap Rock**	**Limestone**
		0.45 w/cm	
Control Mix.	4710 (32.4)	4100 (28.3)	6080 (41.9)
Cem. + FA	4480 (30.9)	4000 (27.6)	5470 (37.7)
Cem. + FA + GGBFS	3450 (23.8)	3360 (23.2)	5400 (37.2)
		0.40 w/cm	
Control Mix.	5590 (38.5)	5490 (37.9)	6720 (46.3)
Cem. + FA	5580 (38.4)	4700 (32.4)	6340 (43.7)
Cem. + FA + GGBFS	4830 (33.3)	3960 (27.3)	6130 (42.3)

Table A.5 Surface Scaling of HSC Mixtures Exposed to Freezing & Thawing Cycles

Mix No.	Scale
1	3
4	1
5	4
8	1
9	3
12	1
13	2
16	2
17	2
20	1
21	2
23	1
24	1
25	2
27	2
30	1
32	1
33	2

Table A-6. Surface Scaling of HPC Mixtures Exposed to Freezing & Thawing Cycles

Mix No.	**Scale**
1	2
2	4
3	4
4	5
7	4
8	3
9	5
37	2
38	4
39	3
40	4
41	4

APPENDIX B

Figure B.1. Control sample of HSC with 0.25 w/c, after 300 freezing & thawing cycles (0 entrained air)

Figure B.2. Control sample of HSC with 0.25 w/c, after 300 freezing & thawing cycles (4% entrained air)

Figure B.3. 30% FA substituted sample of HSC with 0.25 w/c, after 300 freezing & thawing cycles (0 entrained air)

Figure B.4. 30% FA substituted sample of HSC with 0.25 w/c, after 300 freezing & thawing cycles (3% entrained air)

Figure B.5. 25% FA+5% GGBS substituted sample of HSC with 0.25 w/c, after 300 freezing & thawing cycles (0 entrained air)

Figure B.6. 25% FA+5% GGBS substituted sample of HSC with 0.25 w/c, after 300 freezing & thawing cycles (3% entrained air)

Figure B.7. Control sample of HSC with 0.30 w/c, after 300 freezing & thawing cycles (0 air entrainment)

Figure B.8. Control sample of HSC with 0.30 w/c, after 300 freezing & thawing cycles (1.5% air entrainment)

Figure B.9. 30% FA substituted sample of HSC with 0.30 w/c ratio, after 300 freezing & thawing cycles (0 air entrainment)

Figure B.10. 30% FA substituted sample of HSC with 0.30 w/c ratio, after 300 freezing & thawing cycles (1.5% air entrainment)

Figure B.11. 25% FA+5% GGBS substituted sample of HSC with 0.30 w/c ratio, after 300 freezing & thawing cycles (0 air entrainment)

Figure B.12. 25% FA+5% GGBS substituted sample of HSC with 0.30 w/c ratio, after 300 freezing & thawing cycles (1% air entrainment)

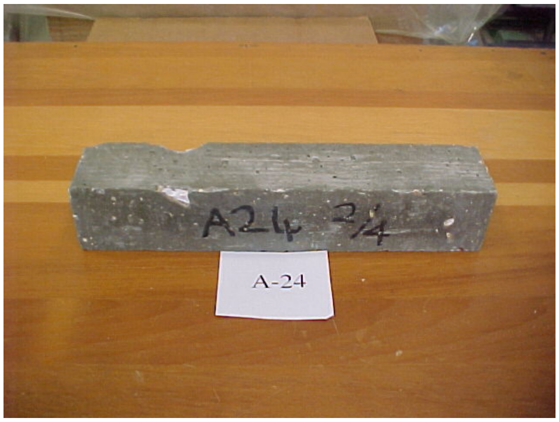

Figure B.13. 25% FA+5% GGBS substituted sample of HSC with 0.30 w/c ratio, after 300 freezing & thawing cycles (4.5% air entrainment)

Figure B.14. Control sample of HSC with 0.35 w/c ratio, after 300 freezing & thawing cycles (0 air entrainment)

Figure B.15. Control sample of HSC with 0.35 w/c ratio, after 300 freezing & thawing cycles (3.5 air entrainment)

Figure B.16. 30% FA substituted sample of HSC with 0.35 w/c ratio, after 300 freezing & thawing cycles (1.5% air entrainment)

Figure B.17. 30% FA substituted sample of HSC with 0.35 w/c ratio, after 300 freezing & thawing cycles (3.5% air entrainment)

Figure B.18. 25% FA+5% GGBS sample of HSC with 0.35 w/c after 300 freezing & thawing cycles (0 air entrainment)

Figure B.19. Control sample of River Gravel utilized HPC with 0.45 w/c ratio, after 300 freezing & thawing cycles

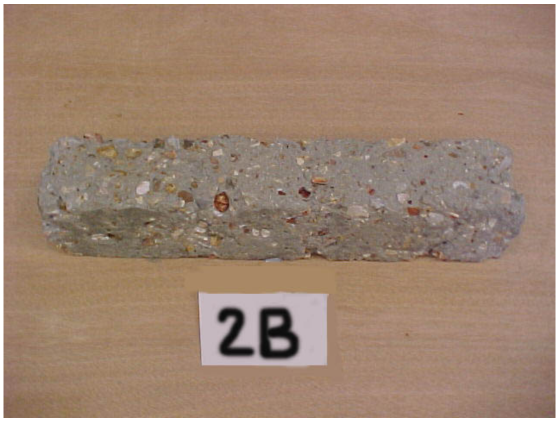

Figure B.20. Control sample of Trap Rock utilized HPC with 0.45 w/c ratio, after 300 freezing & thawing cycles

Figure B.21. 30% FA substituted sample of River Gravel utilized HPC with 0.45 w/c, after 300 freezing & thawing cycles

Figure B.22. Control sample of River Gravel utilized HPC with 0.40 w/c, after 300 freezing & thawing cycles

Figure B.23. Control sample of Trap Rock utilized HPC with 0.40 w/c ratio, after 300 freezing & thawing cycles

Figure B.24. 30% FA substituted sample of River Gravel utilized HPC with 0.40 w/c, after 300 freezing & thawing cycles

Figure B.25. Control sample of Limestone utilized HPC with 0.45 w/c ratio, after 300 freezing & thawing cycles

Figure B.26. 30% FA substituted sample of Limestone utilized HPC with 0.45 w/c ratio, after 300 freezing & thawing cycles

Figure B.27. 25% FA+5% GGBS substituted sample of Limestone utilized HPC with 0.45 w/c ratio, after 300 freezing & thawing cycles

Figure B.28. Control sample of Limestone utilized HPC with 0.40 w/c ratio, after 300 freezing & thawing cycles

Figure B.29. 30% FA substituted sample of Limestone utilized HPC with 0.40 w/c ratio, after 300 freezing & thawing cycles